3D Printing of Rapid Setting Ordinary Concrete Mixtures

By

Friedhelm Stefan Günzel

Supervisor: Prof Riaan Combrinck

Co-supervisor: Dr Pienaar Jacques Kruger

December 2021

Declaration

By submitting this dissertation electronically, I declare that the entirety of the work contained therein is my own, original work, that I am the sole author thereof (save to the extent explicitly otherwise stated), that reproduction and publication thereof by Stellenbosch University will not infringe any third-party rights and that I have not previously in its entirety or in part submitted it for obtaining any qualification.

. . . . . .

Friedhelm Stefan Günzel

Date: December 2021

Abstract

In recent years, significant research and development has gone into 3D printed concrete. This construction technique requires no formwork as in ordinary construction projects. The addition of admixtures increases the complexity of 3D printable mixtures in comparison to ordinary concrete mixtures in which cement, water and aggregate are the main constituents. In this study, more ordinary concrete mixtures are used for 3D printing in order to minimise the complexity of 3D printable mixtures. The combination of a more ordinary concrete mixture with the efficiency of 3D printing as a construction technique, combines the benefits of both construction techniques. The aim was to 3D print ordinary concrete mixtures that have improved buildability characteristics due to a rapid setting behaviour. Three types of rapid setting behaviours were tested in this study: false setting, ordinary Portland cement (OPC) cement replacement with belitic calcium sulfoaluminate (BCSA) cement and flash setting.

The study was conducted in two phases. The first phase was used to characterise the three rapid setting mixtures. Compressive strength, hydration temperature development, setting time and early age compressive strength were tested for the characterisation. In the second phase, the three rapid setting mechanisms were printed in a 3D printer to determine the buildability of the three rapid setting mechanisms. In addition to buildability, the economic feasibility of the rapid setting mixtures was analysed.

It was found that false setting does not significantly influence the mechanical characteristics of concrete. The early age strength gain is not as rapid as for flash setting or with the addition of BCSA cement. Flash setting improves the early ages strength gain of concrete but reduces the long-term compressive strength development. Replacing OPC cement with BCSA cement improves the early age strength gain and does not impact the mechanical properties significantly. Higher cement replacement rates increased the intensity of the rapid setting mechanisms, shorter setting times and higher early age strength was improved. From the buildability study it was found that flash setting has the largest positive impact on the buildability characteristics of 3D printed concrete. The buildability could be increased by 321% with flash setting. OPC cement replacement with BCSA cement resulted in a buildability increase of 214%. False setting was found to be the least effective rapid setting mechanism with a 35% increase in buildability. Flash setting and BCSA replacement are cost effective methods to improve the buildability of 3D printed concrete. False setting is found too expensive to induce and the compressive strength gain at early ages is little compared to the other two rapid setting mechanisms.

The aim of this study was achieved by 3D printing rapid setting ordinary concrete mixtures. Significant buildability improvements could be made, and the rapid setting ordinary concrete mixtures are beneficial for the rapid construction of 3D printed components or structures.

Keywords: 3D concrete printing, flash setting, false setting, BCSA cement, rapid setting

Opsomming

In die afgelope paar jare was daar beduidende navorsing en ontwikkeling in 3D gedrukte beton. Hierdie konstruksie tegniek vereis geen bekisting soos vir gewone bouprojekte nie. Die toevoeging van bymiddels verhoog die kompleksiteit van 3D drukbare mengsels in vergelyking met gewone betonmengsels waarin sement, water en aggregaat die belangrikste bestanddele is. In hierdie studie word gewone betonmengsels gebruik, om die kompleksiteit van 3D drukbare menge te verminder. Die doelwit is om gewone betonmengsels te druk, met beter boubaarheid. Drie tipes vinnige settingsgedrag is in hierdie studie getoets: valsset, vervanging van OPC-sement met BCSA-sement en flitsset.

Die studie is in twee fases uitgevoer. Die eerste fase is gebruik om die drie vinnige settings-mengsels te kenmerk. Druksterkte, ontwikkeling van hidrasie temperatuur, stettings tyd en druksterkte op vroeë ouderdom is getoets vir die karakterisering. In die tweede fase is die drie vinnige settings mengsels in 3D gedruk om die boubaarheid van die drie mengsels te bepaal. Benewens die boubaarheid, word die ekonomiese lewensvatbaarheid van die mengsels met 'n vinnige setting ontleed.

Daar is gevind, dat valsset nie die meganiese eienskappe van beton beduidend beïnvloed nie. Die toename in sterkte op vroeë ouderdom is nie so groot soos by flitsset of met die toevoeging van BCSA sement nie. Flitsset verbeter die vroeë ouderdom sterkte van beton, maar verminder die ontwikkeling van druksterkte in die langtermyn. Deur OPC-sement met BCSA-sement te vervang, word die vroeë ouderdom sterkte van die beton verbeter terwyl die meganiese eienskappe nie aansienlik beïnvloed word nie. Sement met hoër vervangingsyfers het die intensiteit van die flitsset meganismes verhoog, korter settye en hoër vroeë druk sterkte kon gemeet word. Uit die boubaarheidstudie is gevind dat flitsset ‘n positiewe impak op die boubaarheidseienskappe van 3D gedrukte beton het. Die boubaarheid het met flitsset met 321% verhoog. Die OPC sementvervanging met BCSA sement het 'n toename in boubaarheid van 214% tot gevolg gehad. Daar is bevind dat valsset die minste effektiewe vinnige set meganisme is, met 'n toename in boubaarheid van 35%. Flitsset en BCSA vervanging is koste effektiewe metodes om die boubaarheid van 3D gedrukte beton te verbeter. Valsset is te duur bevind, en die toename in druk sterkte op 'n vroeë ouderdom is min in vergelyking met die ander twee set meganismes.

Die doel van hierdie studie is bereik, deur die 3D druk van gewone betonmengsels met vinnig set eienskappe. Aansienlike verbeterings in boubaarheid kan aangebring word, en die vinnige setting van gewone betonmengsels is voordelig vir die vinnige konstruksie van 3D gedrukte komponente of strukture.

Kenwoorde: 3D druk van beton, flitsset, valsset, BCSA-sement, vinnige setting

Acknowledgements

I would like to thank the following people for their contribution towards the completion of this master thesis:

- My supervisors, Prof. Riaan Combrinck and Dr Pienaar Jacques Kruger, who guided, advised, and supported me throughout this research. Their assistance and ideas helped me develop the thesis to what it came out to be.
- My family, who always believed that education is the key to success and allowed me to attend university. They have always believed in me, supported me where they could and trusted that I can successfully complete my engineering degree.
- The laboratory and workshop staff of the Civil Engineering Department at Stellenbosch University, for assisting throughout this research.
- Pretoria Portland Cement, for providing me with the cement used in this study.
- Con van der Colff, for sponsoring the BCSA cement used in this study and providing guidance on its use.
- The National Research Fund, for funding the last year of my studies.
- All fellow master's students who supported me but most importantly made this an enjoyable time and became friends.

Table of Contents

Table of Figures

List of Tables

1. Introduction

1.1 Background and context

During the last decade 3D printing has found its way into modern society, including the construction industry. 3D printing of concrete is still a new subject within the public but has gained publicity and interest at research institutions. The method possesses many possibilities to change the industry and revolutionise construction methods. Reducing the formwork costs, labour cost, optimise construction time and environmental impact (Paul, van Zijl & Gibson, 2018). As with all new developments there are unknowns that are researched and will be resolved with time. The first 3D printed house in Germany has been completed recently in Beckum (PERI, 2021). This itself shows that the printing of concrete is a new process. Germany can be considered as a technologically advanced country and only recently the first building was completed.

There are differences between 3D printed concrete and ordinary concrete construction. In ordinary construction projects a typical three-step process is followed. Formwork is constructed, the required reinforcement is placed inside the formwork and finally the concrete is cast in the formwork. The first two steps are time and labour intensive which explains its major influence on the project cost. The concrete itself is only a small fraction of the overall costs (Han, Yang, Ding, *et al.*, 2021). This is where 3D printing becomes beneficial as it does not require any formwork for construction as the concrete is extruded in layers. Minimal labour is required as the entire printing process is automated. Formwork used in ordinary concrete construction projects typically becomes waste and is not recycled (Sanjayan & Nematollahi, 2019).

Formwork is not required for 3D printed projects and hence it positively influences the environment. On the other hand, 3D printing of concrete has complexities. The concrete used in such projects must meet several requirements. In a fresh state, the concrete must be pumpable and easily extrudable. Since subsequent layers are printed on top of each other, the concrete requires sufficient load bearing capacity. The rate of extrusion, print speed and print path length have to be adjusted to the concrete properties or vice versa (Paul *et al.*, 2018). Multiple admixtures are typically used to achieve the suitable properties for a 3D printable concrete mixture. With increased complexity of the concrete mixture, the production costs also rise (Han *et al.*, 2021). Ordinary concrete mixtures are based on three main components: Cement, aggregate and water. The concrete properties can be adjusted with admixtures to enhance or achieve project specific characteristics (Domone & Illston, 2010). To summarise, 3D printing requires a complicated mix design but is the simpler and more versatile construction technique. Ordinary construction on the other hand uses a simple concrete mixture but requires a more complicated setup process before casting.

A combination of the good characteristics of both construction methods would be the most feasible and effective construction techniques. 3D printing of ordinary concrete mixtures is

no novel approach and the printability of such mixtures has been proven (Van Der Putten, De Schutter & Van Tittelboom, 2019). None the less, further research on 3D printed ordinary concrete mixtures is required. The rheological characteristics of concrete determine the performance in 3D printing. Higher structuration rates improve the buildability of concrete. An ideal printable concrete mixture has a high static yield stress and a low dynamic yield stress. This allows for good pumping and extrusion but sufficient strength to withstand the load induced by above lying layers (Kruger, Zeranka & van Zijl, 2019). Rapid setting of ordinary concrete mixtures with an initial high flowability may be the solution to the problem. Printing an ordinary concrete mixture with good strength gain and printability characteristics saves costs without sacrificing mechanical characteristics. Phenomena such as false and flash setting may be induced to produce a rapid setting concrete. As far as can be ascertained no research has been done to determine if rapid setting ordinary concrete mixes can be printed and what advantages it would have to use such concrete. In conclusion, there is significant room for research with promising outcomes that could have a positive impact on the 3D printing industry.

1.2 Problem statement

This study aims to 3D print rapid setting ordinary concrete mixtures. To counteract the complexity of commonly used 3D printable concrete (3DPC) mixtures, this study uses ordinary concrete mixtures. A combination of an efficient construction technique with a simple ordinary concrete mixture merges the benefits of both, 3D printing and ordinary construction. Minimal admixture addition also ensures the simplicity of the mixture, but the standards set out by ordinary 3DPC mixes should still be met. The influence of rapid setting mechanisms on the concrete characteristics are to be determined as well as their impact on 3D printing. Little work has been done in the field of rapid setting 3DPC mixes which leaves many options and variables to investigate.

1.3 Aim and methodology

The aim of this study is to characterise the effect of rapid setting on the properties of concrete and to determine what influence rapid setting concrete mixtures can have on the buildability of 3DPC. The following methodology was followed to achieve the aim of this study:

1) Determine rapid setting mechanisms that can be induced in concrete

Ordinary concrete mixes are expected to have a slow rate of structuration as well as poor buildability. Rapid setting concrete is considered as a method to improve the 3D printing characteristics of ordinary concrete mixtures. A good understanding of how to induce these rapid setting mechanisms in concrete needs to be gained.

2) Understand the concretes characteristics that are influenced by the rapid setting mechanisms

A characterisation of the various mix designs is used to compare their influence on the properties of concrete. A 3D printable mixture as well as an ordinary concrete mixture are used as the benchmark for comparisons. The obtained results are compared to determine the influence of the rapid setting mechanisms on the properties of concrete.

3) Select the most suitable mixes for 3D printing

From the characterisation, the rapid setting mechanisms and their influence on the concrete's behaviour is well understood. By comparing these characteristics to the ones of the reference mix for printing, the most suitable and promising mixes for 3D printing are to be selected.

4) Print different mixes and compare to reference

The mixes selected during the characterisation for printing must be compared to the standard set out by the reference mix. The objective is to make all selected mixes printable. This may even require alterations to the mix design to change the rheological properties which in return results in better extrudability and placement characteristics. A comparison of the gathered results is used to determine the effect of the rapid setting mixtures and its influence on 3D printing of concrete.

5) Evaluate the economic feasibility of 3D printed rapid setting ordinary concrete mixtures.

The production cost of the current 3D printable mixes used is higher than for ordinary concrete mixtures. If ordinary cement can be printed, major savings can be made and resultingly construction of 3D printed structures becomes cheaper. Therefore, the feasibility to print rapid setting ordinary cement mixtures must be assessed.

1.4 Research significance

This study aims to characterise, and 3D print rapid setting ordinary concrete mixtures. By characterising flash setting concrete, false setting concrete and belitic calcium sulfoaluminate (BCSA) cement cement containing concrete, more insight can be gained regarding methods to induce such setting behaviours as well as the differences between these three setting behaviours. Identifying the influence of the rapid setting mechanisms on the fresh and hardened state properties of concrete will result in understanding the applicability of each rapid setting behaviour to different applications. 3D printing ordinary concrete can have a significant economic impact by reducing the production costs of 3D printable concrete and therefore the cost to print entire structures. In general, the rapid setting mechanisms can be used to obtain the aimed for buildability characteristics by dosing the additives accordingly. With the rapid setting mechanisms, buildability improvements can be made which allows for faster completion of structural components or entire structures.

1.5 Outline of thesis

Chapter 2 contains a review on available literature regarding 3D printing of ordinary concrete using rapid setting mechanisms. A specific focus is placed on the hydration of cement, factors influencing the characteristics of 3D printable concrete and the influence of rapid setting mechanisms on the properties of concrete.

Chapter 3 provides the experimental framework for this study. Information on the materials used in this study is provided and the tests conducted in this study are explained. Furthermore, the mix design development process for the various mixes use in the study is explained.

Chapter 4 shows the results obtained from this study. The first section discusses the results obtained during the Phase 1 characterisation of the various mixes studied. A comparison of setting time, hydration temperature, short-term compressive strength as well as long-term compressive strength development test results is used to select the most suitable mixes for the second phase. In the second section, the buildability characteristics of the selected rapid setting mixtures are compared, and the printability of these mixes is discussed.

Chapter 5 provides the conclusions drawn from this study and recommendations for future work are made.

Following on chapter 5, the references used to gain insight on the topic and analyse the accuracy of the obtained results.

In the appendices, all data gathered from the conducted tests in this study are provided.

2 Literature review

In this chapter, the literature regarding 3D printing of ordinary concrete using rapid setting mechanisms is summarised and discussed. Firstly, an overview on ordinary Portland cement (OPC) is given. The properties of OPC are discussed followed by a detailed discussion of the hydration process and its influencing factors. Secondly, the effect of various admixtures and additives are explained. Thirdly, an overview on 3D printing of concrete is given. The printing process is explained together with the critical characteristics required for good printability of concrete. In addition, critical issues regarding 3D printing are discussed. Lastly, different types of rapid setting cement are introduced. The hydration process is elaborated on these rapid setting concrete mixtures together with adjustments to be considered for when the properties need to be altered.

2.1 Ordinary concrete

2.1.1 Materials and production

In this section a brief overview on the main constituents of concrete and their production processes is given. Concrete is the most used building material in the world (McCarthy, 2008) and has an significant environmental impact. The production of cement contributes 8% to global pollution (Rodgers, 2018). This is a fact that cannot be ignored and must be addressed. On the other hand, concrete can be produced utilising waste material from other industries such as fly ash or recycled brick aggregate. Concrete can be cast into any shape, its properties can be adjusted according to its purpose, it is readily available and provides good strength and durability. All these properties make it an excellent building material suited for a wide range of applications (Zhang, 2011a).

Ordinary concrete has three main components. Namely Portland cement, water and aggregate. The quantities of these constituents vary depending on the application of the concrete. Additives are added to enhance or achieve the required properties or to reduce the production costs of the mix (McCarthy, 2008). More detailed information on the admixtures and supplementary cementitious material used in concrete is provided in the Section 2.2.

Ordinary Portland cement production involves the following steps. Limestone and clay are mined. In a crusher, the particle size is reduced to less than 80 mm (Cement Manufacturers Association, 2020). Several additives can be added to these main components such as shale, fly ash, iron ore or slag. This depends on the chemical composition of the limestone and clay which determines if certain components are sufficient. Additives, such as gypsum are added to make up for the deficit. The mix is then burned in a kiln at 1400 °C - 1500 °C. In a lengthy process the unwanted materials are removed so that only cement components remain. Finally, the burned products are milled to obtain the correct fineness which completes the cement production process. The entire milling and burning process uses vast amounts of energy. Coal is the most used fuel but natural gas, oil, or waste material such as tyres are also used. The emissions during the burning process of these fuels are enormous (Domone & Illston, 2010). Thus, researchers are trying to find ways to minimise emissions. Alternative

sources of energy for the cement production process are considered as well as fillers or cement replacement materials that can be used in concrete to reduce the cement content.

As the world population grows, water becomes a more and more scarce resource, increasing its costs. During 2012, 1.7% of the annually consumed water in the world was used for the overall concrete production process (Miller, et al., 2018). As a result, there is an urgent need for reduction of water usage during concrete production. Water does remain vital for the hydration and hardening process of concrete. Admixtures such as superplasticizers help reduce the required amounts of water for concrete production. Water is not only used for mixing of concrete but is essential for curing. In dry conditions, water evaporates from the concrete which reduces the amount of available water for hydration. Curing can be done by covering the concrete with plastic to avoid evaporation or by regular wetting of the concrete (Harrison, 2003).

Aggregate is volumetrically the main component of concrete. Concrete can contain aggregate in the form of sand and stone. Coarse aggregate or stone is classified by a diameter of larger than 4.75 mm and fine aggregate or sand has diameter of less than 4.75 mm. Aggregate is used to reduce the concrete production costs, improve durability and to decrease the effect of shrinkage or creep. Aggregate is generally locally sourced which then only requires sieving or crushing to attain the correct particle size. The type and shape of aggregate varies from region to region (Moir, 2003). Smaller aggregate sizes tend to be more uniform which improves the concrete strength. More rounded aggregate has less surface area which requires less the water to obtain the same workability as for angular aggregate (Lay, 2003). In 3D printing of concrete, it is unusual to make use of stone. Too large particles could damage the pumps of the printers which would then cause delays.

2.1.2 Properties of concrete

In this section, the properties of concrete are discussed. This includes the fresh and hardened state properties of concrete. Controlling the physical properties of concrete is essential to achieve the required strength and durability characteristics.

2.1.2.1 Setting time

The transition of concrete from a plastic to solid state is described as setting of concrete. During this process, concrete gains sufficient strength for it to hold its shape. Setting of concrete can be categorised in two phases. The first one being the period between addition of water to the cement and loss of workability. The second phase is between complete loss of workability and gaining mechanical strength. Higher or lower setting times are a result of faster and slower hydration rates respectively (Santhanam & Gettu, 2009).

Two tests are commonly used to determine the setting time of concrete, one being the Vicat apparatus and the other the penetrometer (*ASTM C403,2009 ; ASTM C191*, 2009). Both tests are based on the same principle and can be summarised as follows. Concrete gains strength with time and the sample becomes tougher to penetrate. Changes in resistance allow for a quantification of initial and final setting time. For the Vicat test, a needle with a diameter of

1 mm and an attached weight is used to penetrate the concrete sample. Initial set is found when the needle only drops 35 mm into the sample and final set when no penetration is possible. This test is commonly used to determine the setting time of cement paste and not of concrete. The setting time of concrete can be determined using a penetrometer. Different size needles are used to determine the force required to penetrate the concrete. With progressed setting, smaller plungers are used to reduce the physical force required to do the test. The required force measurements are converted to pressure to compensate for the different needle sizes. At 3.4 Pa, initial set is reached and at 27.6 Pa final set (Santhanam & Gettu, 2009).

2.1.2.2 Settlement and bleeding

According to Domone and Illston (2010) settlement is the process in which mix constituents separate and are found in different locations of the concrete batch. Larger particles settle downwards, and fine particles are left at the top of the concrete. A severe case of settlement is segregation. The separation of water from the concrete to the top is defined as bleeding. Both processes can happen together and are observed during or shortly after placement.

The water at the surface weakens the concrete because of the larger availability of water in the area. This produces an imbalance in strength between the top surfaces and the rest of the concrete (Domone & Illston, 2010). High shrinkage is another negative influence that is induced by segregation and bleeding (Jakuja, 2020). According to Jakuja (2020), segregation and bleeding are reduced in concrete that have higher yield stress and lower viscosity.

2.1.2.3 Workability

Good workability is important to be able to complete the placement process of mixing, placing, and vibrating the concrete. A loss in workability during one of these steps can cause defects in the concrete. A concrete with good workability has the following traits: Sufficient mobility to fill all gaps during casting and leaving no voids, good bonding between the concretes constituents and the ability retain the water contained in the mixture which allows it to hydrate correctly (Zhang, 2011a). Workability is therefore dependant on the consistence and cohesion of the concrete mixture (Diekmann, 2019).

The flow table test uses a similar principle as the slump-flow test and is designed for mixes with high to very high flowability. Flowability (consistence) is defined as the ability of concrete to flow. Typically wetter concrete flows more easily than dry concrete (Diekmann, 2019). In the slump-flow test a cone is filled with concrete and lifted. After agitation of the mix with a jolting mechanism. The flow diameter can be measured and compared to the specifications (Domone & Illston, 2010). The test also gives an indication on the segregation risk of the mix (Domone, 2003). In this study concrete is meant to be printed using a 3D printer. This requires a high flow concrete and makes the flow table test the more applicable as a flowability test (Cho, Kruger, Bester, *et al.*, 2020). The flow table test can be used as an indicative test to determine the workability of concrete. It provides insight on the consistence of the concrete and to a certain extent gives an indication on the cohesiveness of the mixture (Diekmann, 2019).

Concrete workability loss at early age can be a result of multiple factors. Higher surrounding temperature and higher cement content can cause a rapid loss in workability due to faster setting behaviour. Rapid setting behaviours induced by an imbalance of sulfate and aluminates may reduce the workability even faster (Domone, 2003). The aggregate and cement fineness impacts the concretes workability. Reduced cement particles size exhibits better cohesion and water retention characteristics. Smoother and well graded sand allows particles to move easier in suspension which improves the workability as well (Zhang, 2011b).

2.1.2.4 Rheology

Different concrete mixes have different flow behaviours. Rheometers are used to characterise the flow behaviour of fluids. A stress growth test is used to determine the static- and dynamic yield stress of the fluid. Using the measured data, the Bingham model can be used to describe the rheological behaviour of fresh concrete (Domone & Illston, 2010).

The plastic viscosity, the resistance of a fluid to flow freely, and yield stress of concrete reduces with increased water-cement ratio. Yield stress is the point at which a solid material starts to flow under force. A proportionality can be found between water-cement ratio and yield stress or plastic viscosity. Higher water content at constant cement content linearly increases the workability of the mix due to a lower yield stress and improved plastic viscosity. The addition of superplasticizer does not have the same effect. The effectiveness of the superplasticizer on the plastic viscosity reduces at higher dosage and the yield stress reduces in a linear pattern. Increasing the fines content using additives such as fly ash or silica fumes for example reduces the yield stress as well. The correct balance between yield stress and viscosity must be determined. Too little viscosity causes segregation or air entrainment which negatively impacts the concrete strength (Domone, 2003).

2.1.2.5 Compressive strength

The most important characteristic of load bearing concrete is strength. All other properties are unimportant if the structural integrity of a structure cannot be guaranteed. A cube test is commonly used to test the compressive strength of concrete. For 3DPC, the maximum aggregate size is less than 40 mm and 100 mm x 100 mm cubes are recommended. Cubes are tested at multiple intervals, typically up to 28 days after casting. After demoulding, the cubes are cured in water up to the test date. The compressive strength is determined by crushing the cubes using a hydraulic machine or a mechanical crushing device. A vertical force is applied on the cube and the failure causing force is recorded (Domone & Illston, 2010).

The compressive strength is strongly dependent on the water-cement ratio (Zhang, 2011a). Lower water-cement ratios lead to higher compressive strength. During the mixing process, a matrix of cement, aggregate and water particles is formed. Less water in the concrete reduces the voids and distance between cement particles. Better interlocking is possible because the hydrated cement grains are closer together. At a water-cement ratio of 0.43, sufficient water is available for the hydration of all cement particles (Domone & Illston, 2010).

Admixtures such as superplasticizers can be used to retain fluidity even at lower water content. Concrete with bad workability characteristics tends to cause compaction and placement issues. This weakens the concrete and reduce the compressive strength. The type of aggregate and cement used plays a role as well. More angular aggregate increases the presence voids that reduce the concretes strength. Higher quantities of cement or finer cement particles will produce higher strength concrete (Harrison, 2003). At high temperature, water evaporates from the concrete. In such conditions curing is important to ensure the availability for water from complete hydration (Zhang, 2011a).

2.1.2.6 Hydration and temperature effects

During the hydration of concrete, heat is developed in the different hydration stages. The reaction between cement and water is exothermic which means heat is produced. A typical hydration curve for concrete is shown in Figure 2.1.

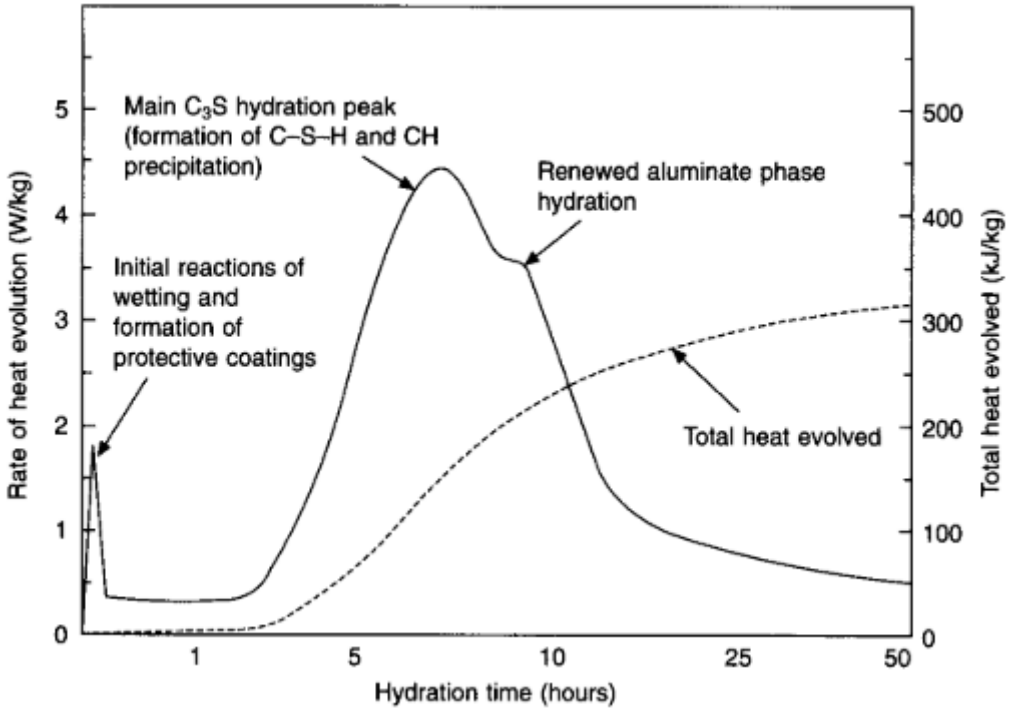

FIGURE 2.1 TYPICAL HYDRATION CURVE OF CONCRETE (MOIR, 2003)

After an initial rapid hydration phase, the rate of hydration slows down which is referred to as dormant or induction period. During these periods, the workability of concrete reduces rapidly, and initial set is reached. After three to five hours, the hydration rate accelerates again. In this period, the concrete rapidly gains strength and reaches final set. At last, the rate of hydration slows down which can be seen in the drop in heat evolution with time. The figure shows that the main hydration phase of concrete lies between 5 and 10 hours after casting. Depending on the hydration rate of a specific concrete, the hydration curve may be shifted for example due to a shorter dormant period for which the peak heat released rate will be reached sooner (Santhanam & Gettu, 2009).

Temperature rises inside the concrete as the hydration progresses and heat evolves. The temperature development inside concrete depends on the quantity of poured concrete, its cement type and content thereof, surrounding environmental conditions as well as the formwork used. Higher volumes of concrete cumulatively produce more heat and the same holds for higher cement content. The formwork used can have insulating properties which enhances a heat build-up inside the concrete because heat is not lost to the surroundings. The temperature between the inside of the concrete and the surrounding ambient temperature can differ greatly. As a result, stresses can build up between the outside and inside of the concrete and may lead to concrete cracking (Moir, 2003; Santhanam & Gettu, 2009).

Higher surrounding temperature results in a faster hydration rate but also reduces the long-term strength. Early age strength is improved with increased temperature because the rate of hydration is faster. As a result, the concrete gains strength more rapidly. Lower temperatures reduce the early age strength development but it has a less significant influence on the concrete strength than higher temperatures (Harrison, 2003).

2.1.3 Hydration process of Portland cement

The reaction between cement and water results in the setting and hardening of the mixture. By interlocking of reacted products (hydrates) and aggregate, the strength of concrete develops as more hydrates are formed. The overall hydration process can be categorised in four main reaction periods. These are the pre-induction, dormant, acceleration and post-acceleration periods (Taylor, 1997).

Beaudoin and Odler (2019) describe the hydration process as follows. The pre-induction period starts immediately when the water and cement are mixed. Tricalcium aluminate (C_3A), tricalcium silicate (C_3S or alite) and calcium sulphate contained in the cement dissolve as soon as the water is added. This produces an ion-rich solution with a high sulphate concentration. The alite reaction forms calcium silicate hydrate (C-S-H) and quickly a supersaturation of this product is found. During the reaction process the cement particles become surrounded with the C-S-H even though only 2%-10% of the C_3S have been dissolved. Due to the precipitation of the C-S-H particles around the cement grains, the hydration process is governed by the C-S-H precipitation and the rate of hydration reduces. Equation 2.1 describes the dissolution of alite in water.

$$CA_3SIO_5 + 3H_2O \rightarrow 3CA^{2+} + H_2SIO_4^{2-} + 4OH^- \quad (2.1)$$

A similar reaction process is followed by the dissolved C_3A. This hydration process is very fast and like for alite, controlled by the rate of C_3A dissolution. The dissolution of C_3A in water is shown by Equation 2.2. In ordinary Portland cement, free Ca^{2+} and SO_4^{2-} combined with the dissolved C_3A form an intermediate hydration product, ettringite (AFt). This product covers the cement particles as well, which once again slows down the rate of hydration.

$$CA_3AL_2O_6 + 6H_2O \rightarrow 3CA2^{+} + 2AL_3 + 12OH^- \quad (2.2)$$

Calcium hydroxide (C-H) is the secondary hydrate formed between C_3S and water. During the hydration of cement pastes, calcium hydroxide is mostly found in the form of portlandite crystals which are equally spread throughout the stiffened cement composition. C_3A is highly reactive and has a fast hydration rate. The rapid hydration can lead to a premature stiffening of concrete in the absence of calcium sulphate. This phenomenon is better known as flash setting and can be distinguished by an early high heat of hydration. The hydration reaction of calcium aluminate hydrate (C-A-H) is shown by Equation 2.3.

$$CA_3(AlO_3)_2 + 6H_2O \rightarrow CA_6(AlO_3)_2.6H_2O \quad (2.3)$$

To prevent this early age stiffening of the cement mix, gypsum is added to the clinker in the milling process. The gypsum may also be added in the form of calcium sulphate anhydrite or calcium sulphate hemihydrate (Beaudoin & Odler, 2019). Equation 2.4 describes the formation of Aft from C_3A, water and calcium sulphate.

$$CA_3(AlO_3)_2 + 3CASO_4.2H_2O + 26H_2O \rightarrow CA_6[Al(OH)_6]2(SO_4)_3.26H_2O \quad (2.4)$$

The hydration process slows down significantly within the first minutes after casting. This indicates the start of the dormant or induction period. The exact reason for this phenomenon is not known and multiple theories exist. During the dormant period, the mix loses workability even though the reaction process is slowed down (McCarthy, 2008).

Four different theories for the dormant period were described by Beaudoin and Odler (2019). The first theory for a dormant period is the impermeable hydrate layer. An oversaturation of C-S-H hydrate leads to the formation of a layer around the C_3S. The non-reacted C_3S is covered with hydrate which prohibits the reaction with water. As a result, the hydration is held up. During the dormant period two processes happen that result in a continuation of the C_3S hydration. As the C-S-H molecules age, the layer formed becomes porous and the water can reach the C_3S again. In parallel, an osmotic pressure builds up that prohibits the hydration. A breakdown or uptake of the layer through the pressure results in an acceleration of the hydration.

The second theory is of the Electric-double layers. The initial hydration of C_3A goes along with a dissolution process that produces a SiO_2-rich surface layer. This layer absorbs Ca^{2+}ions which produces an electric double layer that prohibits the entering of further water into the solution. The hydration slows down, and the induction period starts. With time a gradual perturbation of the electric double takes place, and the hydration accelerates again.

The Nucleation of $Ca(OH)_2$ is the third possible theory. During the initial C_3S hydration, $Ca(OH)_2$ dissolves. No calcium hydroxide is formed during this stage even under oversaturated conditions. This is referred to as the poisoning effect of the $Ca(OH)_2$ by the silicate ions produced during dissolution. Both, dissolution, and hydration, are slowed down which then is the start of the dormant period. Eventually, the $Ca(OH)_2$ concentration reaches such a saturation level that the poisoning effect is overcome. The hydration accelerates again which means that solid calcium hydroxide and C-S-H precipitates again.

The fourth and last available theory is the one of C-S-H Nucleation. In contrast to the other theories above, in this theory the product precipitated on the C_3S surface does not act as an obstruction. As the $Ca(OH)_2$ reaches saturation level, the formation of 'first-stage' C-S-H decelerates. The 'second-stage' C-S-H starts forming after the thermodynamic barrier is broken. None of the theories have been proven to be the single and correct reason for a dormant period. A combination of the above-mentioned theories may also be possible .

Three to twelve hours after the mixing process, the reaction rate starts to increase significantly again. The acceleration period is the 'main' reaction period in which the concrete significantly gains strength. The precipitation barrier is crossed and the hydration of C_3S gains in speed again. In addition, a second-stage formation of C-S-H takes place. In parallel with this, ettringite (AFt) is continuously formed. The rate of Aft formation in this case depends on the reactivity of the C_3A and $C_2(A,F)$. Hydrates containing less water molecules such as dihydrate or hemihydrate result in a faster reaction whereas anhydrite has a low reactivity. During this period the concrete sets and gains strength. As the hydration reactions progress, a decline in Ca^{2+} and SO_4^{2-} concentration can be found and all calcium sulphate in the mix becomes dissolved (Beaudoin & Odler, 2019). Equation 2.5 describes the dissolution of C_3S and the formation of calcium silicate hydrate, C-S-H.

$$2C_3S + 6H_2O \rightarrow 3\,CH + C_3S_2H_3 \qquad (2.5)$$

The final reaction phase is the post-acceleration phase. A decline in non-reacted material results in a decline in the rate of hydration. Beta-C_2S and C_3S still hydrate to form calcium hydroxide or calcium silicate hydrate respectively. The hydration of C_2S only starts at about 14 days after production. C_3S on the other hand hydrates to about 80% after 28 days (Moir, 2003). The quantities of calcium hydroxide formed are less due to the decline in belite concentration. After all available C_3S and gypsum is depleted, the ettringite reacts with C_3A or $C_2(A,F)$ to form monosulphate (AFm). The chemical equation for AFm formation is shown in Equation 2.6 (Danner, Justnes, Geiker, *et al.*, 2016).

$$C_6[AL(OH)_6]_2(SO_4)_3.26H_2O \rightarrow 3CaO.Al_2O_3.CaSO_4.12H_2O \qquad (2.6)$$

AFm is a stable hydration product that does not react any further. The limiting factor for the hydration process is the availability of water for dissolution or for hydration of C_3S. The hydration process is controlled by the permeation rate. In a scenario where enough water is available in the mix, the hydration process ends when all C_3S has dissolved and hydrated. With increasing age, the C-S-H molecules increase in SiO_4 chain length (Beaudoin & Odler, 2019). C-S-H is the main product produced during hydration. As the main hydrate, C-S-H hydrates contribute significantly to the strength of concrete. The hydrates have multiple chemical variations in composition and thus no exact molecule description is used. Thus, x and y in the chemical formula allow for this variation, shown by Equation 2.7. McCarthy (2008) points out that the Si/Ca ratio generally lies between 0.45-0.50. A variation between the 'first-phase' and 'second-phase' C-S-H exists. This variation can be found in its distinct silicate anion structures or their CaO/SiO_2 ratio (Beaudoin & Odler, 2019).

$$3CAOx.SIO_2 + xH_2O \rightarrow YCAO\text{-}SIO_2\ (x+Y-3)\text{-}H_2O + (3-Y)CA(OH)_2 \quad (2.7)$$

2.1.4 Factors influencing Portland cement hydration

The hydration and hydration kinetics of Portland cement depends on multiple factors. The overall hydration process depends on the suspension rate of the four phases described in the previous section, the rate at which hydrates are formed/growing and the diffusion of ions through the concrete mixture. These three factors can be mitigated in order to accelerate or decelerate the hydration proceedings (Beaudoin & Odler, 2019).

The most important factor regarding the hydration and strength of concrete is the water-cement ratio (McCarthy, 2008). Lower water-cement ratios yield higher strength if the mix remains cohesive during mixing. Finer cement particles and a higher specific surface result in more exposure to the water molecules which in return results in better hydration of the cement (Beaudoin & Odler, 2019).

As previously discussed, temperature influences the hydration of cement. The overall rate of reaction increases with rising temperature. Concrete mixed at higher temperature shows accelerated hydration (Domone & Illston, 2010).

The pre-induction phase hydration process can be accelerated with a higher reactivity of the silicates and aluminates. This can be induced with availability of K^+-ions and Nano-$CaCO_3$. Na^+-ions or calcium sulphate decelerate the hydration process. The quality of the alkalis determines their reactivity which in turn influences the hydration rate. Better quality products have a higher dissolution rate and lower quality, a lower dissolution rate (Beaudoin & Odler, 2019).

The composition and processing history of clinker plays a significant role in the hydration kinetics. Unwanted ions contained in the raw clinker as well as the burning conditions influence the reactivity of alite, the main influencing constituent on the hydration rate. In the cement production process, the clinker is burned, and it is essential that its behaviour can be predicted. This ensures that a good quality of cement can be produced and used by the consumer. Depending on the calcium sulphate proportions in the clinker, additional amounts may be added since the calcium sulphate regulates the setting times of the cement. Two types of mills can be used for clinker production, ball mills and rolling mills. Faster setting times can be observed for cement produced in ball mills. This is related to a calcium sulphate distribution that is less favourable in the hydration process. In the clinker produced in ball mills, the C_3S and C_3A exhibit a higher phase reactivity. Less decay of calcium sulphate dihydrate to calcium sulphate hemihydrate takes place (Beaudoin & Odler, 2019).

Apart from the clinker properties there are other factors that have an influence as well. The mechanical effectiveness of the C-S-H can be increased with the quantity of gypsum added to the cement. This was observed by Gauffinet-Garrault et.al, 2012, under the condition that the quantities of aluminates remained the same. Not only the quantity but also the form of calcium sulphate, which in most cases comes in the form of gypsum, plays an important role. A more soluble gypsum can delay the setting time much better than a less soluble one.

Some general factors playing a role are admixtures and the condition under which hydration takes place. This includes curing temperatures and curing conditions which may be in the form of air or water curing. It is vital for the hydration and hardening process that the surrounding environment doesn't reduce the water content in the mix due to dry conditions. Many admixtures or additives are available to alter the properties of cement mixes (Beaudoin & Odler, 2019). In a subsequent section, the effects of admixtures and additives are discussed in more detail.

2.1.4.1 Accelerated formation of individual hydration products

Calcium silicate hydrate (C-S-H) is the primary product of the reaction between C_3S and water. Alizadeh *et al. (2009)* studied what influence the addition of C-S-H seeds may have on the C_3S hydration. "Seeds" is a term used to describe the process in which pre-hydrated compounds are used to alter the hydration process. It was found that the addition of seeds has a significant accelerating effect on the hydration. Measurements taken in the study showed that the acceleration phase occurred up to 6 hours earlier than usual. This is a result of three effects. Firstly, the dormant period eradication due to the availibility of numerous nuclei that promote the hydration process. Secondly, more hydrates can grow simultneously which boosts the initial hydration. Thirdly, the consequences of the diffusion barrier as well as the volume taken up by C_3S are reduced which leaves more space for hydration on the dormant period and acceleration stage. Another accelerating factor is the addition of calcium carbonate to the mix, in the form of limestone. The effects have greatest significance in the early hydration phases. Smaller particles and higher dosages result in boosted reactions which is associated with a higher SO_3 content as well as an alteration of the hydrating C_3S surface and its nucleation (Beaudoin & Odler, 2019). An increased $\beta C_2S/C_3S$ ratio decreases the reactivity of alite. The addition of sulphate or metakaolin increases the reactiveness of C_3S. This acceleration leads to a quicker depletion of gypsum and an accelerated C-S-H formation (Zunino & Scrivener, 2019)

The hydration reaction of tricalcium aluminate varies with and without calcium sulphate. In the case where no or little calcium sulphate is available, plate-like AFm crystals are rapidly formed and flash setting occurs. Such setting behaviour can be noticed by heat development in the concrete during mixing. Beaudoin and Odler, 2019, suggest adjusting the availability of sulphates to the amounts of aluminates in the cement. The availability of sulphates can be influenced in two ways. Either too little quantities of calcium sulphate are available, or the available calcium sulphate does not dissolve fast enough. In both cases more aluminates than sulphates are available which causes flash setting of concrete. Aldonic acids, that form part of lignosulphonates, can be used to achieve the opposite, a decelerated reaction. On the other hand, the availability of calcium sulphate results in the formation of ettringite as a main hydration product. The occurrence of the dormant period is described as a result of the ettringite that forms a barrier around the C_3A. Calcium sulphate addition to the mix results in a decelerated rate of hydration (Beaudoin & Odler, 2019).

The reactivity and availability of C_3A influences the setting behaviour of cement as well. A higher availability of dehydrated gypsum (hemihydrate) than aluminates cause the formation of secondary gypsum, calcium sulphate dihydrate. The plate-like gypsum crystals formed interlock and cause false setting of concrete (Beaudoin & Odler, 2019; Moir, 2003). Figure 2.2 summarises the different setting behaviours that result from varying aluminate to sulphate rations.

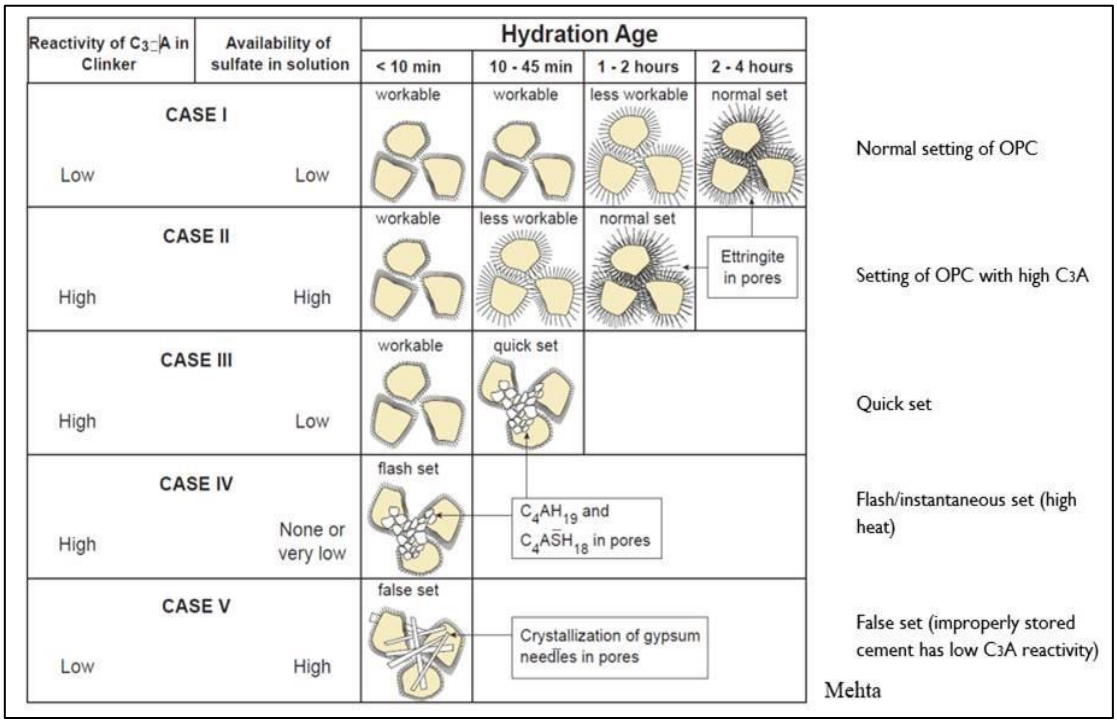

FIGURE 2.2 SETTING MECHANISMS DEPENDING ON THE C_3A AND SULPHATE AVAILABILITY (KUMAR MEHTA & MONTEIRO, 2014)

In contrast to the C_3S hydration, the addition of calcium carbonate restrains the C_3A hydration. An improved hydration reaction can be induced with the addition of calcium carboaluminate hydrate. A similar effect can be achieved with the addition of gypsum or calcium hydroxide. These additives delay the conversion of ettringite to monosulfoaluminate. Calcium carboaluminate produces a faster gypsum depletion which in return accelerates the hydration. The produced ettringite is transformed quicker to monosulfoaluminate, which is a stable hydrate formed by C_3A (Beaudoin & Odler, 2019).

The ferrite phases have varying configurations of calcium aluminoferrite (AFm/Aft) that lie between $C_2(A_{0.7}F_{0.3})$ and $C_2(A_{0.3},F_{0.7})$. Mixes containing lime and gypsum produce mostly Aft phases and without gypsum, AFm phases. The hydration process follows a similar pattern to that of C_3A. The reactivity of the calcium aluminoferrite depends largely on the iron content. Higher iron content reduces the reactivity and vice versa. As for C_3A, the addition of gypsum and calcium hydroxide decelerate the hydration of the ferrite phase. An accelerated ferrite phase can be achieved by elevated temperatures and smaller particle sizes (Beaudoin & Odler, 2019).

2.1.5 Physiochemical factors influencing cement hydration

Beaudoin and Odler (2019) described the influence of physiochemical factors on cement hydration. The setting of concrete happens due to the stiffening of multiple cement grains. Not the bridges between hydrated particles but the connections in between coagulated grains cause the hardening process. Ionic and electrostatic forces add towards the solidity of concrete.

Coagulation is defined as the change of a liquid to a solid. It is the first step that governs the setting of concrete. The bonds formed between particles are a result of interparticle attractions, physiochemical factors, that induce coagulation in the cement. Calcium ions produced during the dissolution of cement are essential for coagulation. A minimum concentration of calcium ions is necessary for coagulation to happen. An oversaturation on the other hand can hinder the coagulation process through dispersion of particles. This is a result of the calcium ions influence on the zeta potential of the mixtures particles. At a too low concentration of Ca^{2+}, the zeta potential of C_3S, C-S-H and the clinker is negative. This then causes a spreading of particles. At a medium concentration of 1-10 mmol/L Ca^{2+}, the zeta potential is small (<40 mV) and strong coagulation is possible. Peak coagulation rate occurs at a Ca^{2+} concentration of 4 mmol/L. The formation of an electric double layer (EDL) and van der Waals forces govern the coagulation process. The EDL creates long-range repulsive forces and the van der Waals forces governs the short-range stability.

As previously mentioned, the setting of cement/concrete is a result of strengthening of bonds between coagulated cement particles. The concrete starts to coagulate, particles are attracted to one another, which then cumulatively causes flocculation of the cement. Finally, the bonds formed start to rigidify, and setting occurs. Hydration products are not formed randomly but due to attractions between specific ions that bond to form a particular hydration product. The zeta potential of particles and coagulation is influenced by the availability of calcium ions. As discussed in Section 2.1.4, the type of hydration products formed is also influenced by the availability of calcium ions. This means that the availability of calcium ions is the main influencing factor for the setting behaviour of cement (Beaudoin & Odler, 2019).

The flocculation process, zeta potential, EDL and Stern layers are described and discussed in more detail in the sections to follow.

2.1.5.1 Flocculation

Flocculation is the process that describes the stiffening of the cement paste. It refers to the bonding and interlocking of hydrated cement particles with chain-like molecules. Bonds are formed between multiple particles and this results in large flocks (McCarthy, 2008). This phenomenon is caused by the zeta-potential and van der Waals forces. The process is reversible before the start of the dormant period. When the van der Waals forces and electrostatic repulsion are not counteracting, particles that are free in suspension can attract one another. Interparticle bonds can be created between particles and a stiffening of the mix

occurs. A lower electrical repulsive force allows flocculation to take place easier (Donaldson & Alam, 2008).

Deflocculation is particularly important for 3D printing. This helps with the process of concrete reagetation during the pumping process. The concrete needs to regain its fluidity and plasticity to be placeable and pumpable.

2.1.5.2 Zeta potentials

A particles electro kinetic behaviour is described by its zeta potential. The charge or potential of the particle determines how strong the coagulated particles are held together. Repulsion occurs if particles have the same charges. From Figure 2.3 the decreasing zeta potential with increasing radius can be seen where the charge development around a negatively charged particle and electric potential is depicted. Excluded from this diagram is a diffusion layer that lies to the right of the shear plane (Beaudoin & Odler, 2019).

The zeta potential determines the extent of coagulation. This potential varies and it is dependent on the amounts of calcium in the mix. Between 1-10 mmol/l of Ca^{2+}, a weaker zeta potential is produced, and coagulation is promoted. Well spread C_3S, C-S-H and clinker in the mixture produce low concentrations of Ca^{2+} with a corresponding charge of less than 30 mV. Higher Ca^{2+} concentrations increase the Ca/SO_4 ratio that determines the mediums zeta potential. Thus, independent on how the ions were sourced it dependents on the amounts of calcium and sulphate ions are available in the mix. The higher the Ca^{2+} concentration in the medium, the smaller the mean diameter of the particles formed. The particle zeta potentials are positive and large because of the increased calcium ions concentration (Beaudoin & Odler, 2019). Positive zeta potentials result in a better adsorption of superplasticizer onto the particle surface. An increasing water-cement ratio increases the zeta potential as the calcium to solids ratio is larger (Gauffinet-Garrault, 2012).

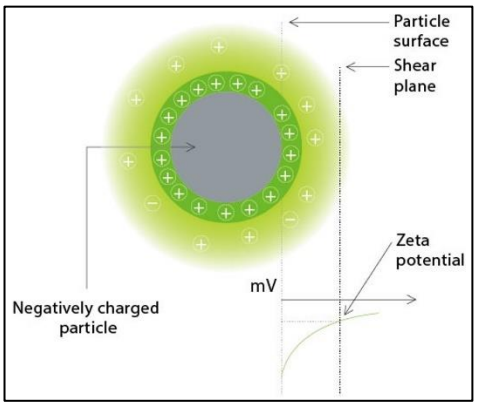

FIGURE 2.3 ZETA POTENTIAL MEASUREMENTS ON NEGATIVELY CHARGE PARTICLE (HORIBA SCIENTIFIC, N.D.)

2.1.5.3 Electric double layer (EDL)

Harrison *et al.* (2015) explain that during the mixing process of a concrete mixture, dissolution and adsobtion of ions occurs. This leads to different surface charges of particles that can either be positive or negative. These surface charges result in the formation of an electric field

that attracts their corresponding counterions. The electric double layer (EDL) is formed between the counterions and the charged surface. This is shown in Figure 2.4, for a negatively charged particle (Butt & Kappl, 2018). Two regions exist, the inner and the outer region. The inner region is formed by the adsorbed ions and the charged surface of the particle. The outside region ends where the electrostatic potential equals to zero. Shorter bonds can be formed at lower particle charges. Figure 2.4 shows a total potential energy diagram with ψ(r) being the sum of the repulsion (ψE(r)) and attraction curve (ψL(r)). The attraction of particles happens at the point of secondary minimum. The lower the potential at this point, the easier bonds can be formed.

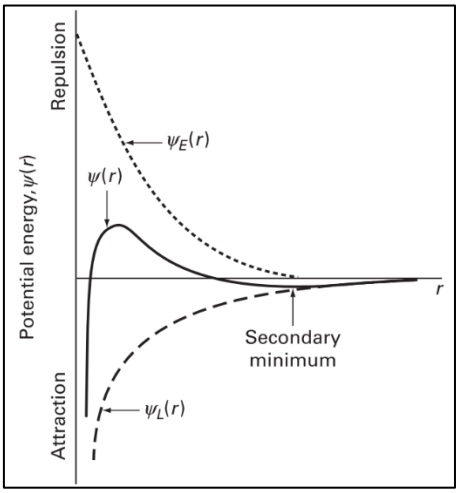

FIGURE 2.4 TOTAL POTENTIAL ENERGY CURVE (BUTT & KAPPL, 2018)

The EDL is described as a "cloud of ions of both signs". This layer has significant effects on the properties of a cement mix and regulates its rheological properties when no superplasticizer is used. These may be rheology, thixotropy, coagulation and flocculation, bleeding or even the adsobtion of superplasticizer. Synergy between EDL's is dependent on the diffusion layer and Stern layer (Harrison, Todd, Rudge, *et al.*, 2015).

2.2 Admixtures and additives

The fresh, hardened and chemical properties of concrete mixes can be altered with the addition of admixtures or additives. Their specific effects on the mix depend on the reactivity, size, and charge of the added material. Gypsum, limestone, fly ash all form part of the huge amounts of optional mineral additives that are used in concrete. Superplasticiser, accelerators, and retarders are admixtures added to concrete. Their addition depends on its purpose to change the properties of concrete (Danner *et al.*, 2016; Domone & Illston, 2010). In the following section different admixtures are discussed with a focus on their effect on the rate of hydration and rheological behaviour.

2.2.1 Admixtures

Superplasticizers are commonly used water reducing admixtures in concrete. It improves the workability of concrete mixes and can be used to reduce the water-cement ratio for concrete,

which reduces permeability and increases compressive strength. A water reduction of 12% - 30% can be achieved at dosages of 0.6 to 2.0% of cement. It is significant considering the amounts of water used in the construction industry and that water becomes a more and more scarce resource. A secondary retardation effect can also be induced with the addition of superplasticiser (Dransfield, 2003). Negatively charged superplasticiser is adsorbed onto the positively charged cement particles. This then wards off flocculation and reduces the amount of water captured inside the formed flocs. As a result, less water is required to obtain the same rheological behaviour (Burgos-montes, Palacios, Rivilla, *et al.*, 2012).

In this section, the various existing types of superplasticisers are characterised with their mode of action and effects on the mix.

2.2.1.1 Lignosulphonate based superplasticiser (LS)

The LS uses electrostatic repulsion as mode of action to disperse the water particles in the mix. LS is formed as a biproduct of the paper and pulp industry, which makes it a renewable and low-priced superplasticiser (Breilly, Fadlallah, Froidevaux, *et al.*, 2021). Burgos-montes et al. (2012) found that the LS was the least effective superplasticiser tested and produced the worst rheological outcomes. It is therefore often referred to only as a plasticiser and not a superplasticiser. The strongest adsorption was found for this plasticiser even though it has the lowest molecular weight. The LS only has a small electrical contribution due to its low zeta potential. The LS based plasticisers can be calcium or sodium based. No differences were found between these two types in terms of retardation. Only at 4% addition, a setback of gypsum dissolution and C_3A hydration is induced. No significant effects on the ettringite production in the mix were obtained by the addition of LS. Changes in the ettringite crystal shape from needle like to oval can be observed (Danner, Justnes & Geiker, 2015). Breilly et al (2021) found that through chemical alterations of the LS, the performance and properties can significantly be improved. The modified LS has the potential to be a renewable and cheaper alternative to the other petroleum based SP's, but further research is required to achieve a similar effectiveness.

Compatibility issues when using LS plasticiser occur when anhydrite is contained within the calcium sulphate used for the cement production. Anhydrite is the slowest dissolving calcium sulphate source, and the addition of LS reduces this rate further. As a result, the available sulphate to form ettringite together with C_3A is reduced. C_3A hydrates at higher rates and the aluminate phases are formed. This causes the cement mix to set much faster. Depending on the quantities of aluminate phases formed, flash setting can be found (Wang, Pang, Lou, et al., 2012).

2.2.1.2 Polymelamine based superplasticiser (PMS)

Electrostatic repulsion is the mode of action for the PMS. Compared to the other superplasticisers, the highest zeta potential can be measured for the PMS which can be referred to its strong electrical contribution (Burgos-montes *et al.*, 2012). Concrete mixes using melamine-based superplasticiser tend to segregate and exhibit bleeding. This is an

advantageous characteristic that can be used in mixes that have a high paste content (Dransfield, 2003).

2.2.1.3 Polynaphthalene sulphonate based superplasticiser (PNS)

PNS superplasticiser is produced by using sulphuric acid and naphthalene sourced from petroleum or coal tar in a polymerisation process with formaldehyde. Calcium and sodium are used to neutralise the product. In contact with water, sulphur trioxide and sodium are released which causes electrostatic repulsion when adsorbed onto cement particles (Dransfield, 2003). PNS has the largest molecular weight and displays the worst adsorption properties compared to the PMS, LS or PCE. The dispersive action is induced by electrostatic repulsion. With the addition of PNS superplasticiser, the zeta potential drops to strongly negative charge (Burgos-montes *et al.*, 2012).

2.2.1.4 Polycarboxylate ether superplasticizer (PCE)

The newest type of superplasticiser are the PCE's. Carboxylate ether groups of different lengths are fixed to the backbone sourced from acrylic acid. Depending on the ether side chain lengths the properties of the superplasticiser can be altered. In contrast to the other superplasticisers described, the mode of action for the PCE is the formation of a steric obstacle. Sodium dissolves off the ether chains, which results in a negatively charged particle. The superplasticiser can then bind onto the cement particles (Dransfield, 2003). The ether side chain length determines the effectiveness of the steric repulsion. The adsobtion process is less compared to the PNS, PMS or LS. Due to its minimal electrical input, the addition of PCE results in a zeta potential of close to zero. It was found that the PCE lowers the yield stress of concrete mixes effectively. Lower dosages of PCE are required than for the other SP's tested by Burgos-montes *et al (2012).* Krivenko et al. (2018) found a significant increase in compressive strength by adding 1% PCE and 2% Na_2SO_4. This effect was more influencial at early ages and 1.5 times higher compressive strength was measured after two days.

The molecular layout of the different SP's plays a significant role in the effectiveness of the type of SP used. A linear chain of hydrocarbon atoms forms the backbone of each PCE molecule. Ether and carboxylate side chains of the molecule vary in quantity and length. Alonso et al. (2013) were provided with some information on the SP's used in their study. All three types of superplasticisers had the same ether side chain length but different molecular weights and backbone length. Another important aspect is the carboxylate to ether proportion. A higher ratio means that more charged ether chains are available. The SP with the lowest carboxylate to ether ratio produced better repulsion. More ethers side chains reduce the yield stress of the mix more effectively at the same added dosage. Higher carboxylate to ether ratios or higher carboxylate contents produces better adsorption of the SP. The SP with the highest carboxylate to ether content was absorbed the best in the study (Alonso, Palacios & Puertas, 2013).

From this section it is evident that PCE type superplasticiser has the least potential to cause compatibility issues and that its plasticising action is the most effective.

2.2.1.5 Citric acid

Retarders are used to retain workability for longer time periods by extending the setting time of cement. Citric acid has been found to work well as a retarder for calcium sulfoaluminate (CSA) cements and belitic calcium sulfoaluminate cement (Nguyen, Kunther, Gijbels, *et al.*, 2021; Rosero, 2020).

Calcium sulfoaluminate cements form ettringite as the primary hydration product and monosulphate as a byproduct. Since the formation of ettringite is rapid, the formation of these hydrates must be retarded to retain workability over longer periods. Citric acid retards the formation of ettringite which ensures a longer period of good workability. Higher citric acid contents increase the retardation period further (Purnomo, Sumarni & Saputro, 2019). In addition to the increased setting time, the compressive strength was improved with citric acid (Nguyen *et al.*, 2021). At a content of 0.15% citric acid, the largest compressive strength improvement can be achieved for CSA cements (Purnomo *et al.*, 2019). The retardation effect results from a reduced dissolution rate of ye'eliminate, the main source of aluminates in CSA cement, that hydrates to form ettringite. The hydration with and without gypsum are shown in Equation 2.8 & 2.9.

$$C_4A_3S + 2CS + 38H \rightarrow C_6AS_3H_{32} + 2AH_3 \quad (2.8)$$

$$C_4A_3S + 38H \rightarrow C_6ASH_{12} + 2AH_3 \quad (2.9)$$

In the presence of gypsum, ettringite is formed. After depletion of available gypsum in solution, monosulphate is formed (El Khessaimi, El Hafiane & Smith, 2020). With the addition of citric acid, ye'eliminate hydration is prevented and neither ettringite nor monosulphate can be formed.

2.2.2 Mineral additives

2.2.2.1 Calcium sulphates

The hydration of cement is a rapid process if calcium sulphates are not added to the clinker. To prevent the fast setting of cement, calcium sulphates are added in the form of calcium dihydrate, hemihydrate, and anhydrite. As described in Section 2.1.3, the gypsum delays C_3A's rate of hydration by forming an intermediate product, ettringite. This allows for longer setting times.

The dissolution is directly influenced by the surface area of the gypsum particles added. More refined gypsum dissolves better and faster. This leads to a faster utilisation of the gypsum and can be noted by larger amounts of heat released. As a result, the overall hydration and hardening process is faster. Mixtures that form ettringite, exhibit lager yield shear stress at higher apparent viscosity (Bullard, Jennings, Livingston, *et al.*, 2011).

Depending on composition of the calcium sulphate source, the reactivity and hydration speed of the cement mix is influenced. The fastest rate of dissolution can be found for hemihydrate, followed by dihydrate and the slowest dissolution speed is found for anhydrite. Mixes

containing higher hemihydrate content display faster hydration speeds. In the same way, mixes containing higher anhydrite concentrations hydrate at the lowest rate. The best strength development can be obtained when gypsum (dihydrate) is used as the sulphate source (García-Maté, De La Torre, León-Reina, *et al.*, 2015).

2.2.2.2 Limestone

Another common component or additive in cement mixtures is limestone. It may be used as raw material for cement or as powder-based additive to the cement mixture. The carbon footprint of limestone production is much lower than for Portland cement. Thus, replacing cement with limestone has a positive environmental impact (Bentz, Ardani, Barrett, *et al.*, 2015).

An increased compressive strength is achieved when limestone is added at a low extent. The same holds for the yield stress. Minor amounts of limestone increase the yield stress but at larger doses these reverses. This results in a decrease in both yield stress and compressive strength. Melamine based superplasticizers combine favourable with limestone due to its highly negative charge. The addition of limestone results in a greater consumption of admixtures (Burgos-montes *et al.*, 2012). The smaller the limestone particle size, the better its influence on the concrete properties. Limestone in the form of calcite speeds up the formation of hydrates. Higher early age strength and resultingly reduced setting time was found for the addition of calcite. Higher compressive strength is achieved due to enhanced formation of hydrates in the presence of limestone (Bentz *et al.*, 2015). Ground limestone generally has varying particle size distribution. Varying sized voids between cement particles can be filled by the limestone particles and improve the particle packing density. This reduces the water requirements and improves durability of the concrete (Belov, Barkaya & Kuliaev, 2019).

2.2.2.3 Fly ash

During the burning process of coal in electric power plants, fly ash is produced as a by-product in fine power form. This pozzolanic material, exhibits cementitious properties when mixed with water. Together with lime and Portland cement, this mixture then has properties like those of a pure Portland cement mixture according to Lewis *et al.* (2003). Silicon oxide contained in fly ash reacts with calcium hydroxide to form C_3S and water as shown in Equation 2.10.

$$3CA(OH)_2 + SiO_2 \rightarrow 3CAO.SiO_2 + H_2O \qquad (2.10)$$

The reaction produces additional alite in the presence of calcium hydroxide which then hydrates to form C-S-H. Therefore, fly ash can be used as a cement extender. The addition of fly ash results in a better spread of cement particles which enhances the rate of reaction. Then again, the fly ash reaction described is limited during the first day of hydration. Depending on the replacement rate this retards the overall rate of reaction during the first 24 hours. Hereafter the rate of reaction is accelerated due to additional amounts of alite

available for hydration. The heat of hydration can significantly be reduced with the use of fly ash as cement replacement which then increases the setting time as well.

Other benefits are the improvement of compressive strength, easier pumpability as well as reduced segregation issues. The fine and well-rounded fly ash particles in a cement mix has the advantage that less voids are in the mix which results in a more fluid mixture. This also improves the overall quality of concrete by having a better surface finish (Lewis, Sear, Wainwright, *et al.*, 2003). Major rheological improvements can be made with the addition of fly ash. Less SP is required to get the same rheological properties due to a lower water demand to attain the same workability. Lower amounts of LS are required and more PMS and PCE according to Burgos-montes et al. (2012).

2.2.2.4 Silica fumes

Silica fumes are an offshoot of silicon metal or ferrosilicon alloys. The produced smoke during the burning process is filtered and collected as silica fumes. It is also classified as a pozzolan. Silica fumes are often used in high strength concrete (The Silica Fume Association, 2014). Silica fumes have a high specific surface area which causes an increased admixture uptake to achieve the same rheological properties. The very fine particles increase the water demand of cement mixes significantly. More water is required to achieve the same workability. The zeta potential in the mix can also be lowered with silica fumes (Rodriguez, 2019).

Strength improvements can be made with the addition of silica fumes. Similar to fly ash, a pozzolanic reaction takes place between silica fumes (SiO_2) and calcium hydroxide which precipitated from the reaction of C_2S/C_3S and water. Hydrates are formed which add to the strength build-up of the cement particles. The addition of silica fumes also increases the packing density of particles. Cement particles lie closer together and stronger bonds can be formed between the particles due to better interlocking of hydrates (Lin, Yan, Wang, *et al.*, 2019).

2.2.2.5 Sodium aluminate

As discussed in Section 2.1.4, the concentration of sulfate ions determines the type of hydration processes. Higher contents of sulfate ions cause false setting and lower contents flash setting. By increasing the aluminate content in the mixture, the sulfate ion concentration decreases. For this study, sodium aluminate ($NaAlO_2$) was used as source of aluminates.

Sodium aluminate has proven to be a useful accelerating admixture. The alite and belite hydration is accelerated with the addition of sodium aluminate (Andersen, Jakobsen & Skibsted, 2004). Han, Wang, Shi *et al.* (2014) found reduced setting times for mixes containing sodium aluminate up to 4% replacement rate. At higher dosages, no significant changes can be found. Quick setting time correlates with rapid early age strength gain. Contrarily, the addition of sodium aluminate reduces the long-term compressive strength of concrete.

Significant changes in hydration temperature development during the first 24 hours are induced with the addition of sodium aluminate. Higher initial peak temperature for higher contents were found during the pre-induction period. During the acceleration stage, the

hydration temperature was reduced. A lower temperature was measured for higher replacement rates. It is suggested that the hydration of silicate phases is prohibited and therefore the hydration temperature is reduced (Han, Wang, Shi, *et al.*, 2014).

In a SEM image analysis by Han *et al.* (2014), the main hydration product during the first 24 hours was found to be monosulphate (AFm). Sodium aluminate dissolves in water to form sodium hydroxide (NaOH) and aluminum hydroxide ($Al(OH)_3$). The presence of sodium hydroxide increases the dissolution rate of both calcium silicate and calcium aluminate allowing for a more rapid formation of their respective hydration products. Aluminum hydroxide forms AFm/AFt together with calcium sulphate and calcium hydroxide depending on the sulphate to aluminate ratio. At sulphate to aluminate ratios larger than three, AFt is formed else AFm (Han *et al.*, 2014). Overall, the quantity of AFm and C-A-H is increased with the addition of sodium aluminate. Reduced formation of ettringite was found as well (Andersen *et al.*, 2004).

2.2.2.6 Alkaline activation

Different approaches exist to enhance the reactivity of components contained in Portland cements. One approach that has shown promising results is the use of alkaline activation to accelerate the hydration process. Silicates and sodium carbonate are commonly used alkaline activators.

Krivenko *et al.* (2018) determined that an accelerated initial hydration is achieved due to interaction between the alkaline activator and gypsum dehydrate. The alkali activator binds onto the calcium sulphate which controls the setting behaviour of cement. Ettringite formation is barred by the unavailability of calcium sulphate and the rapid aluminate reaction takes place. Natural salts, such as Na_2SO_4 may also be used as alkali activator to control the rate of reaction. A 2% addition of natural salts by mass, produced a 30% increase in compressive strength after two days compared to the reference sample. The highest compressive strength gain was found for 5% replacement. The addition of alkali's increases the pH of the concrete which is good for reinforcement due to less corrosion (Krivenko, Sanytsky & Kropyvnytska, 2018).

The dosage of alkaline activator controls the rate of reaction. Higher contents result in a more rapid setting behaviour. In a study on Australian slag and different alkali activators, it was found that sodium silicate had the greatest effect. Shorter setting times were found for increased sodium contents (Bakharev, Sanjayan & Cheng, 1999).

Depending on the cement composition, some alkaline activators are more suitable than other. In principle, the alkaline activator is used to change the cement composition which induces a distinct setting behaviour. Not all cements have the same composition so different alkaline activators work better for different cements.

2.2.3 Conclusion

Cement hydration is dependent on psychochemical factors as well as interparticle interactions. These influence the hydration behaviour but can also be used to manipulate the

hydration process. The concentration and effectiveness of calcium sulphate can be seen as the basis to control the hydration of cement. Admixtures and mineral additives are used to improve, prohibit, or alter certain hydration steps to change the rheological and mechanical characteristics of cement. In addition, external factors such as temperature also impacts the cement hydration.

2.3 3D Printing of concrete

Within the last decade the development of a new construction technique has made significant progress, namely 3D printing of concrete. This construction technique is versatile as different materials can be used and the design possibilities are almost unlimited in form and shape (De Laubier, Wunder, Sven, *et al.*, 2018). This method is commonly used in manufacturing of plastic parts, but the development of concrete printers has made significant progress. This development and progress have come so far that the implementation of this method in industry has taken place. Many issues in the current construction industry can be addressed by using 3D printing (Kruger, 2019). A more economical use of the materials, lower labour cost and faster construction periods are the main benefits (Bentz, Jones, Bentz, *et al.*, 2018). CAD models are generally used to prescribe the printing path, this allows for more complicated shapes due to no formwork requirements and unlimited mobility of the nozzle (Paul *et al.*, 2018). As with every new technology, many unknowns and variables need to be determined and quantified in order to ensure a viable and safe construction method. Within this section the important aspects regarding material use and physical behaviour of 3D printable mixes are discussed.

2.3.1 Process

The 3D printing process is quite simple to understand. A concrete mixture is produced with suitable properties for its function. These properties cover multiple aspects such as pumpability, extrudability, shape retention or thixotropy. Only if all these properties are right, the printing of concrete is possible. The concrete is pumped through a pipe which is connected to an automated control mechanism that allows for accurate placement. The arm movement is prescribed by the CAD model for the specific project. Placement happens in thin successive layers at a specified rate. Free movement of the arm within the projects boundaries allows for increased complexity of the structures shapes, since no formwork is required for the layering process (Paul *et al.*, 2018).

Paul *et al.* (2018) summarised the different types of available 3D printer types as follows. The exact method of printing varies with the type of printer and nozzle. Printers generally are one of the following three types. Gantry printers, a rectangular frame in which the nozzle is mounted moves horizontally and vertically inside the frame. The size of such printers is not limited by the size of the project. The frame is erected outside the structures boundaries which allows the structure to be printed on its inside. Crane printers look very much like the lifting cranes used on most large construction sites. A central position of the cranes allows for smaller cranes to be used. The printing process happens by rotation of the crane and upwards

movement with each layer. Robotic printers function in a similar way. A freely movable arm moves the nozzle that extrudes the concrete.

The printing speed and type of nozzle varies largely. The printing speed needs to be maximized to ensure efficiency and reduce the open time of concrete. 3D printable concrete requires a certain amount of open time to ensure shape retention when layers are placed above. This also varies with the nozzle type used. Circular, square, rectangular or ellipse shapes can be used. A large variety of sizes for these shapes have been used and tested. Their size varies with the properties of the concrete printed and the type of tests/projects (Paul *et al.*, 2018).

A 3D printable concrete mix must be pumpable. The concrete needs to be extrudable without any signs of segregation and retain its original printed shape. This is achieved with a highly viscous cement mix, which in return increases the pressure required to pump the concrete. One can also use accelerators to enhance the setting mechanism of less viscous mixes. Another important factor is the formation of a smearing layer inside the pipe that ensures good pumpability (Bentz *et al.*, 2018; Paul *et al.*, 2018).

2.3.2 Constituents of 3D printable concrete

The designing process of a 3D printable mix is more complicated than for ordinary concrete mixes. Additives and mineral admixtures are used as supplements to obtain the correct rheological properties. Three different mix designs are tabulated in Table 1 below. All mixes have similar constituents, but the quantities vary. This shows what adjustments are required to produce a 3D printable mix. Typical 3D printable concrete mixes have low water-cement ratios of 0.23-0.41 (Paul *et al.*, 2018). For this study, ordinary concrete is considered as printable material. Higher water-cement ratios are expected to retain pumpability and extrudability.

TABLE 2.1 DIFFERENT MIX DESIGNS FOR 3D PRINTABLE CONCRETE

Mix design by	Cement (kg/m^3)	Sand (kg/m^3)	Water (kg/m^3)	SP (kg/m^3)	Fly-ash (kg/m^3)	Silica fumes (kg/m^3)	Fibres (kg/m^3)	Other
Kruger, (2019)	579	1167	261	1.48% by mass of binder	165	83		VMA (0.13% mass binder) & Nano-particles (varying)
Narrela et al., (2019)	430	1240	180	10	170	180	-	-
Le et al., (2012)	579	1241	232	16.5	165	83	1.2 (PP)	-

2.3.3 Rheological properties

The physical properties from fresh to hardened, all form part of the spectrum of rheological properties. Pumpability, interlayer bond strength, extrudability and buildability are part of the fresh state properties that can be estimated by their shear strength, open time, green strength, or viscosity. All these measurements give an indication to whether the mix is printable or not and if the requirements can be fulfilled (Paul *et al.*, 2018). Different measurements can be taken to establish these properties and are elaborated on in this section.

Paul *et al.* (2018) define the term shape retention as the ability of a concrete mix to keep its initial shape or form after placement. Each layer is placed with a specific width and thickness. Under the load of successive layers, the deformation must be minimal to ensure structural integrity. The printed layer must gain sufficient strength to avoid deformation.

The time between mixing and initial setting is referred to as open time. For 3D printable concrete it is vital that this period is long enough to ensure that the mixture does not set in the pipe during placement. Such setting can result in blockage of the pipe or at the nozzle. Too rapid setting before placement of the following layers leads to cold joints. The Vicat apparatus can be used to establish the setting time of a concrete mix (Paul *et al.*, 2018).

In ordinary concrete mixtures the green strength is of little importance. There is enough time for the concrete to harden before any loads must be carried. For 3D printable concrete this is different. A new layer is placed on top of another in a certain time interval. This means that the mix must gain or have enough strength during this period to sustain the load placed on top and retain its shape (Paul *et al.*, 2018). Measurements for the green strength can be done with the uniaxial unconfined compression tests (UUCT). Concrete cylinders are tested at different time intervals and the strength development over time can be plotted (Wolfs, Bos & Salet, 2018).

A concrete mix can be classified as pumpable when it does not lose its fresh properties under the force of a pump. A sliding pipe rheometer can be used to quantify the pumpability of the mixture (Paul *et al.*, 2018). Concrete mixtures with low yield strength and low viscosity are typically easily pumpable (Muthukrishnan, Ramakrishnan & Sanjayan, 2021). The required material for 3D printing needs to be easily flowable to reduce the required pressure for the pumping but needs to be stiff enough at the point of extrusion to retain its shape. Mixes with ample amounts of paste and strong enough interparticle bonding between the components are compatible for printing. A smearing boundary layer on the wall is developed in the pipe and bleeding under the pumping pressure is prohibited (Paul *et al.*, 2018).

Extrudability refers to the ability of a material squeezed out of a pipe, through a nozzle and into the desired position. A thixotropic 3D printable concrete mix is pumpable and retains its shape after placement. The term thixotropy is explained in more detail in the Section 2.3.4. Agitation of the concrete mixture by the pump breaks the formed structures and it reflocculates after extrusion. It may also be the case that the material does not reflocculate

rapidly but that its viscosity is of such a nature that it retains its shape. Issues that may be encountered with the extrusion process are blocking or bleeding due to smaller nozzles than the pipe or partitioning of the mix components (Paul *et al.*, 2018).

The buildability of concrete is linked to its green strength. The concrete layers need to support subsequent layers on top. Minimal deformation and no collapse are vital for numerous layers to be printed on top of each other. Ordinary concrete is cast into formwork and does not have to be self-supporting until it reaches enough strength. As described by Paul et al. (2018) different approaches can be used to enhance the buildability of 3D printable concrete. A change in nozzle type towards a lager contact area or adding supports to the printed layers with other layers. This may be done with a zig-zag pattern between two straight layers. The deformability of concrete can be tested with a slump cone.

The environment in which the concrete is printed in, plays a significant role. Increased temperatures can affect the rheological properties negatively. An additional factor is the rate at which the layers are printed. More time means that hydration can progress which results in a better buildability (Paul *et al.*, 2018). Kruger (2019) proved that an increased SP dosage increases the workability and flowability of concrete significantly, which in return decreases the buildability of the material due to its self-compacting concrete like behaviour. The addition of 1% nano-silica proved to increase the buildability of the mixture as well as a increased rate of hydration. This was noted in a reduced setting time. Both are important characteristics to produce 3DPC.

2.3.4 Thixotropy

For a concrete mixture to be printable and meet the required rheological properties, it needs to exhibit a thixotropic behaviour. This means that at rest, the material stiffens up but through agitation it regains it fresh properties. Such behaviour is ideal for 3D printing of concrete because less energy is required for pumping, but after placement the concrete preserves its shape. These characteristics are scientifically described by the rate of structuration (A_{thix}) and re-flocculation rate (R_{thix}) described by Kruger (2019). The buildability of concrete is dependent on its thixotropic behaviour. After placement, the concrete needs to regain strength for it to be able to carry the load of the above lying layers. The higher this strength is, the more layers can be printed in succession which means that the material has a better buildability (Kruger, 2019).

From a rheological perspective the yield stress development under stress determines its suitability for 3D printing. A balance between a high static yield stress to ensure buildability but a low dynamic yield stress so that pumping does not require too much energy is essential to the properties of 3D printable concrete. The stress development over time under a constant shear rate for a thixotropic material is shown in Figure 2.5. An external force is applied to the mix to reagitate and transfer the material, in general done with a pump. The bonds built during the flocculation process are broken and the viscosity of the material decreases. At the point where the static yield stress is overcome, the material becomes

flowable and the yield stress drops significantly up to the dynamic yield stress. The material has become fully flowable and the lower this value, the less energy is required to pump the material, but it also prevents segregation due to too much force on the material.

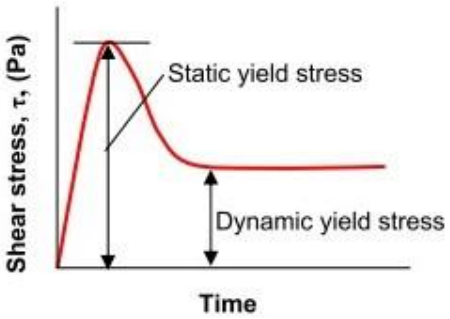

FIGURE 2.5 STATIC AND DYNAMIC YIELD STRESS DEVELOPMENT OVER TIME (Germann Instruments, 2010)

A thixotropic material used for 3D printing needs to regain its stability very quickly through re-flocculation to prevent concrete run-off from the printed position. The initial flocculation occurs due to attractive Van der Waals forces whereas the re-flocculation is a result of Brownian motion that rebuilds the particle bonds. As soon as the material is not agitated anymore, a rapid re-flocculation of the material that is characterised by a change in shear stress from dynamic to static (Kruger *et al.*, 2019; Mewis & Wagner, 2009).

2.3.4.1 Particle interactions

This behaviour is a result of multiple psychochemical particle interactions which are described in Section 2.1.5. The combination of attractive Van der Waals forces, particle electrical potentials as well as the effects of Brownian motion, weakening with increasing particle size, are the dominating factors leading to a coagulation of particles. Coagulation occurs when the maximum attractive forces, primary minimum in Figure 2.6, are present between particles. As this bonding effect is rather unwanted and the more favourable flocculation, secondary minimum, should be induced. Electrostatic, steric and polyelectrolyte stabilisation can hinder coagulation and produce the less strong flocculation bonds (Kruger *et al.*, 2019; Mewis & Wagner, 2009).

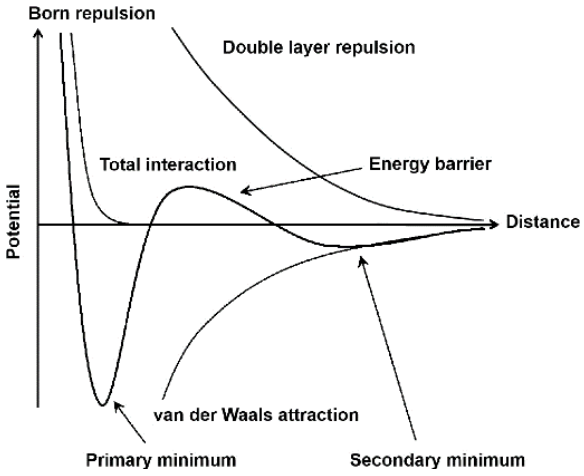

FIGURE 2.6 ELECTROSTATIC STABILISATION POTENTIAL ENERGY CURVE (KATERYNA LOZA, 2019)

According to Kruger (2019), electrostatic stabilisation is caused by the interaction of two particles electric double layers. The overall electric potential reduces, total interaction, which results in increased distances between particles. At greater interparticle distances a secondary minimum is developed. Flocculation occurs and coagulation is prevented. The attraction intensity depends in the depth of the secondary minimum. The buildability performance of 3D printable concrete benefits from stronger flocculation.

The adsorption of macromolecules on the surface of particles brings about steric stabilisation. These macromolecules are surface tension reducing surfactants or non-ionic polymers. Anchoring of particles can happen as tails type, loop type or as a combination of these anchoring types. For the tails type, the particles are connected at its ends whereas for the loop type the anchoring can happens at multiple positions along the length of the particle's backbone. A repulsive force is the result of the synergy between the particle layers. The forcefulness of flocculation depends on the depth of the electrostatic energy developed between the particles. In contrast to electrostatic stabilisation, steric stabilisation only leads to a single potential minimum. A too great potential minimum value can lead to a coagulation as a type of bonding and should be avoided.

Polyelectrolyte stabilisation disperses particles through electrostatic and steric effects. Naphthalene Sulfonate Formaldeyde (NSF) or Polycarboxylate Ether (PCE) superplasticisers can be used to create the dispersive effects. The exact functional details are described in the Section 2.2.1. Dosing of the superplasticiser is important to ensure that flocculation and thixotropic behaviour of the material is present, but that no coagulation happens or that the V_{min} is zero which leads to no flocculation (Kruger, 2019).

2.3.4.2 Effects of nanoparticles on thixotropic behaviour

Kruger (2019) found that the addition of nanoparticles produced significant results and its effectiveness is undoubtably. At typical particles sizes of nanoparticles of 100 nm, the particle interactions are impacted, and rheological improvements can be made. Gravitational and inertia forces are dominated by Van der Waals and polyelectrolyte forces as well as Brownian motion. This means greater re-flocculation rates due to improved Brownian motion can be achieved and the stronger flocs are created measurable at higher yield shear stresses. These are advantageous effects for 3D printing of concrete, stronger and faster bonding after placement.

Due to the large specific surface ratio of nanoparticles, more stiff and viscous mixtures can be produced. The synergy between particles and physical particle properties are boosted due to the greater available surface. Increased flocculation and structuration rates (A_{thix}) are important characteristics of 3DPC. The re-flocculation rate, R_{thix}, describes the rapid rebuilding of shear stress capacity in a few hundred seconds after removal of the agitating force. As mentioned before, the interchange between dynamic and static shear stress is important for 3DPC to be pumpable but also to be able to create a structure. The rate of structuration, A_{thix}, is measured over a longer period and is affected by hydration, accelerators, retarders and so forth. The rheological measurements taken are the same as for

R_{thix}, but the external effects differ. To characterise thixotropic material behaviour, the use of R_{thix} is recommended by Kruger as it characterises the immediate properties of the concrete mixture (Kruger, 2019). Both A_{thix} and R_{thix} are discussed in the following section in more detail.

2.3.5 Buildability

Concrete with good buildability characteristics gains yield strength rapidly over a short period. Two methods are typically available to improve the buildability characteristics of 3D printable concrete. One method uses small batches of concrete that exhibit rapid strength gain and continuously mixing new batches during the printing process. The other uses admixtures to induce rapid strength gain by adding these at the nozzle (Muthukrishnan *et al.*, 2021).

In 3D printing, the bottom layer is considered as the critical layer for failure. Two failure modes are typical for 3DPC: elastic buckling or plastic failure. A combination of both these failure modes is also possible. Plastic failure is caused by too high stresses induced in the bottom layers by the above lying layers that cause yielding of the material. Elastic failure may be caused by too low stiffness of concrete, irregular or skew placement of layers or a combination of both. Such failure mechanisms can be prohibited with increased yield stress capacity. This once again can be achieved in two ways (Muthukrishnan *et al.*, 2021; Suiker, Wolfs, Lucas, *et al.*, 2020). Firstly, the thixotropic behaviour of the concrete can be improved by accelerating the re-flocculation rate. Secondly, the strength gain of the concrete is accelerated with admixtures (Muthukrishnan *et al.*, 2021). Figure 2.7 displays typical failure modes encountered in 3D printing of concrete.

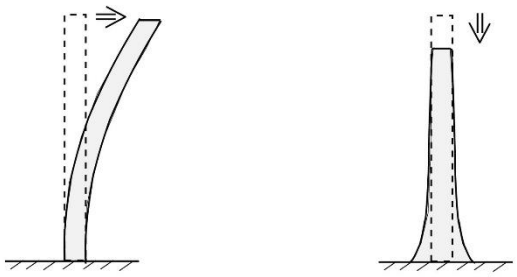

FIGURE 2.7 FAILURE MODES OF 3D PRINTED CONCRETE SEGMENTS (SUIKER *ET AL.*, 2020)

Kruger *et al.* (2019) proposed a novel bi-linear thixotropy model for 3D printable concrete in Figure 2.8. The model assumes that the re-flocculation process only commences after deposition of the material and stoppage of agitation. Completion of re-flocculation is achieved when the material regained its static yield stress capacity. R_{thix} describes the rate at which the static yield stress is regained. After this yield strength capacity is reached, the structuration of the material starts and is described by A_{thix}.

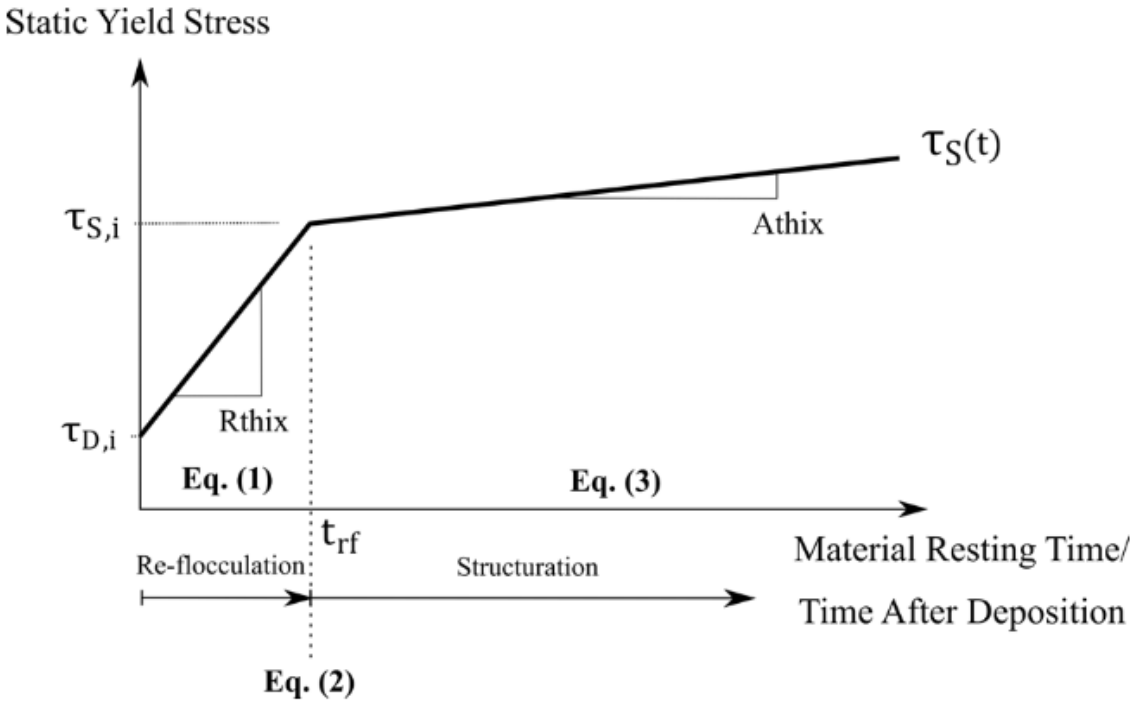

FIGURE 2.8 YIELD STRESS DEVELOPMENT OVER TIME (Kruger *et al.*, 2019)

The mathematical equations of this model describe the development in yield stress capacity. This model holds for both thixotropic and non-thixotropic materials. For non-thixotropic materials the R_{thix} value is zero and thus static yield stress equals dynamic yield stress. Equation 2.11 describes the yield stress development after the force on the material is removed and the re-flocculation starts.

$$\tau_s(t) = \tau_{D,i} + R_{thix} * t \qquad (2.11)$$

The variables being:

$\tau_S(t)$ - Static or apparent yield stress varying with time (Pa)

$\tau_{D,I}$ - Materials initial dynamic yield stress (Pa)

R_{thix} - Re-flocculation rate (Pa/s)

t - Time after agitation was stopped (s), where: [$t \leq t_{rf}$]

The findings made by Kruger (2019) show that too little SP induces coagulation because of a deep electrostatic potential minimum (V_{min}). At higher SP dosages, the V_{min} depth is reduced and found at a greater distance away from the particle centre. As a result, for 3D printing of concrete favourable flocculation occurs. Great care must be taken with regards to the dosage of SP. Too much can move the V_{min} too far away from the particle and weaken the van der Waals forces to such an extent the re-flocculation rate is lowered. This was proven in the study by Kruger (2019) with an addition of +15% SP. Increased flocculation rates were found for the addition of 1% nano-silica but decreased at 2% addition. These findings prove that

there are fine margins of additive addition that need to be determined for optimised 3D printing.

After the initial static yield stress is reached, the structuration of the material is launched. The yield stress at any point in time can be calculated with Equation 2.12. Once again, a linear model describes this behaviour. All variables can be measured with rheological tests.

$$\tau_S(t) = \tau_{S,i} + A_{thix} * (t - t_{rf}) \quad (2.12)$$

The variables being:

$\tau_S(t)$ - Static or apparent yield stress varying with time (Pa)

A_{thix} - Structuration rate (Pa/s)

t - Time after agitation was stopped (s)

To solve Equation 2.12, the value for t_{rf} must be determined using Equation 2.13. All variables once again can be obtained with measurements on the material.

$$t_{rf} = \frac{\tau_{S,i} - \tau_{D,i}}{R_{thix}} \quad (2.13)$$

The variables being:

t_{rf} - Re-flocculation period length

$\tau_{S,I}$ - Stress increase (s)

$\tau_{D,I}$ - Materials initial dynamic yield stress (Pa)

The information gathered in the rheological testing can be used to predict the buildability of a concrete mix. With increasing number of printed layers, the stress induced on below lying layers also increases linearly. The rate at which the stress increases is dependent on the speed of printing and is known as the building rate. By combining the building rate and the rheological model in Figure 2.8, one can determine the buildability of a concrete mix. At the point where the stress induced by the printed layers is higher than the yield stress of the material, failure is predicted to occur. More successive layers can be printed for a material with higher buildability (Kruger, 2019).

A practical buildability test can be used to obtain the actual buildability of a material and compare it to the results from the theoretical model. As many as possible layers are printed until failure is reached. A plastic failure mode is required to verify and compare the results from the model. Two aspects must be considered for plastic failure to happen. The first one being the printed shape. A structure with the same moment of inertia in each direction is preferred so that no weak axis buckling can occur before plastic failure of a printed layer. Therefore, a circular column is selected as printing shape because it has the same moment of inertia about all axes. The second factor is the rate at which layers are placed. At a too low rate, the concrete structurates too fast and no failure occurs. The placement rate is

dependent on the printing path length and printing speed. By adjusting both parameters, one can ensure that plastic failure occurs. A print speed of 60 mm/s and a circumference of 785 mm were prescribed as a good starting point for the buildability test (Kruger, 2019). Adjustments to these parameters can be made in accordance with the project parameters.

2.3.6 Mechanical properties

The mechanical properties of 3D printable concrete probably provide the most important topic of research in the field. Researchers aim to reach and exceed the properties of ordinary concrete to make 3D printing a more competitive construction technique. The following section discusses the current state of research on the mechanical properties of 3D printable concrete.

2.3.6.1 Compressive strength

The compressive strength of concrete mixtures is dominated by its water-cement ratio and the use of large aggregate such as stone. The curing conditions and air content have a significant impact on the outcome of the compressive strength tests as well as any form of defects in the samples. These defects may be damages but also segregated particles in the mix. It is also important to note that the testing direction plays a significant role. For normal concrete cubes, this effect is less significant but for 3D printed concrete mayor differences between the testing directions can be found. Higher compressive strengths are measured perpendicular to the layers compared to testing along the layers/joints (Paul *et al.*, 2018). The printed shape also influences the compressive strength characteristics. A lower strength loss was found for straight-line printed shapes than for curved printed shapes (Le, Austin, Lim, *et al.*, 2012).

2.3.6.2 Interlayer bond strength

When casting ordinary concrete structures, the time gap is minimised to ensure that no cold joints are formed and bonding between the different pours is ensured. The same holds for 3D printed concrete and is one of its critical characteristics. Better bond strength between filament layers can be achieved by reducing the time intervals while printing the layers. Hydration between particles of different touching layers, creates an anchoring effect and thus a better bonding (Paul *et al.*, 2018).

Reinforcement between layers, coarseness of the printed surface, cracks, compressive strength of the concrete sample or the effects caused by normal forces on the conjunctions of the layers are factors influencing the interlayer bond strength. The forces induced between layers are a consequence of different shrinkage processes of the layers (Paul *et al.*, 2018). The correct balance must be found between bonding of layers and buildability. Sufficient time is required for strength gain but can cause interlayer bond strength problems if the hydration progressed too far (Le *et al.*, 2012). The interlayer bond strength is affected by the availability of moisture between layers, roughness of the surface, air entrapment or adverse thixotropy. It is noteworthy that the bond strength between layers is significantly weakened by pass times, time between successively printed layers, longer than the initial setting time (Moelich,

Kruger & Combrinck, 2021). This means that too rapid setting behaviour could induce interlayer bond strength problems as the initial setting time is short and may be close to the pass time.

2.3.6.3 Drying shrinkage

Two properties of 3D printable concrete mixes that can create drying shrinkage issues are a high concentration of fine particles and increased paste content. A larger surface to mass ratio of finer particles causes an increased water demand which in return increases the shrinkage in the drying process. The same happens for mixes with elevated paste contents (Paul *et al.*, 2018).

2.3.7 Critical issues in 3D printing

Ordinary concrete construction cannot be imagined without steel reinforcement. It provides the necessary tensile strength the concrete often requires. The reinforcement is fitted, and the concrete is poured around it. In 3D printing this becomes a difficult process. Three methods are currently used for adding reinforcement in 3D printed concrete. Firstly, the reinforcement is pre-placed, and the concrete is printed around. The second option is to add the reinforcement while printing and the third one is to add it after the printing process. These techniques all come with their own challenges and advantage. Up to this stage no ideal method of adding reinforcement is prescribed. According to Paul et al., the addition of fibres can improve the strength development significantly (Paul *et al.*, 2018).

The buildability of concrete is mostly limited by the green strength and setting time of the concrete. In large projects where the printing path is long, a long setting time is advantageous since successive layers are not printed in quick succession. On the other hand, scenarios where the print speed is limited by the buildability of the concrete, rapid setting behaviour would be advantageous. Accelerators can be used to overcome this problem. The addition of such accelerating admixtures must be timed correctly to avoid setting before the concrete is extruded. The rheology of such rapid setting behaviour has only been studied in theory but has not been practically implemented (Bentz *et al.*, 2018).

On the one hand 3D printing has many benefits when it comes to manufacturing costs and time saving. Even the electricity costs for running the printer are minute the labour and formwork costs on traditional construction sites (Han *et al.*, 2021). On the other hand, the initial cost to build or purchase a 3D printer is immense. These cost will reduce as the process develops and becomes more readily available, but currently it plays a major role (De Laubier *et al.*, 2018). In addition, the concrete currently used for 3D printing projects is more expensive than what is used on traditional construction sites. Additives used to improve the concrete properties for printing increase the production cost significantly (Han *et al.*, 2021). In an ideal scenario, traditional concrete should be printable and have the properties of printable concrete.

2.3.8 Conclusion

It is evident that 3D printing of concrete requires refining of concrete characteristics for a wider implementation in the industry. Several mineral additives and admixtures are used to make concrete printable which increases the complexity of the mixtures. The complexity and the other identified issues can potentially be solved by using rapid setting OPC cement-based mixtures. Rheological characterisation and mechanical strength test would be required for adjustments of the properties to meet the 3D printing requirements.

2.4 Rapid setting cement

2.4.1 CSA cement

Another form of cement is calcium sulfoaluminate cement, CSA ($Ca_4(AlO_2)6SO_4$ or C_4A_3S). Its most differentiating property compared to OPC is its rapid setting characteristic (Winnefeld, Martin, Müller, *et al.*, 2017). CSA cement is produced from limestone, calcium sulphate and material with a high aluminum content. The aluminum can be sourced from expensive materials such as bauxite. As a result, the production costs for CSA are higher compared to OPC (Canbek, Shakouri & Erdoğan, 2020). Tricalcium silicate (C_3S) is removed from the cement and replaced with CSA cement (Bescher & Kim, 2019). CSA cement production requires lower burning temperatures and little limestone. As a result, between 50-85% less CO_2 is emitted during CSA cement production than in OPC cement. Its use in the 3D printing industry has been tested and has shown promising results (Ingaglio, Fox, Naito, *et al.*, 2019).

2.4.1.1 Hydration

The hydration process of cement is described in Section 2.1.3 can be summarised as follows. The availability of calcium sulfate induces an intermediate hydration step that increases the setting time. Ettringite and aluminium hydroxide are initially formed and only later the calcium hydroxide and C-S-H crystals.

Little or no calcium sulfate availability means that the intermediate ettringite formation may only happen at a low level. The main component of CSA cement, ye'eliminate a type of sulfoaluminate, reacts with water to produce aluminium hydroxide and monosulphate. The setting times are controlled by the ration of calcium sulphate to ye'eliminate. The lower the ratio, the faster the cement sets. The setting times of CSA cement can be further reduced by adding more reactive calcium sulfate, such as hemihydrate or anhydrite, instead of gypsum. Ye'eliminate dissolves faster with the highly reactive calcium sulphates. Winnefeld et al. (2017) studied the influence of replacing gypsum with anhydrite. It was found that the hydration process after a week was at a comparable stage than without anhydrite, but higher strength could be determined in the early stages of hydration. These findings were backed up by Ingaglio et al. (2019) that showed higher ettringite formation in the first 5 minutes compared to OPC.

2.4.1.2 Rheological behaviour and use for 3D printing of concrete

In this study the CSA's behaviour and properties to produce a simple 3D printable mix are of specific interest. Even though the CSA cement itself is more expensive than OPC, the reduction in admixture usage to produce a printable mix may compensate for it.

When one considers the setting times of CSA, the initial setting is found to be significantly lower even at higher water-cement ratios than for ordinary printable mixtures. On the other hand, the compressive strength is reduced with the usage of CSA cement (Ingaglio *et al.*, 2019). Higher ettringite formation in the early hydration stages is the reason for improved early age strength. Other advantageous properties are that CSA cements have good frost resistance and it is less susceptible to corrosion (Li, Gao, Wang, *et al.*, 2020).

3D printable concrete requires a good structural build up performance as well as a regulatable cement paste behaviour. A mix that flows easy when pumped but stiffens up just after its placement is required. Ordinary CSA cement mixtures do not perform too well when printed. A limited thixotropic behaviour in combination with non-ideal structural performance results in poor printability (Chen, Liu, Li, *et al.*, 2020). Adding metakaolin to the CSA cement paste improves the static yield stress and thixotropic behaviour. A better flocculation can be observed which directly correlates with the improved thixotropic behaviour (Chen, Yang, Zheng, *et al.*, 2020). Another additive that improves the printability of CSA cement is bentonite. Its ability to bind water improves the rheological properties of the mix. Providing bentonite in the correct quantities can be used to improve the rheological characteristics of the concrete (Chen, Liu, *et al.*, 2020).

During an attempt to reduce the bauxite content in the CSA clinker, industrial waste material was used. The addition of fly ash or red mud can be used to reduce the bauxite content of 40% by half without compensating strength (Canbek *et al.*, 2020).

A blend between OPC to CSA cement was suggested by Khalil, Aouad, El Cheikh *et al.* (2017) for a manually printable concrete mix. The good characteristics of each cement type are used to develop a printable mix. The OPC is used for its long-term strength development and the CSA to obtain the rapid setting. No significant difference in temperature was observed during the hydration process even though the setting time was quicker compared to an OPC mix. A total of 25 layers could manually be printed before collapse. Changes in compressive strength due to replacement of OPC with CSA were only noted for the manually printed specimens. The casted cubes did not show this difference. The following mix proportions were used:

- 93% OPC
- 7% CSA
- Sand to cement ratio = 2
- Water-cement ratio = 0.35
- Superplasticizer = 0.26%

The manual printing process used was less accurate than in a 3D printer. Inclined printing was also tested successfully (Khalil *et al.*, 2017). Adding anhydrite to the OPC/CSA blend improves

the dynamic behaviour of the mix as well as the rate of structuration (Huang, Li, Yuan, *et al.*, 2019).

The use of CSA cement to produce a simpler mix for 3DPC seems promising by blending it with OPC.

2.4.2 BCSA cement

Belitic calcium sulfoaluminate (BCSA) cement is an unblended type of CSA cement. The cement is made up of three main components that vary in quantity - CSA, belite and calcium sulphate. As the name suggests, BCSA cement has belite (C_2S) as its main component. As a result of the increased belite content, BCSA cement contains less CSA in the form of ye'eliminate. Higher quantities of C-S-H precipitate due to a larger availability of belite. BCSA cement is produced by milling and processing only a single clinker. Low shrinkage and rapid hydration are the main advantages of this cement type.

Table 2.2 shows the differences in phase composition between CEM I and BCSA cement. CSA is used to replace alite and aluminate in BCSA cement. The belite content is also significantly higher than in OPC. Calcium sulphate is used to control the setting behaviour of both cement types. In BCSA cement, ye'eliminate reacts with calcium sulphate and water to form ettringite. Since large quantities of ettringite are rapidly formed the concrete gains strength quickly (Rosero, 2020). In OPC, the calcium sulphate reacts with aluminates to form ettringite as well, but this prohibits the formation of calcium aluminate hydrate which causes flash setting.

TABLE 2.2 TYPICAL MINERALOGICAL COMPOSITION OF CEM I AND BCSA CEMENT (ROSERO, 2020)

Component	Notation	CEM I	BCSA Cement
Alite	C_3S	59	-
Belite	C_2S	17	45
Aluminate	C_3A	7	-
Ferrite	C_4AF	9	2
Ye'eliminate	C_4A_3S	-	30
Calcium sulfate	CS	2	15
	Other	6	8
	Total	100	100

The rapid setting characteristic of BCSA cement makes it a good solution in projects where time is limited. Such projects could be emergency repairs of structures that need to be reopened quickly. Rapid gain in flexural strength makes BCSA cement a good alternative for road and highway repairs (Bescher & Kim, 2019).

BCSA cement requires no blending with OPC as it is less expensive than other CSA cement types. None the less, it still has the rapid setting and strength gain characteristics. BCSA cement shrinks little compared to OPC containing mixtures and provides good long-term strength (Rosero, 2020).

The use of BCSA cement also has disadvantages. The rapid setting of the cement can cause problems during placement and the cement itself is much more expensive than OPC. Higher water contents are required for complete hydration of BCSA cement in comparison to OPC. The purchase price of BCSA cement is higher than OPC which makes the concrete more expensive to produce (Rosero, 2020).

2.4.2.1 Hydration

The hydration of BCSA cement is like CSA cement. Ye'eliminate reacts with calcium sulphate to from ettringite and aluminum hydroxide. The quantities of calcium sulphate are such that all ye'eliminate can hydrate to form ettringite. When calcium sulphate is depleted in solution, calcium monosulphate is formed. Aluminum hydroxide, ettringite and monosulphate precipitation influence the short-term strength development of BCSA cement. Belite only hydrates from 3 days after casting onwards, forming calcium silicate hydrates and calcium hydroxide. These hydration products control the long-term strength development (Bescher & Kim, 2019; Borštnar, Daneu & Dolenec, 2020; Rosero, 2020).

2.4.2.2 Rheological and mechanical characteristics

This section considers admixtures and modifications that can be used to adjust the rheological and mechanical characteristics of BCSA cement. Changes in workability or setting time may be required to suite different application purposes where the cement is used.

The slump of BCSA cement mixes can be increased with the additional of water. Higher water content improves the concretes workability but reduces its strength (Rosero, 2020). As previously mentioned, BCSA cement is characterised by short setting times. Researchers report initial setting times between 10 and 20 minutes (Chesnut, 2020; Soriano, 2019).

Citric acid can be used to control the setting time of BCSA cement. The hydration of ye'eliminate is hindered with the addition of citric acid depending on the quantity used. The setting time can be increased between 45 minutes and 4.25 hours at dosages of 0.35% to 2.0% citric acid with respect to BCSA cement content. It enhances the fluidity of concrete and impacts the compressive strength only slightly. A linear relationship can be found between citric acid dosage and setting time (Rosero, 2020; Soriano, 2019). Chesnut (2020) recommends a citric acid dosage of 0.35% of binder content that allows sufficient time for placement and casting. The effectiveness of citric acid is decreased at higher temperatures. At elevated temperature the hydration process is accelerated which then reduces the setting time and reduces the effectiveness of the retarder (Zou, Zhang & Wang, 2020). Burris and Kurtis (2018) found that citric acid is more effective on BCSA than on CSA type cement. The authors concluded that the use of citric acid can ensure sufficient workability over longer time periods. In return, CSA type cement can be used in large scale projects since the setting behaviour can be controlled with citric acid without compensating too much on mechanical properties.

In a study by Su *et al.* (2019) it was found that the plasticising effect of PCE type superplasticisers is limited for BCSA type cements. The PCE does not hinder the rapid

formation of ettringite and therefore the concrete stiffens up rapidly. Nonetheless, the early age fluidity can be improved by using PCE.

The usage of citric acid as a retarder in BCSA cement/concrete mixtures has no significant influence on the compressive strength according to Soriano (2019). At early ages the increased compressive strength capacity is not as significant as after a week. Higher dosage citric acid resulted on average in higher compressive strength. It is postulated that better workability characteristics reduce the number of voids and therefore strength is improved. The early age compressive strength development can be improved by increasing the temperature of water. This effect tends to even out with time. Soriano (2019) argues that due to a lower initial rate of hydration, hydration products are packed more evenly which increases strength. Borštnar *et al.* (2020) studied the influence of temperature on the hydration kinetics of BCSA cement and obtained similar results. At higher temperatures, the rate of hydration is accelerated, and better early age compressive strength is developed. At lower temperatures, the hydration rate is slower initially, but better long-term strength development was found. C-S-H is responsible for long-term strength development. The precipitation of C-S-H hydrates is decreased at higher temperatures which in return negatively influences the compressive strength at later stages. More stable C-S-H crystals are formed at lower temperatures.

2.4.3 Rapid setting behaviours of OPC

Two unwanted scenarios on a construction site are flash and false setting of cement. During normal hydration of OPC, the C_3A hydration is controlled by the addition of calcium sulphate and its corresponding ettringite formation. Imbalances of sulphate concentration cause rapid stiffening which prohibits proper casting because of early setting.

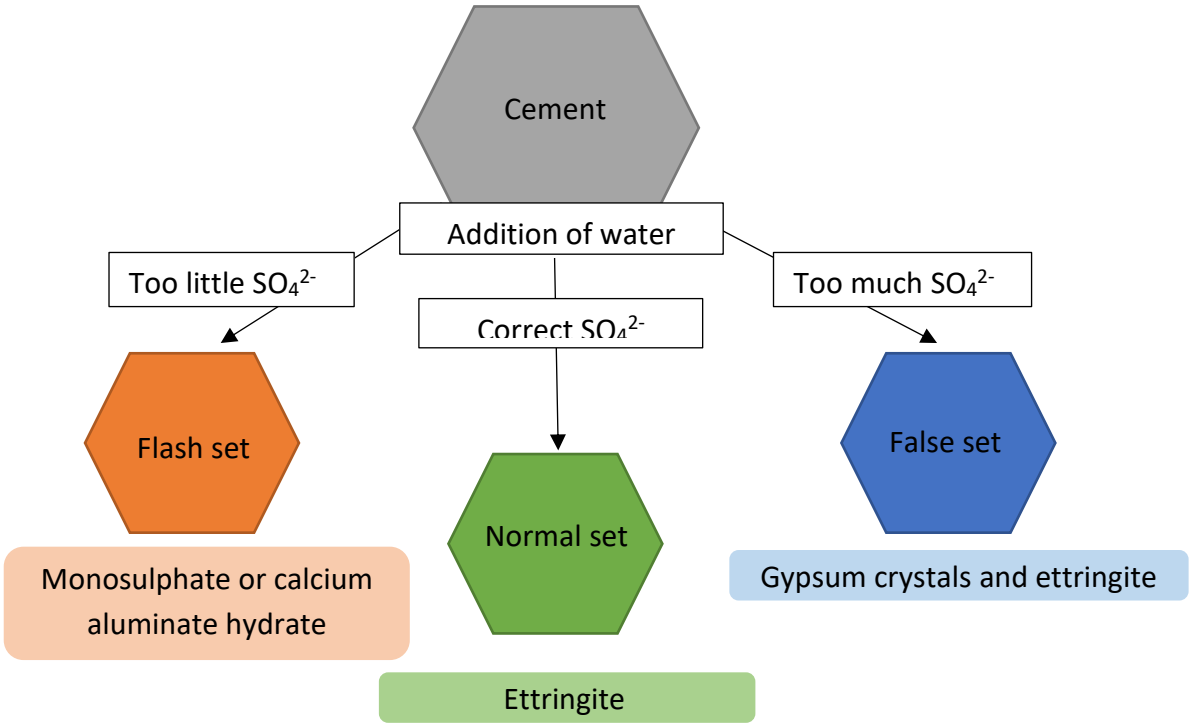

FIGURE 2.9 SETTING BEHAVIOUR DEPENDING ON THE SULPHATE CONCENTRATION (MOIR, 2003)

Calcium sulphate is added in the form of gypsum during the cement production. In general, too little gypsum causes flash setting and too much gypsum causes false setting (Wei, Li, Xiao, *et al.*, 2006; Gauffinet-Garrault, 2012). Figure 2.9 displays the setting behaviour induced by different sulphate availabilities and the resulting hydration products formed.

2.4.3.1 Flash Set (Quick set)

Flash setting of cement is linked to a rapid stiffening and large heat of hydration. The distinguishing characteristics of flash set from false set are the formation of AFm phases as well as the high heat of hydration. The hydration of C_3A is affecting the heat of hydration. During flash set, the hydration of C_3A is not delayed as insufficient quantities of calcium sulphate are available. There are multiple scenarios under which this reaction occurs, and these are described in the following sections. It is important to note that the high heat of hydration and reaction processes happening influence strength development negatively. The formation of excessive amounts of calcium monosulphate (AFm) instead of C-S-H is one reason for the loss in strength. A reagetation of the mix damages the hydrated crystals and these cannot be rebuilt (Beaudoin & Odler, 2019). Factors such as calcium sulfate types, cement fineness and exact clinker components can have an effect on the development of flash set (Wei *et al.*, 2006). During flash set, the quantities of effective gypsum are too little to delay the C_3A hydration. The effectiveness of the calcium sulphate depends on its rate and quantity of dissolution as well as the concentration in the mix (Rößler, Möser & Stark, 2007).

No Calcium sulphate availability

In the production process of cement, calcium sulphate is added in the form of gypsum. This prevents flash setting of cement by delaying the hydration process. Thus, flash setting happens when there is little or no calcium sulphate available. AFm crystals that have a plate like shape form rapidly without calcium sulphate in solution. A fast stiffening within five minutes is characteristic for flash setting. This reaction is not found in cements where the C_3A content is little (Beaudoin & Odler, 2019).

Pyrocatechol

Another option to induce this phenomenon is to hinder the gypsum dissolution. This can be done by using pyrocatechol (PCC), a benzene type used in the production of perfumes or pesticides. Quantities as low as 0.027% of cement paste can accelerate the cement hydration process significantly. An accelerated C_3A hydration can take place that leads to flash setting of the cement due to inhibition of calcium sulfate dissolution (Justnes, 2010).

Brykov *et al* (2018) tested the effect of PCC on OPC cement as well as CSA cement. In mixtures with OPC, the addition of PCC causes much faster stiffening of the cement paste. The study showed that C_3A sets immediately when PCC is added to the mix. For CSA cement, the addition of PCC results in slower setting of the cement paste. This effect initially seems controversial. The C_3A can hydrate faster because the PCC prevents a dormant period in which its hydration is delayed. On the other hand, in mixtures such as CSA cement where no gypsum is present to bind on, the PCC binds the calcium and aluminum ions together. This means that

the aluminates cannot hydrate, and the setting times are increased. No effects were found on the setting behaviour of the other hydration products formed with the addition of PCC. Both Justnes (2010) and Brykov *et al.* (2018) could not exactly find the exact reason for flash setting of the mixtures. It was proposed that the availability of dissolved calcium sulfate is reduced with the addition of PCC.

Use of accelerators

Within the mining industry the use of shotcrete to stabilise mining tunnels is common practise. Accelerators are added into the mix to produce rapid setting. Two types of accelerators are mainly used, alkali-free and alkaline. The alkali-free accelerator contains mainly aluminum sulphate which in a dissolved state, speeds up the formation of AFt for hydration of C_3S and AFm for hydration of C_3A. Their use is more environmentally friendly and higher compressive strength can be achieved in comparison to alkaline accelerators. The accelerated ettringite and monosulphate formation causes the cement mixture to stiffen up rapidly. An early age strength development can clearly be observed (Liu, Ma, Tan, *et al.*, 2020; Maltese, Pistolesi, Bravo, *et al.*, 2007).

Source of calcium sulphate

Maltese et al. (2007) studied the influence of the reactivity of the added calcium sulphate. Gypsum, alpha- and beta-Hemihydrate as well as anhydrite were tested. A direct correlation between dissolution rate and reactivity could be found. Table 2.2 shows that a slower dissolution time correlates with a faster setting time. Maltese *et al.* (2007) argue that lower concentrations of calcium sulphate ions enhance the strength characteristics of ettringite crystals. Less ettringite crystals are formed but their size is increased, and the hydrates are better shaped. As a result, better interlocking is created than for the larger amounts of small crystals and this therefore stiffens up the cement paste. Garcia-Mate *et al.* (2015) confirmed these results, hemihydrate also known as bassanite dissolves more rapidly in water than anhydrite. Maltese *et al.* (2007) found that the exposure of β-hemihydrate to moisture reduces its dissolution rate. This results in a slower formation of ettringite which in return accelerates the C_3A hydration and causes more rapid stiffening of the concrete.

TABLE 2.3 DISSOLUTION RATE AND SETTING TIME OF CALCIUM SULPHATE SOURCES (STANDARD DEVIATION IN BRACKETS) (MALTESE *ET AL.*, 2007)

Calcium sulphate source	**Dissolution rate (Ca-ions g/(l*min)**	**Setting time Initial/Final**
Gypsum	48 (+- 5)	2h30min / 8h30min (+-30min)
α-Hemihydrate	60 (+/−6)	1min38s / 6min30s (+-30s)
β-Hemihydrate	92 (+/−9)	1min6s / 3min5s (+-20s)
Anhydrite	7 (+- 1)	40s / 1min18s (+-10s)

Lignosulphonate & Anhydrite

The clinker composition and calcium sulfate sources have a great impact on the hydration behaviour of the cement. High anhydrite content in the calcium sulfate added to the clinker can induce flash setting when mixed with lignosulfonate superplasticizer. The already lower solubility of anhydrite is further reduced with the addition of lignosulfonate plasticizer. Less calcium sulfate is therefore available to react with C_3A and form ettringite. On the other hand, more C_3A hydrates in the presence of calcium lignosulphonate plasticiser and forms C-A-H since less calcium sulphate as available to hinder the hydration of calcium aluminate hydrate. As a result, the mix gains stiffness rapidly. The lignosulphonate superplasticiser has a similar effect as the accelerators used for shotcrete. The fewer ettringite crystals formed are larger with the addition of calcium lignosulphonate plasticiser. Larger plate like ettringite crystals are less effective in covering C_3A and preventing the formation of C-A-H. Thus the mixture stiffens up faster, due to the formation of C-A-H and a few large ettringite crystals (Wang *et al.*, 2012).

Sodium aluminate

As previously discussed, rapid setting of concrete can be induced with the addition of sodium aluminate ($NaAlO_2$). Sodium aluminate rapidly dissolves in water and binds with free calcium ions dissolved from C_3A, C_3S or C_2S to form C-A-H. It was determined that sodium aluminate accelerates the hydration of alite and belite in white Portland cement even at low temperatures with increased chain lengths of C-S-H hydrates. In the presence of sodium aluminate, the formation of ettringite is reduced and more monosulphate and C-A-H is formed (Andersen *et al.*, 2004). In a study by Han *et al.* (2014) the setting time of concrete was continuously reduced to a few minutes with sodium aluminate up to a 4% replacement rate. Higher sodium aluminate contents did not have any significant influence.

2.4.3.2 False Set

False setting is different to flash setting. The setting times are longer, about 10 minutes. This varies with the intensity of the reaction happening. The strength development of false setting concrete is not affected by the reaction. This can be related to the low heat of hydration which is like the normal hydration reaction of concrete. Reagetation of the cement mix breaks up the formed crystals and the plasticity of the mix can be regained through mixing. After the force is removed, the crystals start forming again (Beaudoin & Odler, 2019). Large gypsum and syngenite crystals are formed during false setting that interlock and cause stiffening of the concrete (Chung & Lee, 2011).

Secondary gypsum formation

Beaudoin and Odler (2019) argue that, the most common reason of false setting is a result of secondary gypsum formation. This happens at low concentrations or no content of C_3A and high concentration of calcium sulfate. The calcium sulfate in the form of hemihydrate contained in the cement precipitates and forms calcium sulfate dihydrate. Calcium sulphate hemihydrates rate of dissolution is faster than calcium sulphate dihydrate (gypsum) and

results in an accelerated secondary gypsum formation. Larger fast precipitated amounts of secondary gypsum interlock and then cause the rapid stiffening of the cement paste, false set. Another factor playing a role in the hemihydrate hydration is the anhydrite to dihydrate ratio. Due to incorrect proportions, the formation of ettringite is interrupted and AFm or calcium aluminate hydrate forms. This may even happen under the condition that ample amounts of hemihydrate are present in the mix (Beaudoin & Odler, 2019). The formation of hemihydrate in the cement can be a result of using ball mills for grinding the clinker. Due to the high temperatures in the milling process, the gypsum dehydrates to hemihydrate (Beaudoin & Odler, 2019; Wei *et al.*, 2006)

Syngenite formation

Accordin to Chung *et al*. (2011) and Krivenko *et al*. (2018) Alkali sulphates in cement can induce as different form of false setting by forming syngenite. At high sulphate content, alkalis bind with a sulphate to form alkali sulphates. Arcanite, thenardite or calcium langbeinite are typical examples of alkali sulphates. These alkali sulphates rapidly react with water to form syngenite. Equation 2.14 describes the rapid hydration process of arkanite (K_2SO_4) and calcium sulphate that induces an intense production of syngenite:

$$K_2SO_4 + CaSO_4{\cdot}2H_2O \rightarrow K_2SO_4{\cdot}CaSO_4{\cdot}H_2O + H_2O \qquad (2.14)$$

As a result, the excessive amounts of syngenite rapidly stiffen the cement by interlocking of particles, and hence inducing false set. The amounts of free gypsum are significantly reduced in this reaction process (Chung & Lee, 2011; Krivenko *et al.*, 2018). The syngenite reaction is more likely to produce false setting than flash setting as it is a more rapid stiffening behaviour of concrete (Chung & Lee, 2011). At high concentrations of alkalis it can occasionally lead to flash setting of cement (Beaudoin & Odler, 2019).

2.4.4 Conclusion

It can be concluded that the characteristics of BCSA and CSA cement hydration can be adjusted to meet the set-out rheological and workability requirements of any project. The rapid stiffening characteristic in combination with promising strength development of BCSA and CSA cement, gives optimism for good buildability in 3D printing. OPC cement flash sets due to low or no availability of calcium sulphate and the corresponding ettringite formation that prevents rapid setting. The unavailability of calcium sulphate in solution is a result of low quantities in cement or influence of admixtures reducing its dissolution. False setting is a result of over availability of calcium sulphate to form secondary gypsum or the presence of alkalis that form syngenite in the presence of calcium sulphate. Flash setting is a more extreme and faster setting behaviour than false setting. The setting time characteristics of CSA/BCSA cement at flash setting are similar.

The use of rapid setting cement in any of the described rapid setting behaviours indicates that good buildability results can be achieved when 3D printing such mixes.

2.5 Concluding summary

A literature review on the important aspects considering 3D printing of ordinary cement with aid of rapid setting mechanisms is provided in this chapter. The literature review presented in such a way, that three focus points of this study can be well understood. Firstly, ordinary concrete and how its hydration processes work and what effect admixtures have. Secondly, the important aspects considering 3D printing of concrete for this study. Thirdly, what rapid setting behaviours can be found in OPC, or which cement types can cause rapid setting in concrete.

In the first section of this chapter, a brief background was given on concrete constituents: cement, water and aggregate. It was found that the use concrete has a significant environmental impact, and the usage of cement as critical component must be optimised. Subsequently, the main properties of concrete and its influencing factors were discussed. An explanation of the hydration process of concrete clarified that calcium sulphate concentration controls the hydrational processes of cement.

In a separate section, different admixtures and mineral additives with their positive effects on concretes characteristics were presented. PCE type superplasticiser was found to be the most suitable for this study. Using calcium sulphate or sodium aluminate was found to work well as false and flash setting inducing agents.

In the second section, the process of 3D printing was explained and the critical rheological aspects influencing buildability were laid out. Rapid re-flocculation and structuration are required for good buildability characteristics of a concrete mix. Following this, some critical aspects of 3D printing were discussed. It was suggested that these problems could potentially be solved by using rapid setting ordinary cement mixtures.

In the third section, rapid setting cements were introduced. The advantages and disadvantages of rapid setting CSA/BCSA cement were discussed. Multiple ways to induce flash and false setting ordinary Portland cement mixtures were provided. It is shown that these setting behaviours are once again dependent on the calcium sulphate availability and ratio of aluminates to sulphates.

From this literature study it is evident that 3D printing of different rapid setting ordinary concrete mixtures, flash- and false setting concrete, is a novel approach. The study aims to improve buildability characteristics of printable concrete with mix design that contain as little as possible additives or admixtures. Better buildability characteristics increase the printing speed which can then be used to complete construction projects or 3D printed components in less time. Little work has been done on comparing the characteristics of rapid setting concrete mixtures which provides further reason for this study.

3 Experimental framework

This chapter gives the procedures and tests followed in this study. Firstly, the material used to produce the concrete mixes is provided and the reasoning for the addition of admixtures is discussed. Secondly, the mix design development process is described, and the final outcomes are presented. Lastly, the procedures followed for the various tests are described in detail.

3.1 Materials

3.1.1 Water

Municipal potable tap water, consistently sourced from the same tap in the laboratory, was used throughout this study. For consistency purposes the water was stored at 23 °C in a plastic container for a minimum of 24 hours before use.

3.1.2 Binder

A CEM I 52.5N Portland cement was used in this study. This binder has a high purity (95% OPC and 5% minor constituents) and therefore reduces the risk of variation in the results. Pretoria Portland Cement (PPC) supplied the material from its De Hoek production plant. An X-Ray Fluorescence analysis (XRF) was done on the CEM I 52.5N and the results are shown in Table 3.1.

TABLE 3.1 CEMENT ELEMENTAL ANALYSIS AND COMPOSITION

	CEM I 52.5N	BCSA
Cement composition	Percentage (%)	Percentage (%)
Al_2O_3	4.21	15.70
CaO	63.86	46.97
Fe_2O_3	3.25	0.69
K_2O	0.55	0.49
Na_2O	0.23	0.10
P_2O_5	0.12	0.10
SiO_2	20.35	13.86
TiO_2	0.21	0.64
Mg0	0.07	1.25
Loss on ignition at 1000 °C	3.44	4.83
Other	2.75	15.35
Total	100	100

The XRF was done for the BCSA cement as well. This cement is used to replace parts of the CEM I 52.5N to induce a rapid setting behaviour in the concrete mixture. Table 3.1 also contains the XRF analysis results of the BCSA.

Differences between the CEM I 52.5N and the BCSA can be observed from the results in Table 3.1. Such variation in composition explains the different setting behaviours of the two

cements. BCSA has a much higher Al_2O_3 content and a reduced CaO content. A higher aluminate content means that the aluminate phase is more extreme and causes rapid stiffening early on. The material classified as “Other” contain mainly sulphur that cannot be measured with the XRF analysis. Research suggests that the sulphur is found in the form of sulphur trioxide (SO_3) and makes up about 15% of the BCSA cement (Bescher & Kim, 2019).

DuraPozz fly ash Class F has been used throughout this study to produce the reference printable mix (REF_3DPC). This concrete mixture also required silica fumes. The micrometric silica, CHRYSO Silica, was obtained from Chryso SA (Pty) Ltd.

3.1.3 Aggregate

The aggregate used was a fine natural pit sand known locally as Malmesbury sand. A 4.75 mm sieve was used to filter out large particles of stone, dirt, or other organic materials in the sand. Fine sands are characterised by more than 90% of the sample passing the 5 mm sieve and not more than 5% dust in the sample (SANS 3001-AG1:2014). A grading analysis was conducted according to SANS 1083:2017 and the results can be seen in Figure 3.1. The properties of the aggregate are listed in Table 3.2.

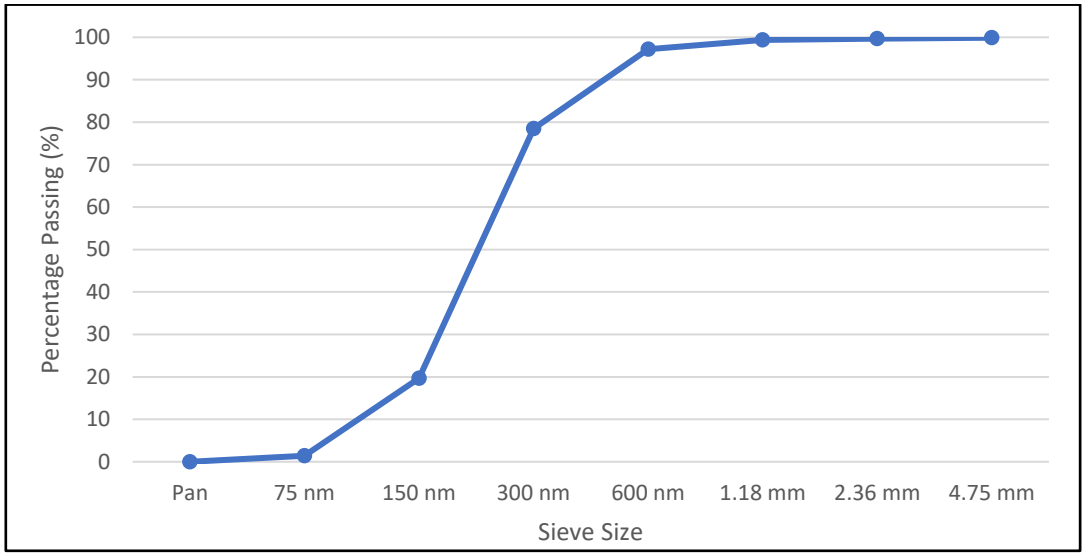

FIGURE 3.1 GRADING ANALYSIS FINE PIT SAND

TABLE 3.2 FINE PIT SAND PROPERTIES

Aggregate	Relative density (kg/m^3)	Fineness Modulus
Fine natural pit sand	2.67	1.06

3.1.4 Admixtures

Several different admixtures were used to create the different setting behaviours of the concrete mixtures.

Polycarboxylate polymer-based superplasticizer (PCE) was used throughout the study. The same batch was used for all mixes produced. Chryso SA (Pty) Ltd supplied the Fluid Premia 310 superplasticizer which was used.

Gypsum, in form of Hemihydrate, was used for the false setting mixes. Calcium sulfate hemihydrate (calcinated) is a dehydrated and more reactive form of gypsum. Clearer false setting can be observed due to an increased rate of reaction (Bessinger, 2020). As specified by Sigma Aldrich (Pty) Ltd the gypsum was calcinated to produce the hemihydrate.

Sodium aluminate anhydrous (Technical) was used for the flash setting mixes. Sodium aluminate is highly reactive in water and is therefore suitable as aluminate source to induce flash setting behaviour. Both the gypsum and the sodium aluminate were sourced from Sigma Aldrich (Pty) Ltd.

As discussed in Section 2.4.2, citric acid was used as retarder to delay the hydration process of BCSA cement for a required amount of time. The citric acid was used in a powder form and was supplied by Kimix Chemical and Lab supplies CC.

3.2 Mix designs

The development of the mix designs went through multiple phases. All mixes were originally based on a mix design proposed by Van Der Putten *et al.* (2020) as 3DPC. This mix only contained cement, sand, and water. The mix could not be replicated as suggested in the study by van der Putten *et al. (2020)* , since the properties of the mix constituents available for this study differ. Slight adjustments were made to achieve the required workability.

All mixes for Phase 1 characterisation were then developed by changing the proportions of constituents to meet the printability standards under the setting behaviour induced by the admixtures. Similar to the suggestions made by Cho et al. (2020), in the trial prints it was found that mini-slump values between 165 mm – 180 mm worked well from an extrudability point of view . The major adjustments were made by altering the water-cement ratio as well as the superplasticizer dosage.

The mix designs for Phase 2 of the study were changed to further improve the printability of the selected mixes. Unpredictable influences like pumping pressure for example, affect the behaviour of the concrete and cannot be anticipated before printing. Therefore, the changes for printability were only made on the concrete mixtures ultimately selected for printing.

All mixes and the exact mix design development procedures follow in the subsequent sections. A layout visualising the progression of each mix design is shown in Figure 3.2. In Phase 1, eight different mixes were characterised: two false setting mixtures (FA_xy), two flash setting mixtures (FL_xy), two BCSA cement containing mixtures (BC_xy), one standard reference mix (REF) and one 3D printable reference mix (REF_3DPC). The term “xy” refers to the replacement rate of CEM I 52.5N. Based on their performance in the rheological and mechanical characterisation tests, the most suitable mixture of each rapid setting mechanism was selected for printing in Phase 2.1. The selection was based on the setting time test, early-

age and 28-day compressive strength and hydration temperature development test results. Thereafter, adjustments were made to each mix tested in the buildability test which are shown in Phase 2.2 to improve the buildability of the mixtures.

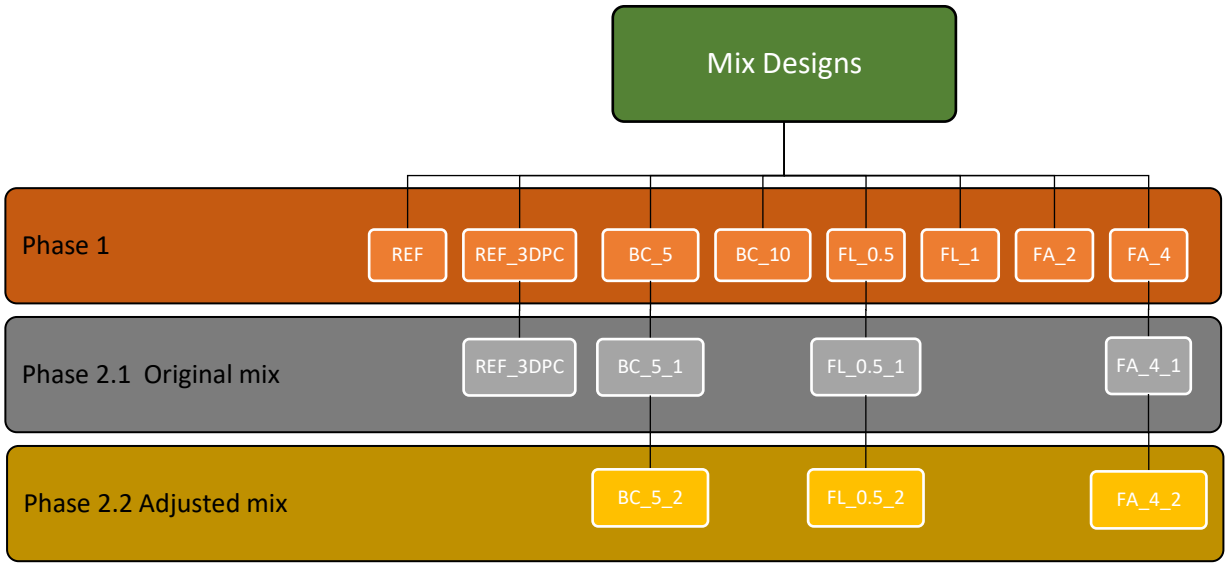

FIGURE 3.2 MIX DESIGN DEVELOPMENT PROCESS

3.2.1 Reference mixes

The standard mix used at Stellenbosch University served as reference mix for 3D printing of concrete. This mix is referred to as REF_3DPC. The mix design is shown in Table 3.3.

TABLE 3.3 STANDARD 3DPC MIX REFERRED TO AS REF_3DPC

	kg/m^3	RD	Litres
CEM I 52.5N	579	3.14	184.4
Sand	1169	2.67	437.8
Water	261	1.00	261
PCE	7.0	1.05	6.7
Fly-ash	165	2.20	75
Silica Fumes	83	2.10	3.5

Van der Putten *et. al* (2020) developed and ordinary concrete mix that can be used for 3D printing of concrete. Where ordinary refers to a concrete mixture only containing cement, sand, and water. This mix was replicated and adjusted so that the similar workability characteristics were obtained with the material available for this study. A test run for pumpability in the 3D printer was used to determine the printability of the mixture. The mix at extrusion was very dry and the addition of extra superplasticiser and water helped solving

the extrusion problem. This mix design was used as the basis for developing all other rapid setting mixes. This reference mix is further referred to as REF and the mix composition is shown in Table 3.4.

TABLE 3.4 REFERENCE MIX FOR STUDY REFERRED TO AS REF

	kg/m^3	RD	Litres
CEM I 52.5N	670	3.14	213.4
Sand	1340	2.67	501.9
Water	284.8	1	284.8
PCE	3.15	1.05	3.00

3.2.2 Flash setting mixes

The starting point for the mix design development was 2 litre mix. A dosage of 2% and 4% binder replacement with sodium aluminate created no workability issues in the small volume mixes. This means that a rapid setting behaviour was observed but still not excessive. An upscaling of both mixes to 18 litres in volume showed that both sodium aluminate dosages were too high. Both mixes stiffened up as soon as the water was added, and no fluidity was achieved at all. The concrete remained dry and sandy, having no fluidity. The binder replacement with sodium aluminate was reduced to 1% and 0.5%.

As expected, the higher dosage of 1% stiffened up the mix faster than the lower dosage. A suction like effect was observed for the higher dose mix after the water was added in the mixing process. According to Han et al. (2014) addition of sodium aluminate increases the water-demand of the cementitious mix. Therefore, the water-cement ratio of the 1% replacement mix was increased to compensate for the higher water-demand and to retain fluidity. Both water and SP content were increased to compensate for the higher water demand and to improve the concrete's workability. The dosage of 1% sodium aluminate was not further adjusted so that the characterisation would show clear results between high and lower dosage addition of sodium aluminate on cement mixtures. The mix design for 1% binder replacement with sodium aluminate is shown in Table 3.5. This mix is referred to as FL_1.

TABLE 3.5 FLASH SETTING AT 1% SODIUM ALUMINATE CONTENT REFERRED TO AS FL_1

	kg/m^3	RD	Litres
Water	321.6	1.00	321.6
CEM I 52.5N	612.3	3.14	195
Sand	1285.7	2.67	481.5
SP (PCE 1.45%)	8.97	1.05	8.54
Sodium Aluminate (1%)	6.12	3.14	1.95
Water-binder ratio	0.52		

A lower content of sodium aluminate proved to have less of an effect on the consistency and flowability of the mix. Only slight adjustments to the mix composition were made to ensure that all mixes characterised in this research have similar mix proportions. Table 3.6 shows the mix composition used for the FL_0.5 mixes produced in the Phase 1 characterisation.

TABLE 3.6 FLASH SETTING AT 0.5% SODIUM ALUMINATE CONTENT REFERRED TO AS FL_0.5

	kg/m^3	RD	Litres
Water	290.1	1.00	290.1
CEM I 52.5N	641.5	3.14	204.3
Sand	1347.2	2.67	504.6
SP (PCE 0.85%)	5.48	1.05	5.22
Sodium Aluminate (0.5%)	3.21	3.14	1.02
Water-binder ratio	0.45		

The two flash setting mixes have different water-binder ratios, denoted in Tables 3.5 and 3.6 as W/C. As previously explained, the FL1 mix required more water and superplasticizer to obtain similar workability.

3.2.3 False setting mixes

False setting of cement can be induced by increasing the calcium sulfate content of the binder. Calcium sulfate is added to ordinary cement to prevent flash setting, but overdoses can induce false setting. A more reactive form of calcium sulfate dihydrate, calcium sulfate hemihydrate, has shown to create more extreme false setting behaviour (Bessinger, 2020).

Initial trials have shown that dosages of 2% and 4%, do not exhibit extreme rapid stiffening but clear false setting. The gypsum contained in the OPC can be dehydrated into its hemihydrate form by placing it in an oven for 48 hours at 150°C. In this form, the hemihydrate can induce false setting due to its higher solubility in water (Chung & Lee, 2011).

For this study, a combination of both approaches, addition of calcium sulfate hemihydrate and dehydration of the cement, have been implemented to get a clear false setting behaviour. The mix compositions for both 2% and 4% binder replacement are shown in Table 3.7 & 3.8 and will be referred to as FA_2 and FA_4 respectively.

TABLE 3.7 FALSE SETTING MIX DESIGN AT 2% CALCIUM SULFATE REFERRED TO AS FA_2

	kg/m^3	RD	Litres
Water	292.3	1.00	292.3
CEM I 52.5N dehydrated @ 150 °C	636.8	3.14	202.8
Sand	1337.3	2.67	500.9
SP (PCE 0.85%)	4.87	1.05	4.64
Calcium Sulfate (2%)	12.74	3.14	4.06
Water-binder ratio	0.45		

The higher dosage of calcium sulphate resulted in a slightly higher water demand of the concrete to obtain the required workability. A higher water-cement ratio is obtained for the FA_4 mix design due to the increased water content.

TABLE 3.8 FALSE SETTING MIX DESIGN AT 4% CALCIUM SULFATE REFERRED TO AS FA_4

	kg/m^3	RD	Litres
Water	295.1	1.00	295.1
CEM I 52.5N	630.6	3.14	200.8
Sand	1324.3	2.67	496.0
SP (PCE 0.85%)	5.57	1.05	5.31
Calcium Sulfate (4%)	25.22	3.14	8.03
Water-binder ratio	0.47		

3.2.4 BCSA cement

BCSA cement is a modern rapid setting cement type. High strengths can be achieved at early ages which makes it interesting for projects with limited time frames. This study considers rapid setting mechanisms and therefore the addition of BCSA cement fits well into the research. In a small volume test series, 2% and 4% replacement of binder by mass were sufficient dosages to show the setting behaviour expected with the addition of BCSA cement. Binder replacements with BCSA of 5% and 10% were rather used for this study. Clear differences in setting behaviour were observed in the trial mixes produced. The mix designs for both BCSA containing mixes are shown in Tables 3.9 and 3.10 and are referred to as BC_5/BC_10.

TABLE 3.9 5% REPLACEMENT BCSA MIX REFERRED TO AS BC_5

	kg/m^3	RD	Litres
CSA Cement	33.5	3.14	11
CEM I 52.5N	636.5	3.14	203
Sand	1340	2.67	502
Water	284.8	1	285
SP (PCE 0.6%)	5.36	1.05	5
Water-binder ratio	0.425		

No changes in SP dosage nor water content were required for the higher BCSA containing concrete mix to obtain good workability.

TABLE 3.10 10% REPLACEMENT BCSA MIX REFERRED TO AS BC_10

	kg/m^3	RD	Litres
CSA Cement	67	3.14	21
CEM I 52.5N	603	3.14	192
Sand	1340	2.67	502
Water	284.8	1	285
SP (PCE 0.6%)	4.02	1.05	4
Water-binder ratio	0.425		

3.2.5 Printable mixes

The mix designs for the first printing trial were the same as described in Sections 3.2.4. The following mixes were selected for printing: REF_3DPC, FA_4, BC_5 and FL_0.5. Mix FA_4 was selected over FA_2 due to its good strength gain characteristics and overall better characterisation performance. Both BC_5 and FL_0.5 were selected due to their less extreme setting behaviour in comparison to BC_10 and FL_1 which could cause extrusion problems. The mix design for the REF_3DPC was not changed since it is a printable reference mix. Mix FA_4 was found to be a printable concrete mixture. Adjustments to this mix were made to improve the buildability as well as printability characteristics. The flash setting concrete and the BCSA containing mixture were unprintable with its original mix design from Phase 1. Therefore, the superplasticiser and water content were increased to make these mixes printable. Table 3.11 and 3.12 show the adjusted and printable mix designs for the respective mixes.

TABLE 3.11 ADJUSTED FLASH SETTING MIX FOR PRINTING

	kg/m^3	RD	Litres
Water	305.0	1.00	305.0
CEM I 52.5N	639	3.14	203.5
Sand	1310.0	2.67	490.6
SP (PCE 1.1%)	7.06	1.05	6.73
Sodium Aluminate (0.5%)	3.20	3.14	1.02
Water-binder ratio	0.48		

The hydration of the BCSA mix was delayed with the addition of Citric acid, acting as a retarder for BCSA cement hydration. This allows for more time before the hydration reaction of the BCSA cement initiates.

TABLE 3.12 ADJUSTED BCSA MIX DESIGN FOR PRINTING

	kg/m^3	RD	Litres
BCSA Cement	33.45	3.14	11
CEM I 52.5N	635.5	3.14	202
Sand	1337.9	2.67	501
Water	286	1	286
SP (PCE 0.825%)	5.52	1.05	5
Water-binder ratio	0.43		
			1000
Citric Acid	125g		

3.3 Pre-experimental procedures

3.3.1 Material preparation

Before every test, the material required for the specific mix was stored for 24 hours in a temperature-controlled room at 23 °C (± 2) and 65 % (± 5) humidity. The constituents were stored in different buckets so that reactions between the materials were prohibited. All containers were covered during the curing period. This ensures that no outside influences could pollute the material.

The main aim of the preparation was to eliminate the influence of varying temperature and humidity on the material. Since all material was stored in the same conditions, environmental

influences such as temperature could not have a significant effect on the reactions in the mix. This facilitates consistency in the obtained results.

3.3.2 Mixing procedure

All mixes produced in this study were mixed according to the same procedure. The only variation was the different mix volumes used. Table 3.13 shows the exact volume used for each test to cast all required samples. Unfortunately, the large differences and quantity of mixes produced required volume changes to save material and therefore reduce the cost of the study.

TABLE 3.13 MIX DESIGN VOLUMES FOR VARIOUS TESTS

Test	Mix volume (Litres)
UCCT	18
Penetration time test	11.5
Hydration temperature test	11.5
Rheology testing	23
Compressive strength test	18
Buildability	40

All material used for each mix was accurately weighed off and stored as described in the Section 3.3.1. Before mixing, the mixing pan and mixer were wiped with a paper towel to ensure that the mixer was cleaned and dried properly.

The dry mix constituents were always added to the pan in the following order: aggregate, additives, and cement. All dry components were mixed for 1 minute. After this, a manual check for any unmixed material at the bottom of the pan was done. The dry components were then mixed for another minute. Superplasticizer was added to the water before addition of water to the dry components. This allows a better and faster plasticising action of the SP. The water-superplasticiser mixture was then added to the mix at a slow and controlled rate while mixing commenced. After addition of water and SP, mixing continued for another 2 minutes. Once again, a manual check was done to ensure that all components were well mixed, and no dry material was stuck at the bottom of the pan. The concrete was then mixed for another minute before the mixing process was completed. As soon as mixing was stopped, the concrete was transported to be used in its specified test.

3.4 Test setups and procedure

The tests in this study were performed on fresh as well as hardened state concrete. These tests were used to characterise the different concrete mixes with their distinct setting behaviours. The promising mixes that yielded the best results in the Phase 1 characterisation were selected for a buildability test.

All tests conducted within the study is explained briefly in this section.

3.4.1 Grading

The grading performed in this study was done according to ASTM C136. This test is used for classification of fine to coarse aggregate. The results can then be compared to the ASTM or SANS standards and conclusions can be made on the applicability of the material for its designated use.

The first step was the sample preparation. A sample of 1 kg was used in the test. The sample was washed with municipal potable tap water until the wash-water from the sample was clear. A flat-bottom pan was used to dry the sample at 110 °C until no changes in weight could be found.

The second step of the test was sieving. Sieves with sizes between 0 mm (Pan) and 4.75 mm were used for the grading process. The material was added to the top sieve and vibrated for 10 minutes. All material in the different sieves was weighed.

Lastly, the third step is to analyze the results and calculate the percentage of material passing and percentage of material retained. The particle size distribution is shown in Section 3.1.3 (*ASTM C136*, 2005).

3.4.2 Flow table test

The workability of all mixes produced was quantified with a flow table test. Cho et al., 2020, suggest that concrete mixes with flow diameters between 150 mm and 180 mm are suitable for printing. These limits were used for the development of the various mix designs. The proposed limits were used as a check during scaling of mixing volumes that the concretes workability remained within printable limits. The slump flow test itself was conducted in accordance with ASTM Test C143 *(ASTM C143, 2015).*

A flow table consists of three components, a flow table on top of a jolting mechanism, a tampering rod, and a circular metal cone. The cone has a top diameter of 60 mm, a bottom diameter of 90 mm and a height of 50 mm. The diameter of the flow table is 250 mm, and the cone is placed in its centre as shown in Figure 3.3.

FIGURE 3.3 FLOW TABLE TEST SETUP

A concrete sample was collected as soon as the mixing process was completed. Before the material could be added to the cone, the apparatus was wiped with paper towel to ensure a clean and dry device. The cone was filled halfway and tampered 10 times. After filling the cone, the sample was tampered again. All excess mortar was scraped off the top of the cone ensuring a smooth and level surface. The mould is then removed in a gentle manner to minimise disturbance of the sample and the jolting mechanism is turned 15 times at one revolution per second. During the turning process the flow table is lifted and dropped 12.7 mm to create a loading that results in a spreading of the sample. A vernier calliper was used to measure the diameter the sample has spread in two perpendicular directions. The average value of the two measurements is then noted as the flow diameter.

3.4.3 Uniaxial unconfined compression test (UUCT)

The irreversible nature of some of the setting behaviours used in this study make it difficult to use ordinary rheology tests such as the rheometer. A test that would produce a strength gain curve with multiple samples was required to be able to compare the strength gain curves of the different mixes. Wolfs *et al.*, 2018, suggested a test that met these requirements and it was implementable for this study, a uniaxial unconfined compression tests (UUCT).

Wolfs *et al.* (2018) prescribes singular circular moulds with an aspect ratio of 2. This means that the sample needs to be twice as high as it is wide. The moulds were cut from PVC pipe with an inner diameter of 74.5 mm (Wolfs *et al.*, 2018).

For each of the 8 mixes tested in the study, the same procedure was followed. All 24 moulds were oiled and placed on a Perspex plate that closes off the bottom of the mould. The mix was produced as described in Section 3.3.2. As soon as the mixing process was completed, all moulds were filled. The samples were tampered three times while filling to remove entrapped air from the sample. Figure 3.4 shows filled, and emptied moulds used in the UUCT test.

FIGURE 3.4 FILLED AND EMPTIED UUCT MOULDS

A 5 kN MTS machine was used for testing. Within its mould the sample is positioned centrally below the head of the machine and the head is lowered onto the PVC mould. To remove the mould from the sample, the mould was manually pressed against the head to ensure a straight line movement. By lifting the head and the mould that is pressed against it up, the sample slips out of the mould due to low friction on the oiled inside surface while the mould moves upwards. After extrusion, the head was lowered onto the sample again and the test

was started. A displacement of 30 mm was prescribed by Wolfs *et al*. (2018) at 30 mm/min speed for the crosshead, and the resulting force recorded using a built-in loadcell. The test was run for 1 minute per sample and after completion a force-time graph could be obtained. A typical graph obtained after test completion is shown in Figure 3.5.

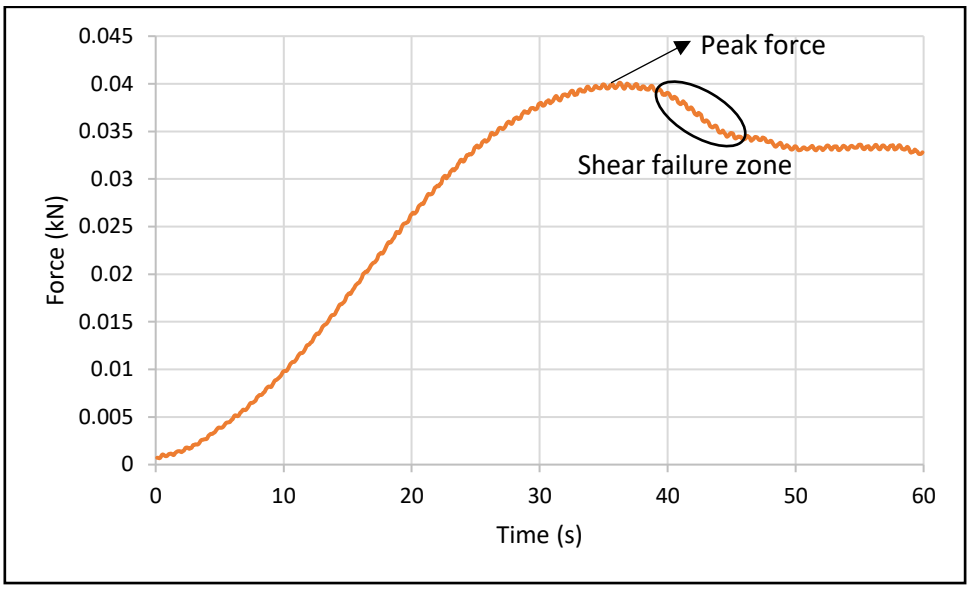

FIGURE 3.5 TYPICAL UUCT TEST RESULT OUTPUT SHOWING FORCE VS. TIME

Within the first 30 minutes of testing, 12 samples were tested at regular spaced 2-minute intervals. At 30-, 60-, 90- and 120-minutes concrete age three samples were tested for each respective time frame. The results used for stress evolution plot were the peak force values obtained from the test data. For all test results it was checked that the maximum value used was the peak compressive force before shear failure occurred. In certain instances, a higher strength was achieved after shear failure which was then not used as the peak force. Figure 3.6 shows a sample in the demoulding phase, a sample at the start of the test as well as a sample that sheared under compression marked with a red line (from left to right).

FIGURE 3.6 SAMPLE DEMOULDING AND CRUSHING PROCESS DURING UUCT TEST

3.4.4 Penetration time test

This study aims to use rapid setting concrete mixes for 3DPC. The setting time test aims to quantify the setting time within the first 12 hours after casting. A Penetration Time Test was used as test method in accordance with ASTM C403.

After the mixing procedures were completed, the concrete was cast into two 150 mm x 150 mm unoiled steel moulds to a height of 140 mm. The code states that the concrete needs to be sieved through a 4.75 mm sieve but all particles used were much smaller than this sieve. Therefore, this step was omitted. The samples were vibrated to remove entrapped air and a slump test was done with the surplus concrete in the mixer.

The test is done with 6 different needle sizes (645-, 323-, 161-, 65-, 32- and 16-mm diameter). An initial trial was used to determine the approximate setting time so that the 6 tests could be conducted at evenly spaced time intervals. Before each test, all surface water was removed, and no measurement was taken within 25 mm of the boundary or twice the diameter away from another test location in the sample. The needle was then pushed 25 mm into the sample over a time of 10 seconds. A reading of the required force for penetration could then be read from the loading apparatus ("ASTM C403 ASTM C191", 2009).

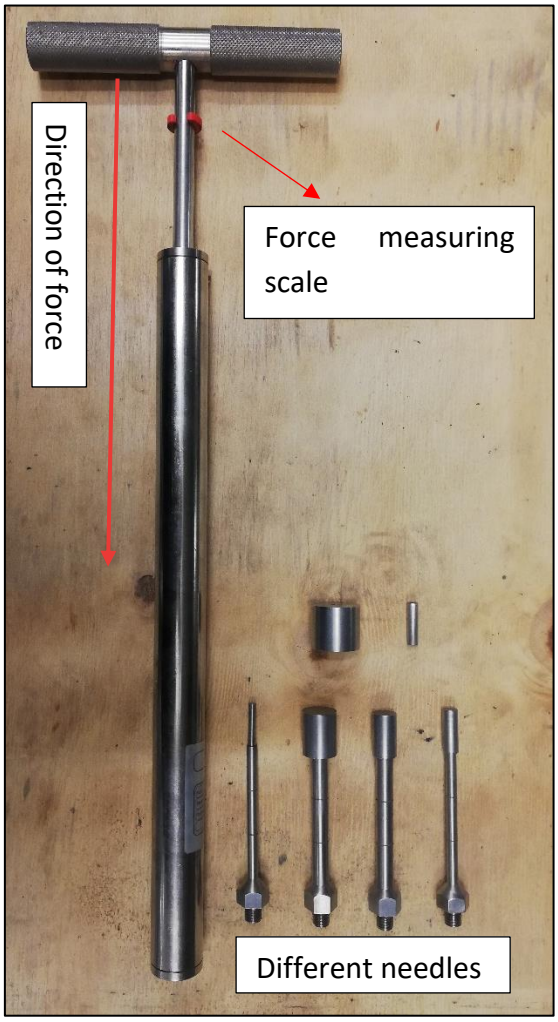

FIGURE 3.7 PENETROMETER

The measured force could then be converted from Newton to MPa by factoring it with the size of the needle base. A plot of Penetration resistance vs. time can then be used to determine the initial setting time at 3.5 MPa and final setting time at 27.6 MPa. All measurements at each time interval were taken from two samples. The average value was then used for the setting time calculations.

3.4.5 Hydration temperature

Hydration temperature measurements were conducted to gain insights on the temperature development of the different mixes. This can help define and characterise certain hydration steps and classify the different setting behaviours.

Vishay NTC Type 10 kΩ Thermistors were used to measure the temperature development of 100 x 100 x 100 mm cast cubes over a period of 3 days. The cubes were kept in their moulds throughout the testing period. All mixing constituents were previously stored in the temperature-controlled room for 24 hours to ensure consistency.

The setup procedure for the test was done as follows. The thermistors were connected to a copper wire and the connections were sealed thoroughly. All thermistors were fixed to a position 50 mm from the bottom of the mould. Figure 3.8 shows the setup before the concrete was added to the mould. As soon as the mixing process was completed, the concrete was added to the mould. It was checked that the thermistors were kept in the middle of the sample. To remove all entrapped air within each sample, the cubes were vibrated for one minute.

FIGURE 3.8 HYDRATION TEMPERATURE MEASURING SETUP

After casting the cubes, the cables were connected to the temperature logger. It was vital to get the setup connected as fast as possible to measure all the early age hydration temperature developments of the concrete. The moulds were also placed in Styrofoam boxes. Duct tape and metal weights were used to ensure that the box lids were sealed properly. Figure 3.9 shows this setup.

FIGURE 3.9 STYROFOAM INSULATION BOX SETUP WITH CUBES FOR HYDRATION TEMPERATURE TEST INSIDE

When the testing period of 65 hours was completed, the data could be extracted. The temperature development of each mix was plotted and analysed.

3.4.6 Rheology testing (Dynamic and static yield stress)

A comparison of the rheological properties between the REF_3DPC mix and the REF mix was done with a German Instruments ICAR Rheometer (Germann Instruments, 2010). The rapid setting mechanisms are not all reversable or reversable for multiple test runs. Therefore, no tests with the rheometer were done on the rapid setting mixes. Nonetheless, the results from the test can provide insight on the different dynamic and static yield stresses, thixotropic behaviour, and structuration rate of the two reference mixes.

The rheometer consists of a cylindrical container and a four-bladed rotating vane connected to a driving motor. Inside the bucket there are 15 10 x 10 mm plastic ribs that prevent shearing along the perimeter. The container has a radius of 143 mm and has a depth of 127 mm. Four blades make up the vane that has a radius of 63.5 mm. The volume of the container is 20 litres but generally about 18 litres of concrete was used for a test. Figure 3.10 demonstrates the fully set up rheometer before the addition of concrete.

FIGURE 3.10 ICAR RHEOMETER (ICAR-RHEOMETER - GERMANN, 2021)

Setting up the rheometer requires connecting of all components and resetting of the device to define the zero-force reading. After this, the concrete can be added to the bucket up to the top of the plastic ridges. The vane is inserted into the bucket. Shaking the bucket ensures that there are no voids around the vane when inserted into the concrete.

Multiple strength growth tests were done to determine the rheological properties of the reference mixes for this study. The influence of the repetitive bond breaking by the rotating vane on the rapid setting cement mixes is not entirely clear. At each time interval the bonds formed during the resting period are broken. After analysis of the test results for the rapid setting concrete mixes, it was concluded that the rheometer influences the setting behaviour of the rapid setting mixes. Therefore, only the rheological properties of the reference mixes are discussed in this study. Other tests would be required to quantify the rapid setting behaviours.

In this study, the static yield stress development over time is of specific interest and can be determined with a stress growth test. The test was run over a period of 1 minute at a rate of 0.025 revolutions per second with increasing resting times between tests as shown in Table 3.14. The shearing rate corresponding to the rotational speed was 1.25 s^{-1}.

TABLE 3.14 RHEOLOGICAL TESTING PROTOCOL FOR STRESS GROWTH TEST

Test No	Concrete age after mixing	Resting time	Test duration	Action
-	00:00 - 01:00	-	-	Transport concrete to rheometer
1	01:00 - 02:00	0 s	60	Stress growth test
2	02:10 – 03:10	10 s	60	Stress growth test
3	03:30 – 04:30	20 s	60	Stress growth test
4	05:00 – 06:00	30 s	60	Stress growth test
5	06:40 – 07:40	40 s	60	Stress growth test
6	08:30 – 09:30	50 s	60	Stress growth test
7	10:30 – 11:30	60 s	60	Stress growth test
8	13:00 – 14:00	90 s	60	Stress growth test
9	16:00 – 17:00	120 s	60	Stress growth test
10	32:00 - 33:00	15 min	60	Stress growth test
11	63:00 - 64:00	30 min	60	Stress growth test
12	124:00 - 125:00	45 min	60	Stress growth test

3.4.7 Compressive strength test

Compressive strength tests were done on all 8 different mixes according to SANS 5863:2006 (SANS,2006c). This test would then be used to determine the influence of the admixtures on the compressive strength of the concrete.

Concrete cubes with dimensions 100x100x100 mm were cast and vibrated for 1 minute. The samples were stored at 23 °C (± 2) and a relative humidity of 65 % (± 5) for 24 hours. After 24 hours the cast cubes were demoulded. The cubes were kept in a curing bath at a temperature of 25 °C. Three cubes of each mix were tested at 1, 3, 7, 14 and 28 days after casting. On the relevant days, the cubes were removed from the curing bath. All sides of each cube were dried before testing. Each cube was weighed, and the outside dimensions were measured so that density and volume could be obtained. A Kingtest Contest 2 MN compression testing machine was used for this test. The cubes were placed in the machine with a steel plate on top. At a rate of 180 kN per minute, the compressive strength of the cubes was tested. The maximum force measured by the machine was noted and the maximum compressive strength was calculated by:

$$\sigma = {}^{F}/_{A} \quad (MPa) \tag{3.1}$$

With the parameters as follows:

σ- Compressive strength of concrete

F- Compressive force at failure (N)

A- Area of the tested cubes (mm^2)

The setup of the machine and the positioning of the cube are shown in the Figure 3.11.

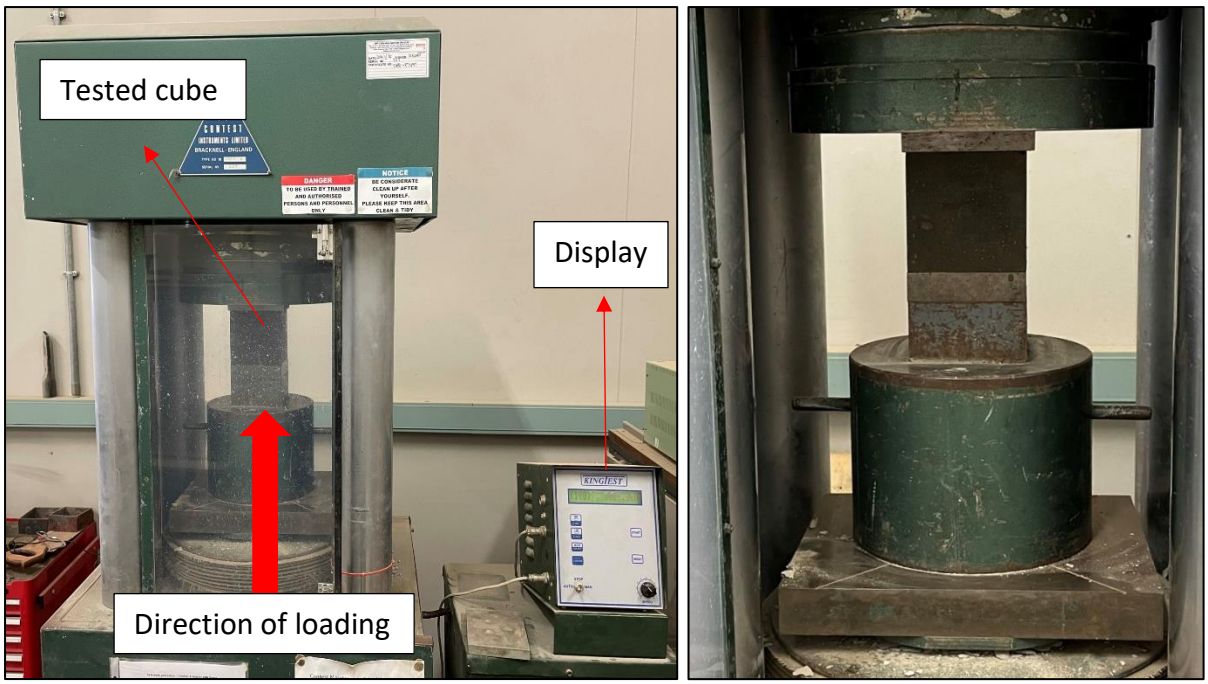

FIGURE 3.11 KINGTEST CONTEST MACHINE AND CUBE SETUP

3.4.8 Buildability

A lower bound model for the buildability quantification of 3DPC mixes was proposed by Kruger *et al.* (2019). The model was verified by printing a circular hollow column and comparing the results from the model to the results from that physical print (Kruger *et al.*, 2019). To compare the buildability of different mixes tested in this study, circular hollow columns were printed. The printing parameters, shown in Table 3.15, were used to set up the 3D printing parameters.

TABLE 3.15 INPUT PARAMETER FOR CIRCULAR COLUMN PRINTING

Printing Parameter	Value
Circumference (l_p)	785 mm
Layer thickness (w_l)	30 mm
Layer height (t_l)	10 mm
Print speed (v)	60 mm/s
Filament aspect ratio (h_l/w_l)	0.33
Diameter	250 mm

After completion of a 40-litre mix, a flump slow test was done to determine the concrete's workability. The concrete mix was added to the hopper and the pump was started immediately to prevent setting of the mixture inside the hopper. In addition, a vibrator was used to keep the concrete flowable throughout the printing period. Before the circular column print was started, approximately 5 litres of concrete were extruded into a bucket to ensure that the pipe was primed. Only when a constant extrusion rate of concrete without any voids was observed, the circular column print was started. A column with the properties shown in Table 3.15 was printed either to failure or to a maximum height of 900 mm at a building rate of 45.86 mm/min. Figure 3.12 shows a circular column printed during one of the prints. The pumping frequency was adjusted during the printing process for the mixes that stiffened up too rapidly to ensure a good printing quality and a constant layer width of 30 mm. A video of the entire print was taken for later determination of the column's failure mechanisms.

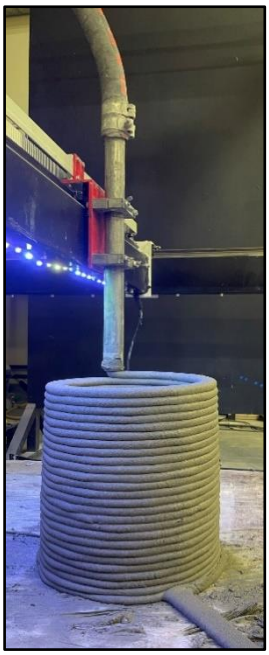

FIGURE 3.12 CIRCULAR HOLLOW COLUMN DURING PRINTING

The first buildability print of each mix was done according to the mix design used for the Phase 1 characterisation. After an assessment of the first print, adjustments to the mix design were made with the aim to improve the buildability of the mixture. Section 3.2.5 discusses the changes made for potential improvements. The same printing procedure was used for all buildability tests. The 3D printer used for this study is shown in Figure 3.13.

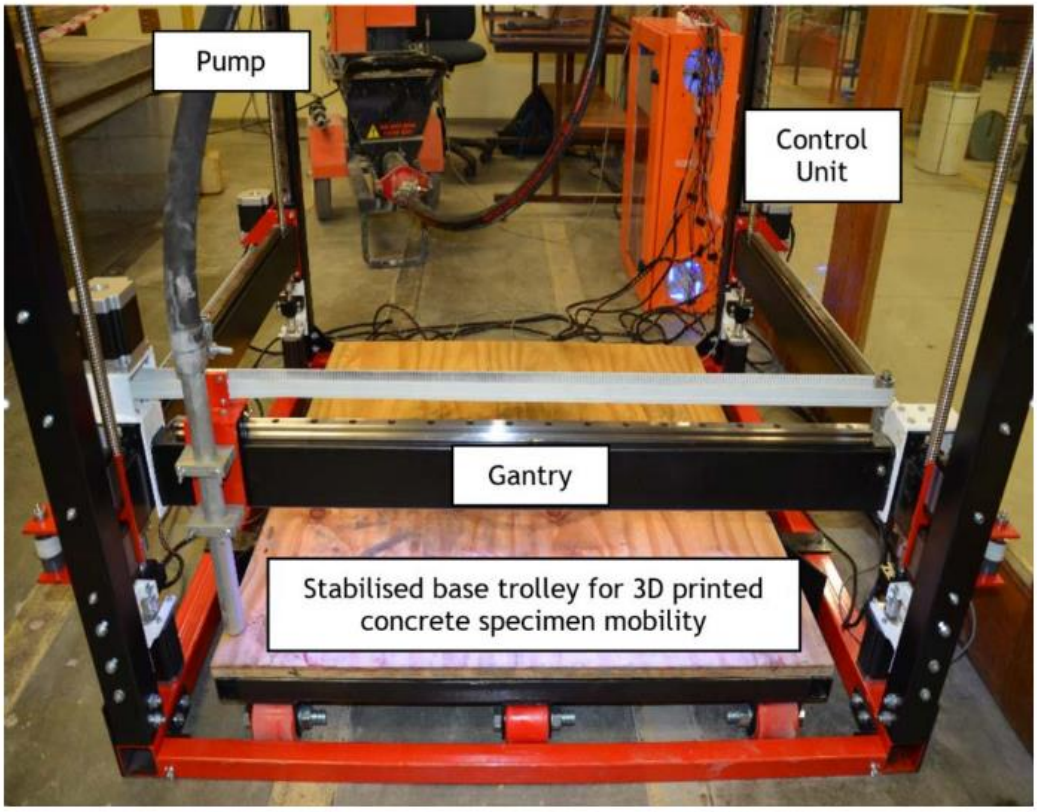

FIGURE 3.13 3D CONCRETE PRINTER USED AT STELLENBOSCH UNIVERSITY (KRUGER, 2019)

3.5 Testing Programme

As described in the preceding sections, the testing in this research was divided into two phases. The first phase being a characterisation of the various mixes. The second phase was the printing of the most promising mixes from Phase 1. Table 3.16 summarises the testing programme followed in this study.

Before the actual testing could commence, all mix compositions were developed, and their setting behaviour was evaluated. Small mixes were prepared, and it was checked that the same setting as described in literature was observed in the samples. The mixes were then tested for pumpability to ensure that printing of such mixes would be possible before all characterisation tests were done. The characterisation was required to determine the most suitable mixes from each of the three different rapid setting behaviours.

TABLE 3.16 TESTING PROGRAMME

Test	Number of samples per data point	Obtained results	Testing period
UCCT	1	Yield stress	0-30 minutes at 2-minute intervals 30, 60, 90, 120 minutes
Penetration time test	2	Setting time	10 hours
Hydration temperature test	3	Hydration temperature curve	3 days
Rheology testing	1	Rheological properties: Static/dynamic yield stress	0-120 seconds 15, 30, 45 minutes
Compressive strength test	3	Compressive strength development	1, 3, 7, 14 and 28 days
Buildability	1	Layers printable in direct succession	Until failure

4 Results

In this chapter, the results obtained are analysed and discussed. The Phase 1 characterisation of the mixes was used to select the most suitable mixes for printing in Phase 2.

The following procedure is followed for the Phase 1 results discussion. Both reference mixes and one of the three other rapid setting types are discussed individually. This will be repeated for all three setting behaviours. Finally, a summary of the results is used to highlight the differences between the three mixes.

For Phase 2, the results obtained are first discussed individually and then they are compared. A possible correlation between Phase 1 tests and the results obtained during printing are compared.

4.1 Phase 1: Material characterisation

4.1.1 Compressive strength

The compressive strength of all mixes was measured between 1 and 28 days after casting. All results shown in the various graphs are an average of three cubes measured at each specific time interval after casting. The error bars on the charts express the standard deviation.

The two reference mixes, REF and REF_3DPC, are shown in all figures. These mixes are the benchmark to which all mixes are compared to. The ordinary concrete mix, REF, shows a rapid strength gain within the first 7 days compared to REF_3DPC. Higher compressive strengths were obtained than for REF_3DPC up to one week after casting. The peak compressive strength measured at 28 days for REF was 41.34 MPa. Continuous cube strength development can be found for the REF_3DPC. A slower strength development compared to REF can be seen within the first week but a higher peak compressive strength of 46.68 MPa was measured 28 days after casting. Increased standard deviation can be observed for both reference mixes at increased concrete age.

Even though the water to binder ratio for REF (0.425) was lower than for REF_3DPC (0.45), lower compressive strength was achieved for REF. The positive influence of the fly ash and silica fumes contained in REF_3DPC on the compressive strength of concrete needs to be considered. Silica fumes and fly ash were found to improve the strength of concrete (Rassokhin, Ponomarev & Figovsky, 2018; Taylor, 1997). At a water to binder ratio of 0.32, this is significantly lower compared to REF. Lower water-binder contents are known to increase the compressive strength of concrete which is shown in the obtained results. At higher water-binder ratio, the porosity of concrete is higher which reduces the compressive strength (Harrison, 2003; Moir, 2003; Taylor, 1997).

Figure 4.1 shows the compressive strength development of the two false setting mixes together with the reference mixes. FA_4 exhibits higher strength than FA_2 throughout the testing period. The majority of strength development is complete after 7 days and only a slight increase in strength can be seen between 7 days and 28 days after casting. A maximum compressive strength of 41.97 MPa was achieved for FA_4. FA_2 shows a slow strength gain

pattern similarly to REF_3DPC in the first 3 days. Between 7 and 28 days after casting, the compressive strength of FA_2 and REF is similar. The maximum compressive strength for FA_2 was 41.78 MPa.

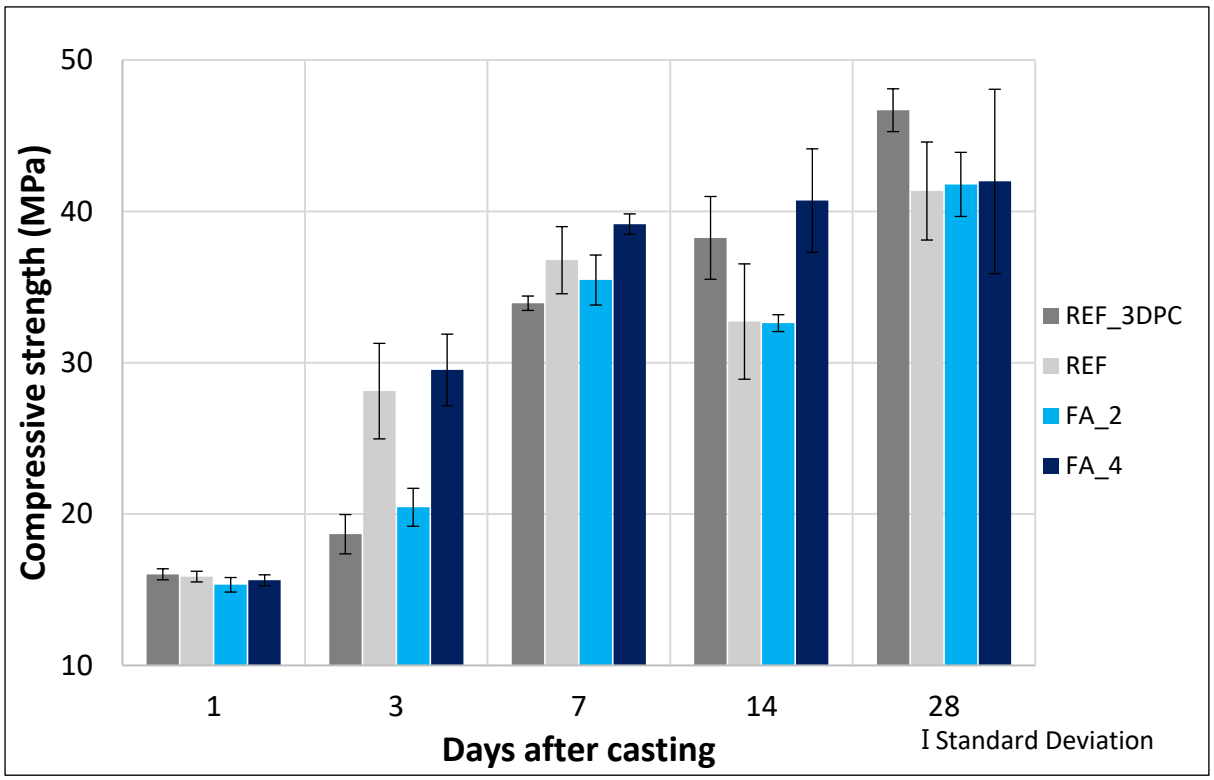

FIGURE 4.1 COMPRESSIVE STRENGTH OF FALSE SETTING MIXES COMPARED TO REFERENCE MIXES

The strength development for the false setting mixes is the same as the REF mix. No significant changes in compressive strength were found between the REF mix and the false setting mix. The addition of calcium sulphate hemihydrate only influences the early age strength development but does not influence the compressive strength. Both false setting mixes have a lower compressive strength after 28 days compared to REF_3DPC. The ettringite formed hydrates further to form monosulphate (Beaudoin & Odler, 2019). As this is a hydration product that is also formed during the normal hydration of OPC cement, it does not affect the compressive strength development and only provides stiffness at early ages.

Figure 4.2 shows the compressive strength development of BC_5 and BC_10 in comparison to the reference mixes. Both mixes show slightly higher compressive strength one day after casting. The BC_5 mix follows the same strength development pattern as REF. No significant differences in compressive strength were found for 5% replacement of OPC with BCSA cement. Overall, the compressive strength measured for BC_5 is marginally higher than REF. A maximum compressive strength of 41.86 MPa was obtained for BC5. The compressive strength development of BC_10 was lower on average than for BC_5 from 1 day after casting onwards. A 28 day compressive strength of 38.36 MPa was measured for BC_10.

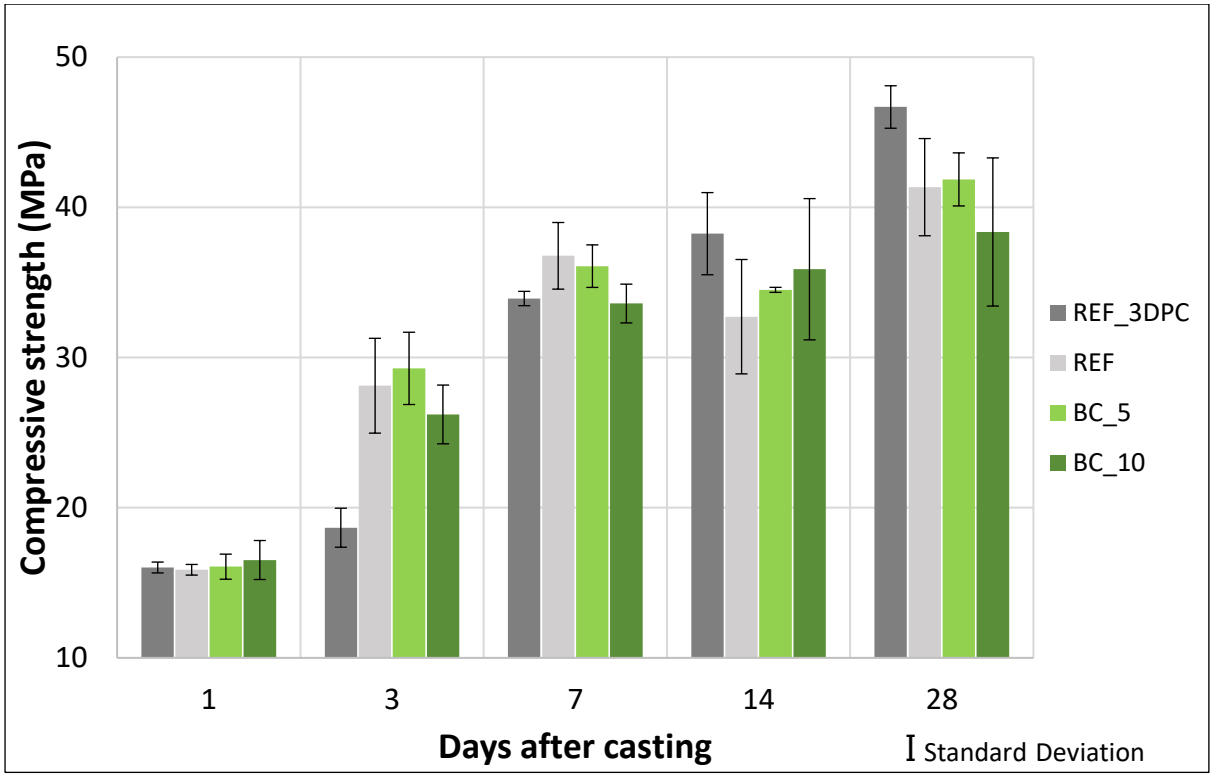

FIGURE 4.2 COMPRESSIVE STRENGTH OF BCSA MIXES COMPARED TO REFERENCE MIXES

The lower replacement rate of 5% has no significant effect on the compressive strength development. A higher replacement rate decreases the 28-day compressive strength. This suggests that BCSA cement limits the compressive strength development at higher replacement percentages. In this study, the replacement rate is still low and higher dosage replacement would be required to confirm this trend. To summarise, the 5% or 10%. replacement of ordinary Portland cement with BCSA cement does not have a major influence on the compressive strength development. No major increase or decrease in compressive strength was found. BC_5 was found to be 1.26% (+- 1.77 MPa) stronger and BC_10 was 7.2% (+-4.93 MPa) weaker than REF 28 days after casting. The hydration of OPC cement is not directly affected with the addition of BCSA cement. Ye'eliminate hydrates to form ettringite which improves the early age strength development. The belite (C_2S) hydration produces C-S-H which improves the compressive strength development at later ages (Rosero, 2020). As a result, the addition of BCSA cement improves the early age strength development as more ettringite is formed in the mixture between OPC and BCSA. The compressive strength is not significantly influenced since sufficient C-S-H is formed.

The compressive strength of the flash setting mixes is shown in Figure 4.3. It is evident that the compressive strength is negatively affected by the flash setting. Both mixes, FL_0.5 and FL_1, show the same pattern for the compressive strength evolution curve. Within the first 7 days after casting the main strength gain phases for both concrete mixes are complete. The major difference is that FL_1 is significantly weaker than both reference mixes. At 28 days after casting, the compressive strength is approximately half compared to the reference mixes. Only a third of the compressive strength was measured one day after casting. A 28-day

cube strength of 21.78 MPa was achieved. The standard deviation of the results is low and confirms the accuracy of the measured results. FL_0.5 has a higher compressive strength than FL_1 throughout the 28-day testing period. A constant lower compressive strength compared to REF is noticeable. REF_3DPC has a lower compressive strength 3 days after casting. FL_0.5 had a peak cube strength at 28 days of 33.19 MPa

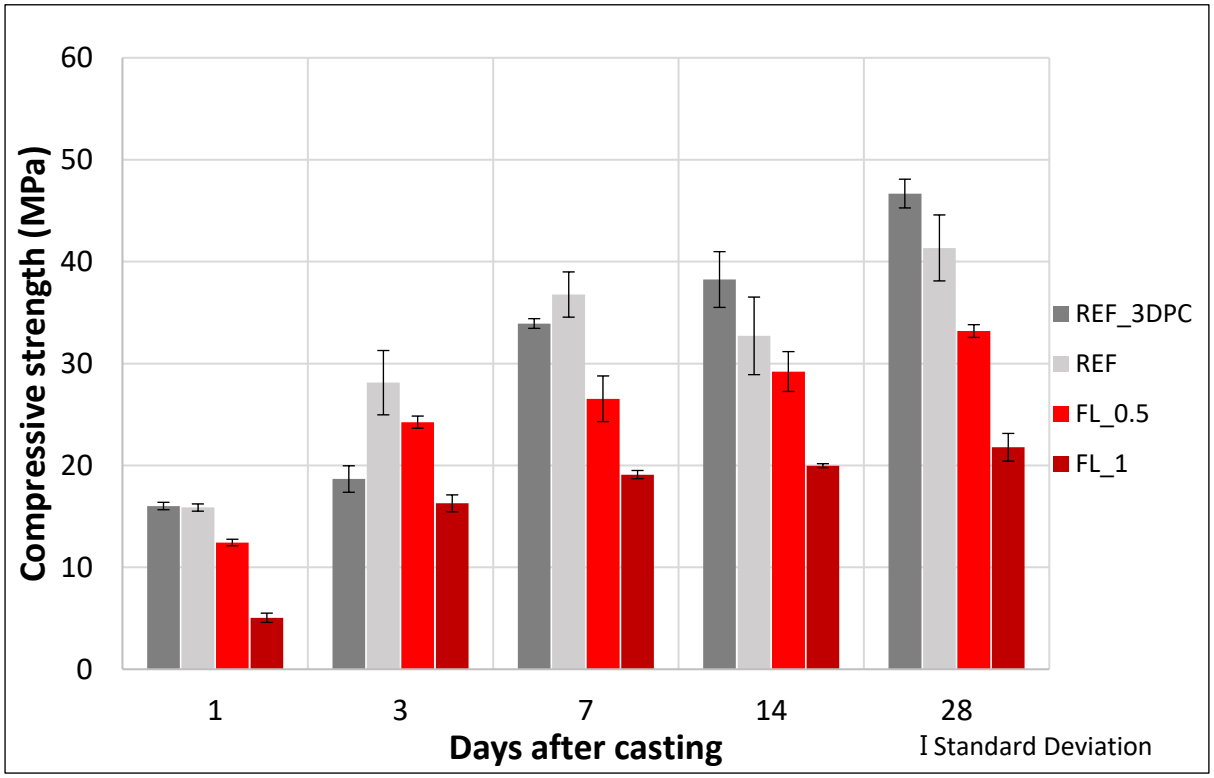

FIGURE 4.3 COMPRESSIVE STRENGTH FLASH SETTING

At lower aluminate content, the flash setting effect is reduced. In return, the reduction of flash setting intensity has a reduced influence on the compressive strength development. Higher compressive strength was achieved for a lower aluminate dosage. The compressive strength of concrete is reduced with the presence of flash setting. The main hydration product formed in the presence of sodium aluminate is ettringite. Due to an increased quantity of ettringite and calcium aluminate hydrate in the presence of sodium aluminate, less calcium silicate hydrate is formed (Han *et al.*, 2014). As the formation of calcium silicate hydrates is essential for the compressive strength development of concrete, lower C-S-H quantities negatively affect the compressive strength (McCarthy, 2008).

Figure 4.4 summarises the compressive strength development of all characterised mixes in this study. All three setting behaviours do not increase the compressive strength of the concrete. Flash setting reduces the compressive strength of the concrete significantly and has a significantly lower compressive strength over the entire testing period. The reduced hydration of silicate phases negatively impacts the compressive strength. Excessive formation of aluminate phases improves the compressive strength at early ages but has no significant impact on the compressive strength development (Beaudoin & Odler, 2019; McCarthy, 2008). The cement replacement with BCSA limits the compressive strength development of the

concrete. Higher compressive strength can be achieved after 24 hours with the addition of BCSA, but the long-term compressive strength is limited as previously mentioned. The highest compressive strengths up to 14 days was achieved with the 4% calcium sulphate containing mix. The compressive strength development of FA_4 is limited 14 days after casting and no significant compressive strength gain is detected at 28 days. At lower addition of hemihydrate, the compressive strength is not really affected. Both BCSA addition and false setting have no significant effect on the formation of C-S-H. As a result, the long-term strength is not much influenced.

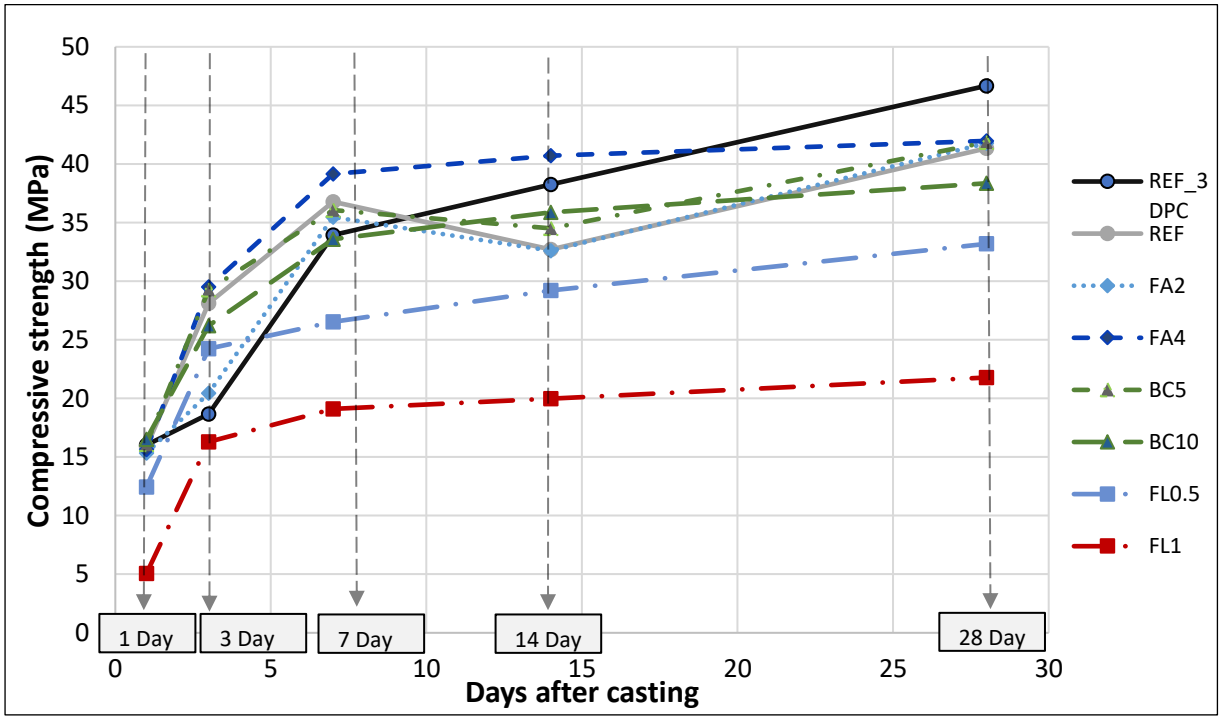

FIGURE 4.4 COMPRESSIVE STRENGTH SUMMARY

To conclude, flash setting reduces the compressive strength whereas BCSA replacement and false setting do not significantly influence the compressive strength significantly.

4.1.2 Rheology

The differences in rheological properties can be understood from the rheometer results of both reference mixes. REF is the base mix off which all rapid setting mix designs were developed. The rheological properties of this mix influence the properties of the rapid setting mixes. Therefore, the comparison of rheological properties of the references can give insight on the difference in behaviour of these mixes. The rheological test results are shown in Figure 4.5.

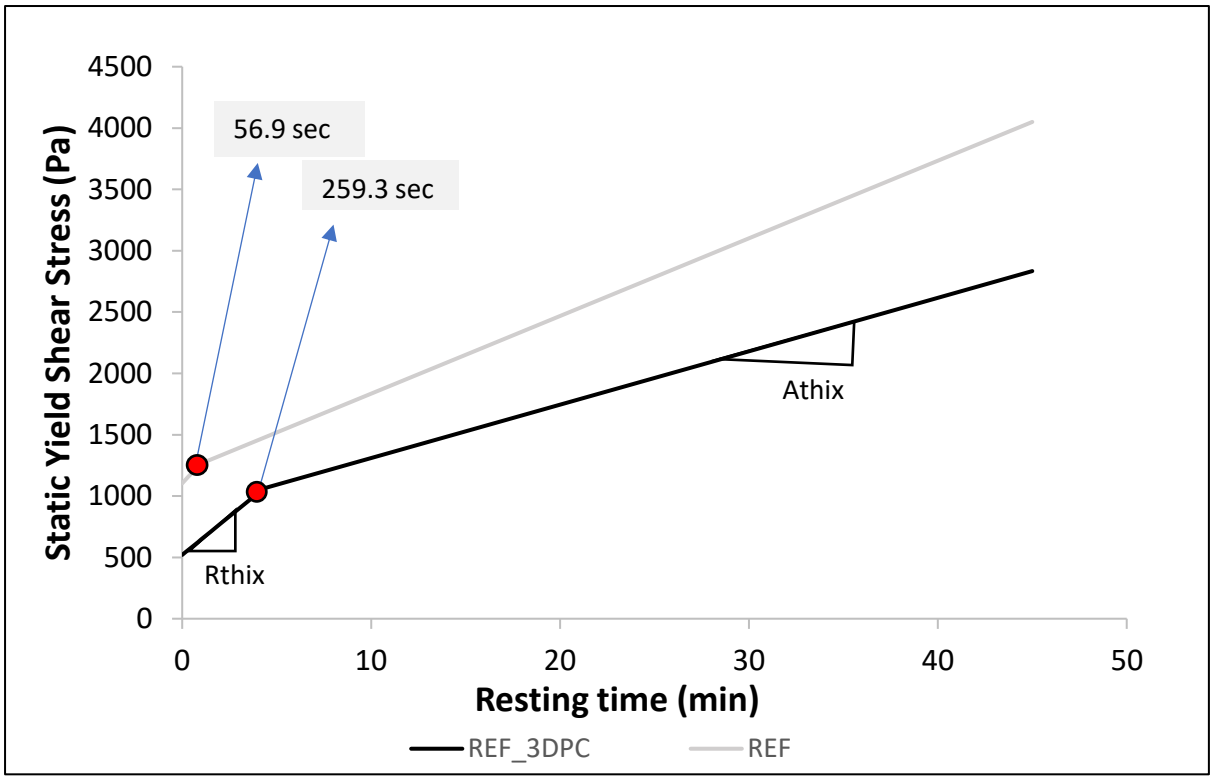

FIGURE 4.5 RHEOLOGY RESULTS FOR REFERENCE MIXES

The concept of Athix and Rthix was introduced by Kruger et. al (2019). The rheology testing for this study was conducted in the same manner to obtain both parameters. The parameters were then used to characterise the rheological properties of both mixes (Kruger *et al.*, 2019).

Figure 4.5 clearly shows that there are differences between the two reference mixes. The initial static yield stress of the REF mix is twice as high as the REF_3DPC. This result makes sense since the REF_3DPC contain fly ash and silica fumes that increase the fines contents which reduces the yield stress of the mix. The re-flocculation period of both mixes is shown for each respective mix. REF_3DPC reflocculates about 200 seconds later than REF. In Table 4.1 the exact duration of Rthix and Athix are shown. REF re-flocculates at a higher rate (Rthix) but for a shorter period. REF_3DPC reflocculates slower but significantly longer. The structuration rate (Athix) of REF is higher than for REF_3DPC. As a result, REF_3DPC takes longer to harden but still continuously gains in strength with time. This makes it an ideal mix for printing as more time is available to place subsequent layers on top of each other without any bonding issues. The static yield stress measured for REF is higher than for REF_3DPC throughout the test. The rapid structuration of REF allows results in a larger strength build up over the same period. More layers can be printed over the same period because the concrete gained more strength. A higher number of printable layers means that better buildability can be achieved.

TABLE 4.1 ATHIX AND RTHIX VALUES FOR REFERENCE MIXES

	SU		GH	
Rthix	2.10	Pa/s	2.77	Pa/s
Athix	0.73	Pa/s	1.06	Pa/s

To conclude, the two reference mixes have different rheological characteristics. From the results shown in Figure 4.5, it can be assumed that the REF mix has a higher buildability than the REF_3DPC mix. The effect of the rapid setting behaviour on the rheological characteristics cannot be determined from a single bath. A multi-batch approach is recommended to determine the rheological properties of such setting behaviours with a Rheometer.

4.1.3 Hydration temperature

The hydration temperature was measured using thermistors embedded in the centre of 100 mm concrete cubes. The results shown in this section are average values measured from three cubes per mix. It is important to note that half the samples were mixed at an ambient temperature of 23 °C and the other half at 17 °C. The ambient temperature affects the temperature of the mixing pan which then effects the temperature of the concrete. Even though the material was stored under constant conditions, the effect of the mixing pan on the concrete temperature was visible in the results. Table 4.2 below displays the measured initial temperature, peak temperature and absolute temperature increase referred to within this section.

TABLE 4.2 HYDRATION CURVE CHARACTERISTICS

			Peak temperature		
Mix	Initial Temperature (°C)	Abs temperature increase (°C)	Peak temperature (°C)	Standard Deviation	COV (%)
REF	24.07	19.53	41.91	0.65	1.55
REF_3DPC	23.38	21.02	43.35	0.64	1.48
FA2	25.43	24.16	46.19	0.71	1.53
FA4	18.09	26.48	44.22	0.12	0.28
BC5*	25.91	22.23	44.38	3.19	7.19
BC10	18.45	23.79	42.23	0.98	2.32
FL0.5*	18.83	20.47	39.30	0.01	0.02
FL1	22.20	20.52	42.29	0.47	1.12

* Data only from 2 samples after elimination of outlier

The data analysed for each hydration curve was collected from 3 samples. Comparing the three data points, samples that were obvious outliers due to malfunctioning of thermistors were eliminated. The measured temperature of a sample was classified as malfunctioning when the temperature plotted followed no sensible pattern. Such patterns are upward and downward spikes visible in the hydration temperature plots that are not observed for any of the other samples. Data collected of temperature curves developed of two samples, and not three as the rest, are marked with a star in Table 4.2.

The two reference mixes are shown in all figures below. Both were mixed at an ambient temperature of 23 °C. Even though both were mixed under the same conditions slight differences can be seen in the initial temperature. The period before the main hydration period is longer for REF_3DPC than for REF. The main hydration reaction starts much sooner for the REF mix than for the REF_3DPC mix. REF_3DPC has a swifter hydration reaction than REF. This is shown by the steeper slope between the start of the main hydration period and the peak temperature. The absolute temperature increase for REF_3DPC is 21.02 °C with a peak temperature of 43.35 °C. REF has a lower peak temperature of 41.91 °C and absolute temperature increase of 19.53 °C. These results indicate a lower hydration temperature development for REF in comparison to REF_3DPC. Both mixes follow the same hydration temperature development from 20 hours onwards.

In Figure 4.6, the hydration temperature development of the false setting mixes in comparison with the reference mixes is also shown. FA_4 was mixed at lower ambient temperature which explains the lower initial measured temperatures.

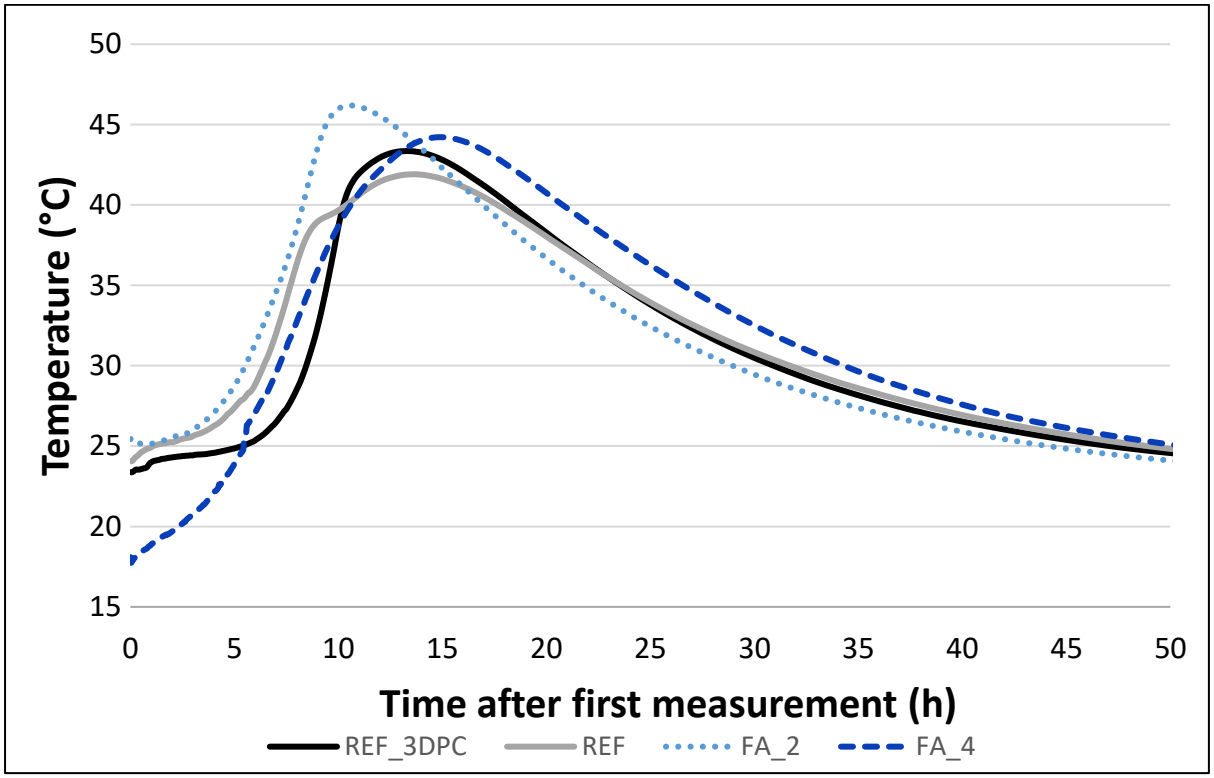

FIGURE 4.6 HYDRATION TEMPERATURE DEVELOPMENT FALSE SETTING

In the first 4 hours after test start, the hydration temperature measured for FA_2 does not increase. This may be an indication for a reduced rate of hydration. Thereafter, as steep rise in temperature can be observed and a peak temperature of 46.19 °C was measured. The main hydration period starts earlier than for the REF_3DPC mix and reaches a higher peak temperature. FA_2's hydration temperature drops faster than of the other hydration curves shown.

The hydration curve for FA_4 differs from FA_2. During the first 5 hours after test start, the temperature rises from about 18 °C to 25 °C. Subsequently, the main hydration period starts. The slope towards the peak temperature is flatter than for FA_2. A peak temperature of 44.22 °C is reached just after 15 hours which is higher than both reference mixes. This is about 4 hours later than for FA_2. The overall hydration temperature curve of FA_4 is delayed compared to the reference mixes and the FA_2.

To summarise, both false setting mixes have a higher peak temperature than the reference mixes. False setting consequently increases the hydration temperature of concrete. In comparison to REF, FA_2 and FA_4 reached at 10.2%/5.5% higher peak temperature respectively. The absolute temperature increase of both false setting mixes are closely together and is the highest of the three setting behaviours tested.

The hydration curves for the BCSA containing mixes compared to the reference mixes are shown in Figure 4.7. BC_10 was mixed at lower ambient temperature than the other three mixes.

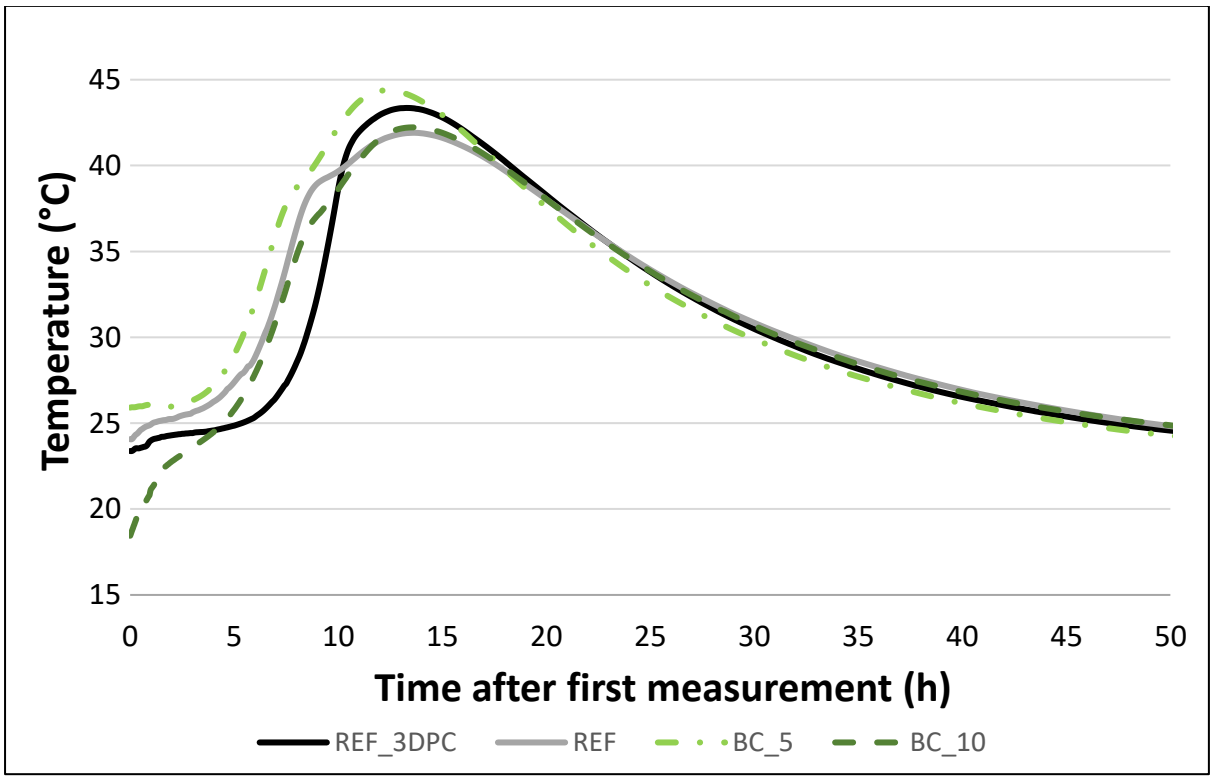

FIGURE 4.7 HYDRATION TEMPERATURE DEVELOPMENT BCSA REPLACEMENT

Even though BC_5 was mixed at about the same temperature as the reference mixes, the initial temperature at test start is higher than the reference mixes. No significant change in temperature can be observed within the first 4 hours after test start. The peak temperature measured at around 12 hours for BC_5 was 44.38 °C. BC_5 reached its peak earlier than all three other mixes shown in Figure 4.7. The shape of the hydration temperature curve of both mixes containing BCSA are similar to the REF mix and not as steep as the REF_3DPC mix in the main hydration phase between 5-10 hours.

BC_10 has a steep initial spike in temperature in the first 2 hours. A flatter slope can be detected up to 5 hours after test start with a plateauing of the temperature rise to 5 hours after the start of thetest. The peak hydration temperature of 42.23 °C was reached at about 15 hours. REF and BC_10 have a similar peak temperature that is reached at the same time. The hydration curve for BC_10 is delayed in comparison to BC_5.

Summarising, the replacement of CEM I 52.5N with BCSA cement increases the hydration temperature at a lower dosage. The lower peak temperature for the higher BCSA containing mix may be a result of the low initial concrete temperature. A higher absolute temperature in comparison to REF for BCSA containing mixes is another indication for a rise in hydration temperature.

Figure 4.8 shows the comparison of the reference mixes to the flash setting mixes. Both flash setting mixes were produced at lower ambient temperature than the two reference mixes. The lowest absolute temperature increase of the three rapid setting concrete types was found for flash setting concrete.

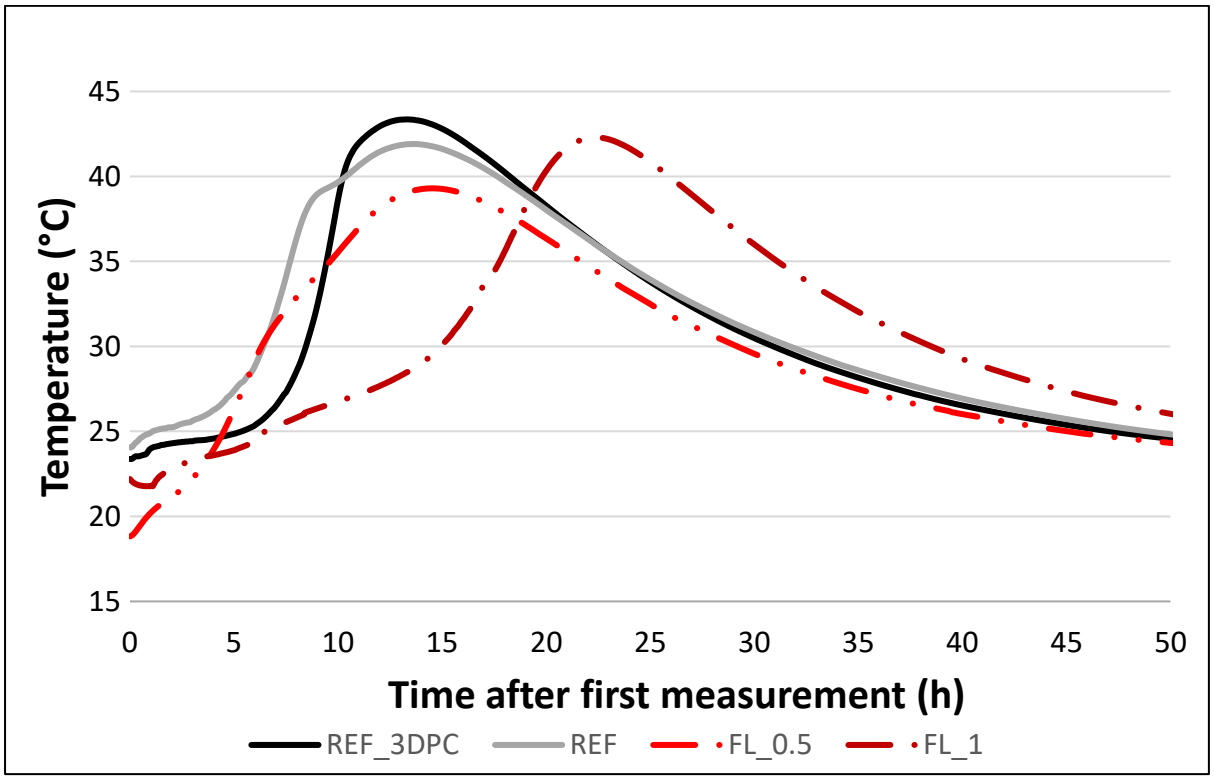

FIGURE 4.8 HYDRATION TEMPERATURE DEVELOPMENT FLASH SETTING

The initial temperature for FL_0.5 is higher than for BC_10 or FA_4. This suggests that hydration is already taking place at and before start of test. Within the first hour after test start, the temperature rises steeply in FL_0.5. The steepness of the slope reduces between 1 and 3 hours after which an increase in slope can be observed again. This suggests that a reduced hydration reaction takes place which can be a form of dormant period. FL_0.5 follows a similar hydration curve pattern to the reference mixes but only reaches a peak temperature of 39.3 °C. A lower temperature than all other mixes characterised. An intermediate peak can be found for FL_0.5 at about 7 hours.

Even though the two flash setting mixes were mixed at the same temperature, the initial temperature measured for the FL_1 mix is much higher than the FL_0.5 mix. This suggests that a reaction has happened between completion of mixing and test start. Han *et al.* (2014) found a peak in heat release rate 5 minutes after casting. This explains the increased initial temperatures of both flash setting mixes. The temperature in FL_1 rises at a flat slope in the first 15 hours but only reaches peak temperature of 42.29 °C between 20 and 25 hours. All other mixes reach their maximum temperature between 10 and 15 hours. The entire hydration temperature curve for FL_1 is shifted and shows a delayed temperature development curve.

To summarise, increased initial temperatures can be observed for flash setting concrete. This is an indication that between completion of mixing and test start, hydration reactions have started. Literature suggests a high temperature development when water is added to the dry mix constituents of flash setting mixes (Beaudoin & Odler, 2019). The obtained results show this suggested temperature development which confirms a typical flash setting behaviour. The extent of the severity of the temperature development may be temperature dependent and needs to be determined in a further study.

The hydration temperature development of all eight characterised mixes is shown in Figure 4.9. In summary, the flash setting mixes don't have higher peak hydration temperatures than the reference mixes. Increased hydration temperature was only found at early ages. False setting seems to increase the hydration temperature significantly and the BCSA containing mixes only have slightly higher temperature development than the reference mixes. The highest peak temperature was observed for FA_2 and the lowest for FL_0.5. The hydration for FA_4 and especially for FL_1 are delayed compared to the other mixes. The main hydration phase for all mixes started at around 25 °C regardless of their initial temperature.

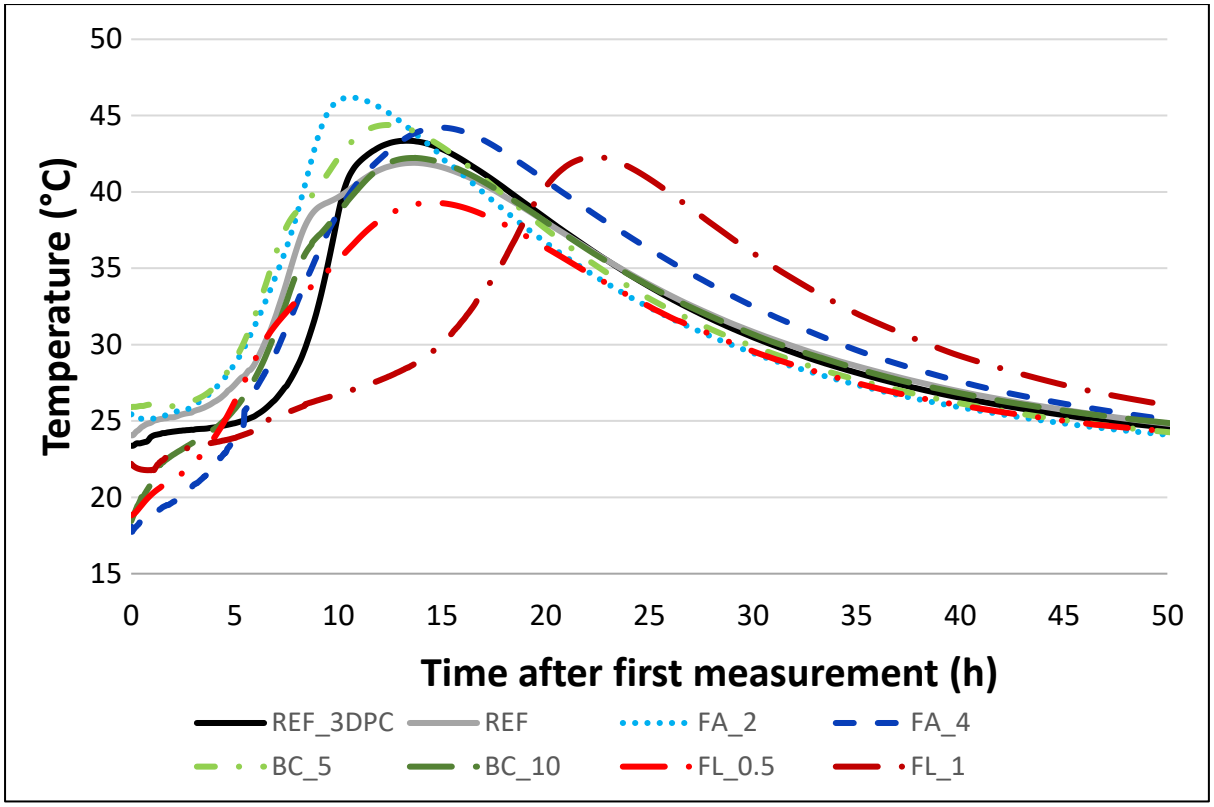

FIGURE 4.9 HYDRATION TEMPERATURE DEVELOPMENT SUMMARY

For the mixes produced at lower temperatures, the initial temperature was lower. The surrounding temperature influences the hydration behaviour. Higher temperatures increase the rate of hydration (Borštnar *et al.*, 2020; Harrison, 2003). BC_5 and FA_2 were both mixed at higher temperature than BC_10 and FA_4. Higher peak temperatures can be observed as well as faster hydration rates which coincides with the information gathered from literature.

4.1.4 Setting time test

As described in Chapter 3, a penetrometer was used to determine the setting times of all mixes. The results discussed are average values measured of 2 separate samples. Figure 4.10 shows the setting time test results.

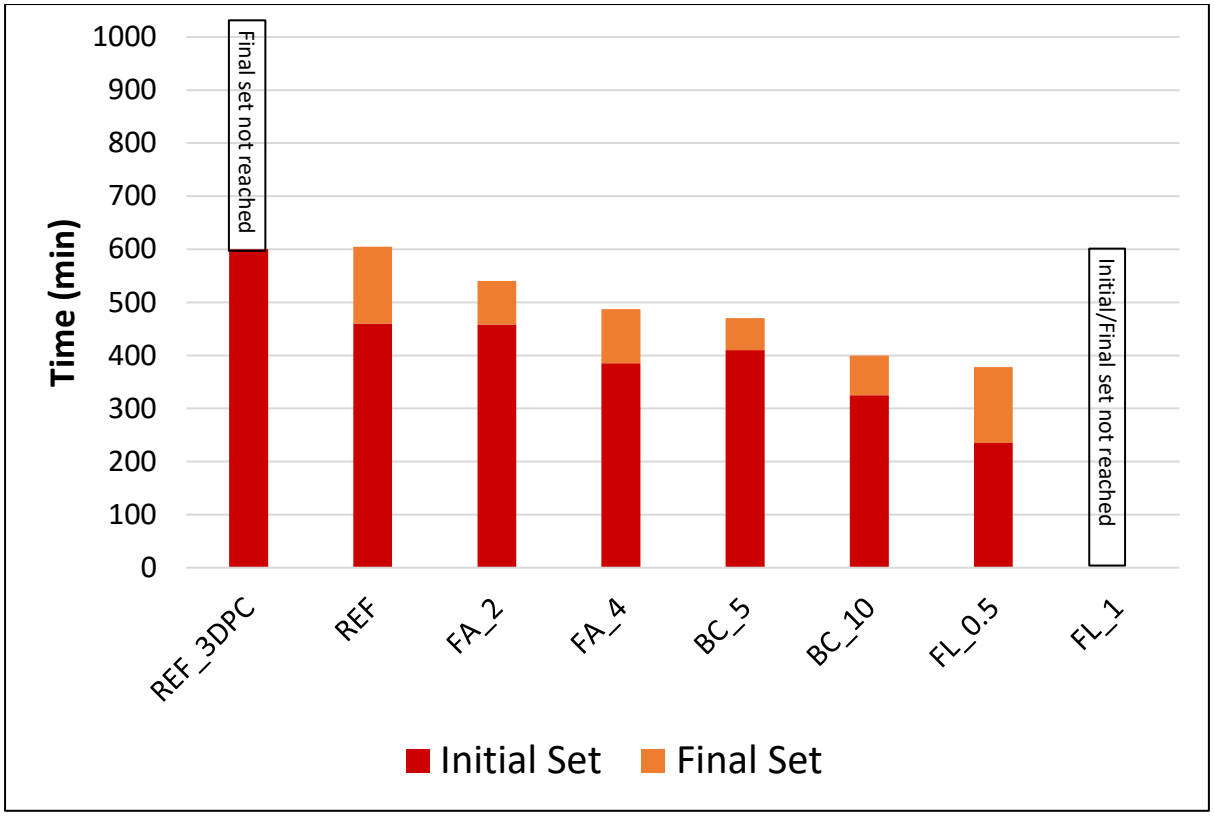

FIGURE 4.10 SETTING TIME TEST RESULTS

Initial set is defined as 3.5 MPa in resistance and final set as 27.6 MPa (ASTM C403, 2009). No initial set and final set could be determined for FL1. The maximum pressure measured after 10 hours was 0.8 MPa. For REF_3DPC no final setting time could be determined, 3.68 MPa was measured after 10 hours. In Table 4.3, these unknown values are marked in red.

TABLE 4.3 SETTING TIMES OF ALL CHARACTERISED MIXES (MIN)

	REF_3DPC	REF	FA2	FA4	BC5	BC10	FL0.5	FL1
Initial setting time	600	460	458	385	410	325	235	*
Final setting time	*	605	540	487	470	400	378	*

***Sample resistance did not reach initial/final set**

REF_3DPC is designed for 3D printing, which requires good printability characteristics and thixotropic behaviour. The results show that this mixture has the largest measured initial setting time of all mixes excluding FL_1. Initial setting for REF_3DPC is completed after 10 hours when most other mixes already reached final set. The false- , flash- and BCSA mixes were all designed as rapid setting mixes.

False setting reduces the setting time the least in comparison to the BCSA containing mixes and flash setting mixes. A higher dosage of hemihydrate in the mix reduced the initial setting time by roughly 1 hour. An increased time between initial and final set can be seen for the higher dosages as well. The false setting provides significant stiffness for initial set, but the

gypsum and ettringite crystals must be broken down and normal hydration must take place to get to final set. Thus, at higher dosages more time is required for hydration.

The BCSA mixes have lower setting times than the false setting mixes. A 5% replacement does not affect the setting time significantly, but the 10% replacement does. It takes approximately 1 hour less to reach initial and final set for BC_10. The interval between initial and final set is the shortest for the two BCSA mixes of all tested mixes. As suggested by Bescher and Kim (2019), BCSA increases the early hydration stages which results in higher early strength and lower setting times.

The shortest overall setting time was measured for FL_0.5. According to Han *et al.* (2014), higher sodium aluminate dosages reduce the initial and final setting times in a linear fashion up to a content of 4%. Similar initial setting times were found in this study, but the final setting time was larger than for Han *et al.* (2019). FL_1 does not set within the measured period. This result confirms the observations made in Figure 5.8. The hydration of the FL_1 mix is delayed and only starts to accelerate after 10 hours. 1.5 hours less than BC_10 and 3.75 hours less than REF less are required for FL_0.5 to reach initial set. The time between initial and final set is about the same as for REF. This means that the BCSA mixes and false setting have a shorter time interval between initial and final set than FL_0.5. The excessive amounts of hydrating aluminates reduce the quantities of hydrated silicates which may influence the time to reach final set.

4.1.5 UUCT

To quantify the rapid setting mechanisms, the uniaxial unconfined compression test was chosen. The test requires undisturbed samples that are tested at different time intervals. Since re-agitation of samples changes the setting behaviours of the rapid setting mixes, this test was a fitting solution to quantify the setting behaviours.

All initial compressive strengths are strongly dependant on the flowability of the mix. A more flowable mix is initially weaker and a less flowable mix stronger. The flow table test results measured before each test are tabulated in Table 4.4.

TABLE 4.4 SLUMP FLOW TEST RESULTS FOR UUCT MIXES

Mix	Slump (mm)
REF	165
REF_3DPC	164
FA2	168
FA4	172
BC5	178
BC10	170
FL0.5	164
FL1	144

The fresh-state compressive force development with time is shown in Figure 4.11. The data points for each mix show the maximum measured compressive force before shearing failure. A trendline was fitted between the points and the equations for each trendline are shown in Table 4.5. The compressive force can be converted into compressive strength by dividing the force by the cylinder area.

The results obtained from the rheology testing of the reference mixes are confirmed with the UUCT test. A steeper trendline slope and higher maximum compressive force were measured for REF in comparison to REF_3DPC. REF's rate of structuration is faster than for REF_3DPC's and a higher initial compressive force was measured as well. The initial compressive force of REF_3DPC is 6.1 N and 30.32 N for REF. That is 5 times more for REF in comparison to REF_3DPC.

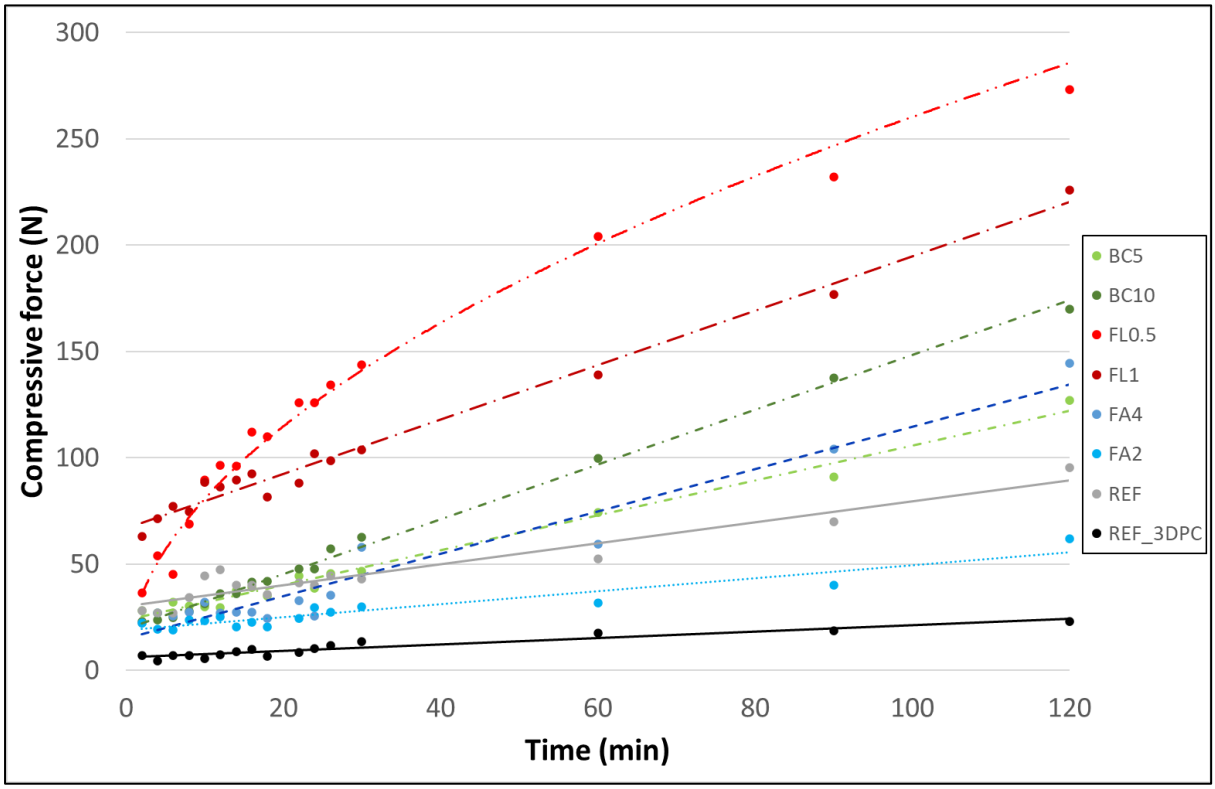

FIGURE 4.11 UUCT TEST RESULTS

Both false setting mixes have similar initial compressive forces of 18.85 N for FA_2 and 23.6 N for FA_4. FA_4, containing more hemihydrate, in theory must show stronger false setting due to higher gypsum crystal and ettringite formation. This can be observed in the trendline that is steeper and therefore means a more rapid strength gain. Initially both false setting mixes are weaker than the REF mix. The higher slump flow values of the false setting mixes result in lower initial compressive force. FA_2 is lower in compressive strength throughout the testing period. FA_4 gains compressive strength rapidly and at about 30 minutes becomes stronger in compressive strength than REF. A lower dosage of calcium sulphate reduces the compressive strength gain rate below the rate of the REF mix. At higher doses, the compressive strength gain rate increases above that of REF.

The BCSA mixes are initially lower in compressive strength than the REF mix. This may be a result of two factors. Firstly, the higher slump and secondly the influence of the BCSA on the mix. BC_5, the mix with a lower BCSA cement content, sets slower than BC_10, with a higher BCSA cement content. This can be seen by the steep slope of the two mixes. As a result, the concrete containing more BCSA sets faster than the mix with less BCSA. The results from Figure 4.11 follow this pattern. Higher compressive strength than REF is achieved at 30 minutes for BC_5 and at 15 minutes for BC_10. A somewhat proportional increase in compressive strength development can be observed for increased BCSA content. The compressive strength development of BC_5 and FA_4 is similar.

The two flash setting mixes have the largest compressive strength development of all the mixes. Both have higher initial compressive strengths than the other mixes. Flash setting is expected to be more severe for higher aluminate contents than for lower aluminate contents. Since FL_1 contains more aluminates than FL_0.5 a higher compressive strength was expected. The results from the UUCT do not show the expected outcome. FL_0.5 achieved higher compressive strengths than FL_1. From the setting time test as well as the hydration temperature development it was found that the hydration of FL_1 was delayed. Rapid initial strength is gained within the first minutes but from there onwards the strength development stagnates. A flatter compressive strength gain curve can be seen for FL_1 in the figure. Therefore, the UUCT results correlate with the other tests. The initial compressive strength is significantly larger of FL_1 than for FL_0.5. Up until 12 minutes after test start, FL_1 has higher compressive resistance than FL_0.5. After 12 minutes, FL_0.5 gains strength more rapidly and reaches a force of 50 N more after 2 hours in compressive strength. FL_0.5 is the only mix where an exponential compressive strength growth pattern was the best fit. Within the first 30 minutes after test start, 107 N in compressive force increase was measured.

TABLE 4.5 EQUATIONS FOR COMPRESSIVE FORCE DEVELOPMENT OF ALL MIXES

Mix	Compressive force with time (N)	R^2
REF	F=0.4917t + 30.316	0.9022
REF_3DPC	F=0.1521t + 6.0986	0.9093
FA2	F=0.3054t + 18.852	0.8972
FA4	F=0.8213t + 23.603	0.9422
BC5	F=0.4917t + 30.316	0.9855
BC10	F=1.2857t + 19.704	0.9966
FL0.5	$F=25.048t^{0.5084}$	0.9877
FL1	F=1.2781t + 66.76	0.9848

In summary, flash setting improves the compressive strength in a period of 2 hours the most. BCSA addition does not improve the compressive strength development as significantly as flash setting but better than false setting. The REF_3DPC mix only gained 16.26 N compressive force during the 2 hours of testing and is the worst performing mix for the UUCT test.

4.1.6 Correlation between tests

A correlation exist between the characterising tests conducted in this study. This section focusses on combining test results between two tests to gain further insight on the mix characteristics.

In Figure 4.12, the time to peak hydration temperature is plotted against the peak compressive force measured during the entire UUCT test. Time to peak hydration temperature (TPHT) is measured between the start of the test and the highest temperature measured throughout the testing period. The UUCT value plotted is the maximum compressive force measured two hours after starting of the test.

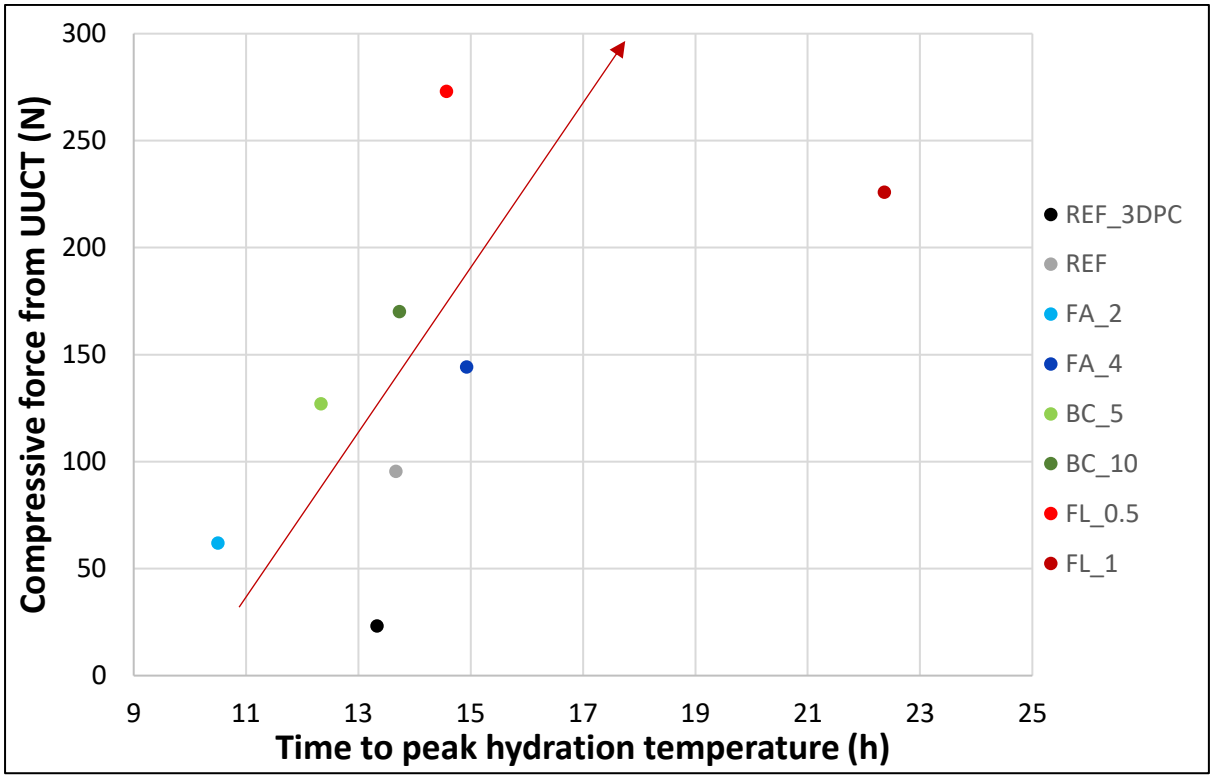

FIGURE 4.12 HYDRATION TEMPERATURE VS COMPRESSIVE FORCE

The time to peak hydration temperature of the two reference mixes are similar. REF has a higher compressive strength and a longer setting time than REF_3DPC. Similar to Figure 4.11, Figure 4.12 visualises the differences in short-term compressive force between the reference mixes. FA_2 has the lowest time to peak hydration temperature. The difference in TPHT between FA_4 and FA_2 is about 4 hours. Once again, the higher UUCT compressive force correlates with a larger TPHT. The same pattern can be seen for BCSA containing mixes, a higher compressive force and TPHT for the mix with a higher BCSA content. For the flash setting mixes, the previously observed pattern does not hold. FL_1 has a much longer TPHT than FL_0.5 but does not have the higher compressive force. From the setting time test and hydration curve, it was found that the hydration process of FL_1 is delayed. This may be an explanation for the lower UUCT compressive force as then main hydration period only starts much later.

From the Figure 4.12, it can be concluded that the mixes containing lower amounts of CEM I 52.5N and consequently higher additive content have an increased TPHT. The influence of the lower mixing temperature must be considered. FL_1, FL_0.5, BC_10 and FA_4 were all mixed at lower temperatures and have higher TPHT. Wade *et al.*, 2010, found that for lower concrete temperatures the setting time is longer and at higher temperatures, the setting time was shorter. The longer setting times at colder temperatures are a result of an extended initial setting time (Wade *et al.*, 2010). Concrete mixed at lower temperatures remains dormant for longer. This in return means that the peak temperature will be reached later because the concrete sets slower.

Figure 4.13 illustrates the relationship between compressive force within two hours after casting and initial setting time. The setting time value for FL_1 could not be measured during the period of testing and therefore the mix was omitted in this chart. Initial setting time is determined from the point where the concrete resistance reaches 3.5 MPa.

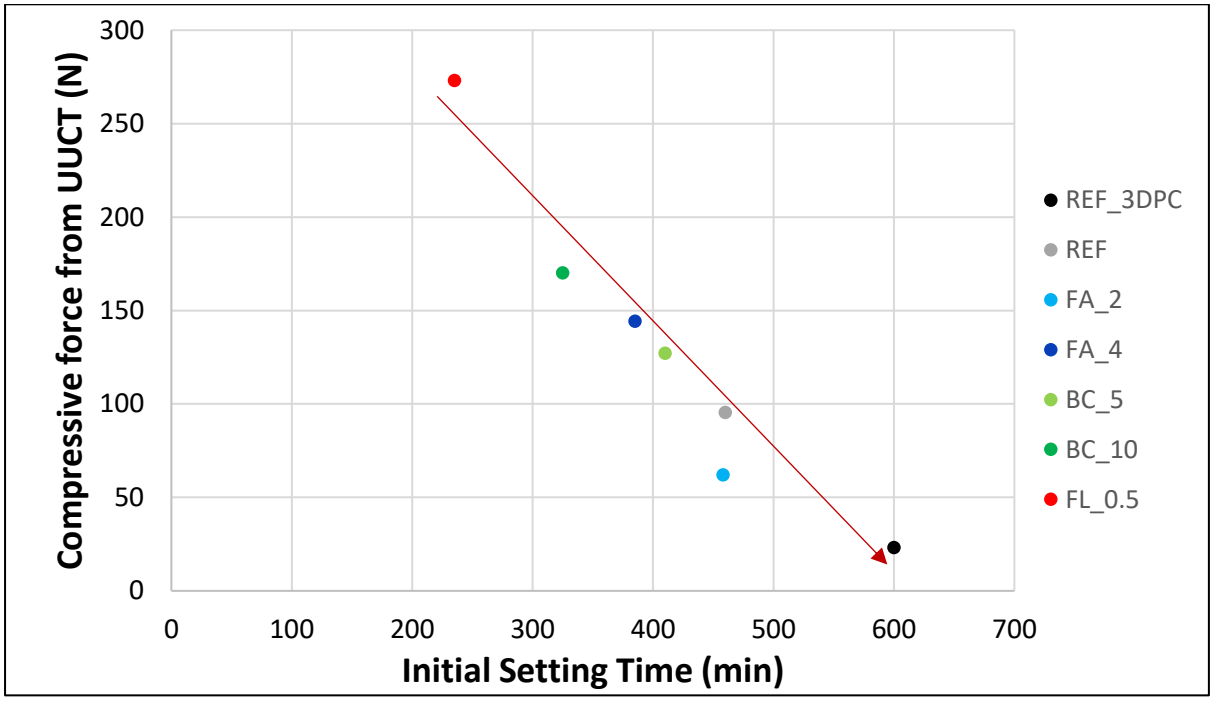

FIGURE 4.13 INITIAL SETTING TIME VS COMPRESSIVE STRENGTH

Overall, a trend can be seen between higher early age compressive force and shorter setting times. This seems intuitive since a concrete that sets faster will have a higher early age compressive strength. REF_3DPC is the mix that sets the slowest. This mix also has the lowest compressive force measured during the UUCT test. FL_0.5 sets the fastest and has the highest UUCT compressive force. A linear trendline gives an indication what compressive strength can be expected from a certain setting time and vice versa. As both these plotted parameters must correlate, plots such as Figure 4.13 help to verify the results obtained from both tests.

No significant correlation could be found between the cube strength results and the other tests conducted. All other tests determine fresh state properties of concrete, and the cube strength test is a hardened state test. Hence, a correlation between the results is unlikely.

4.1.7 Phase 1 concluding summary

The Phase 1 characterisation is used to determine suitable mixes for 3D printing of concrete. All results of each rapid setting behaviour are compared. The most suitable mix for printing can be selected from each rapid setting behaviour.

Clear differences were found between the two reference mixes. REF proved to be a stiffer mix at early ages that sets faster than REF_3DPC. Only in the compressive strength test did REF_3DPC show the better characteristics. The reference mix for printing (REF_3DPC) remains workable for longer which enhances its pumpability characteristics throughout the printing process.

Of the two false setting concrete mixes, FA_4 performed better overall. No significant differences in long-term compressive strength were found. The peak hydration temperature of FA_2 was higher and the hydration process of FA_4 was found to be slightly delayed. A shorter setting time was determined for higher calcium sulfate content. The UUCT test results showed a clear difference between the two false setting mixes. FA_4 proved to gain compressive strength well with time whereas FA_2 was weaker than its base mix and barely gained strength in the testing period.

The test results of the BCSA containing mixes were similar in all characterisation tests. BC_10 had a lower cube strength than BC_5. The long-term compressive strength was limited by the larger replacement rate of CEM I 52.5N with BCSA cement. BC_10 had a reduced setting time as well as improved compressive strength when compared to BC_5. From these summarised results it can be estimated that BC_10 has better buildability characteristics than BC_5.

Both flash setting mixes exhibit a clear reduced cube strength. A higher aluminate replacement rate reduced the cube strength further. A clear delay in hydration was found for FL_1 in the setting time test as well as the hydration temperature curve. The greatest increase in early age compressive strength was found for flash setting. FL_0.5 showed the best early age strength gain characteristics.

The test results from the characterisation phase correlate sensibly. Each rapid setting behaviour has its unique influence on the concrete characteristics and is preferable for a different reason. False setting concrete performed the best in the cube strength test because the addition of calcium sulphate does not significantly influence the hardened state properties of concrete. Adding BCSA to concrete reduces the setting time on average most significantly. Flash setting concrete gains compressive strength the fastest within the first 2 hours after mixing which gives it the best compressive strength characteristics from the UUCT test.

4.2 Phase 2: Printing

After characterising all mixes in Phase 1, the most suitable mixes for 3D printing were selected for Phase 2. The best overall performing mix of each rapid setting behaviour was determined and tested for printing. A circular column was printed to determine the buildability of each

selected mix. The aim of this study was to obtain a printable ordinary concrete with a rapid setting characteristic. Printing quality was only of secondary interest since that would require even more adjustments to the mix. This would make the mix different to the characterised mix and defeats the purpose of the first phase.

The mixes selected for printing were:

- REF_3DPC
- FA4
- BC5
- FL0.5

As a reference for 3D printing performance in a buildability test, the reference mix for 3D printing in the study, REF_3DPC. FA_4 sets faster than FA_2, gains compressive strength more rapid and the cube strength does not differ much. Faster strength gain is advantageous in a test where the maximum number of layers is required. BC_5 did not perform as well as BC_10 in Phase 1, but preliminary printing issues were encountered with BCSA containing mixes. Therefore, the mix with lower BCSA content and in return less risk for issues was selected. FL_0.5 outperformed FL_1 in all tests and was therefore the obvious choice for printing for the flash setting mixes. Its rapid strength gain in the UUCT test presented promising results for good buildability characteristics.

4.2.1 Buildability

A circular column was printed to establish buildability. The layer height printed was 10 mm and a layer width of 30 mm was aimed for. Extrusion rate adjustments were made during prints where needed to ensure the correct layer width. All columns were printed at a print speed of 60 mm/s. The circumference of the column was 785 mm with a corresponding diameter of 250 mm.

All columns were aimed to be printed till failure or to the limit of 90 layers. A poker vibrator was used to keep the concrete flowable in the hopper during the printing period. The vibrator was injected into the hopper and moved through the paste to ensure good pumpability. The following sections discuss the procedure followed to get all selected mixes printable and achieve the maximum possible printing height.

4.2.1.1 REF_3DPC

The benchmark for this buildability study was set by REF_3DPC. This study aims to use rapid setting cement mixtures for 3D printing. All results were compared to the reference mix for printing.

In Figure 4.14, the main information gathered from the REF_3DPC mix is summerised. No further trials were required since this mix was a standard mix that required no adjustments. The mix had an average slump of 158 mm measured in two perpendicular directions. 28 layers could be printed before the colum failed. Figure 4.15 shows the failure mechanism of the column. The images are arranged from just before failure to collapsed.

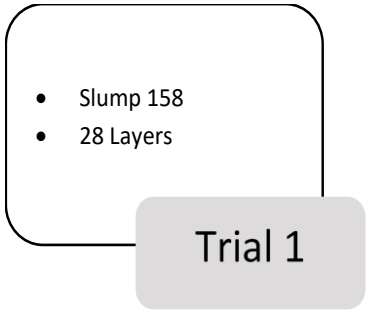

FIGURE 4.14 MIX DESIGN DEVELOPMENT PROCESS REF_3DPC

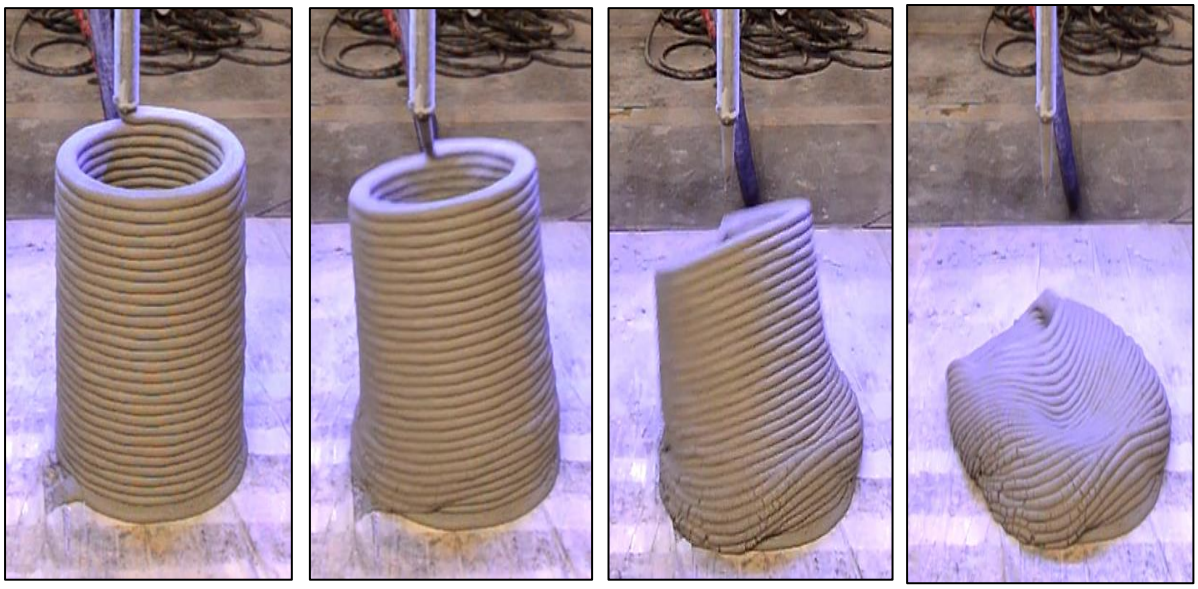

FIGURE 4.15 FAILURE MECHANISM REF_3DPC

Material failure in the form of plastic collapse can be seen in the Figure 4.15. The bottom layers are too weak to withstand the pressure induced by the layers printed on top. Failure occurs in the side where the printing nozzle is located. More load is added on the side where the nozzle is placing the concrete. As a result, the layers underneath start spreading under the load which destabilises the entire column. Buckling occurs and the column collapses.

4.2.1.2 FA_4

The false setting mix chosen for printing, FA_4, was printed in three different trials. The summarised results as well as the changes made between trials are shown in Figure 4.16. Figure 4.17 shows the failure mechanisms of FA_4 during the first trial.

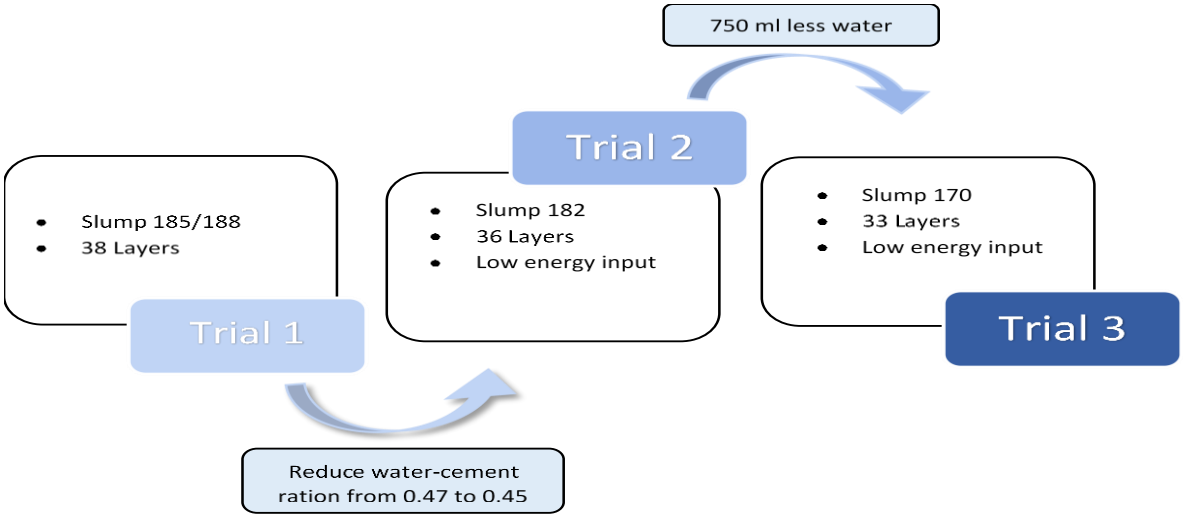

FIGURE 4.16 MIX DESIGN DEVELOPMENT PROCESS FA_4

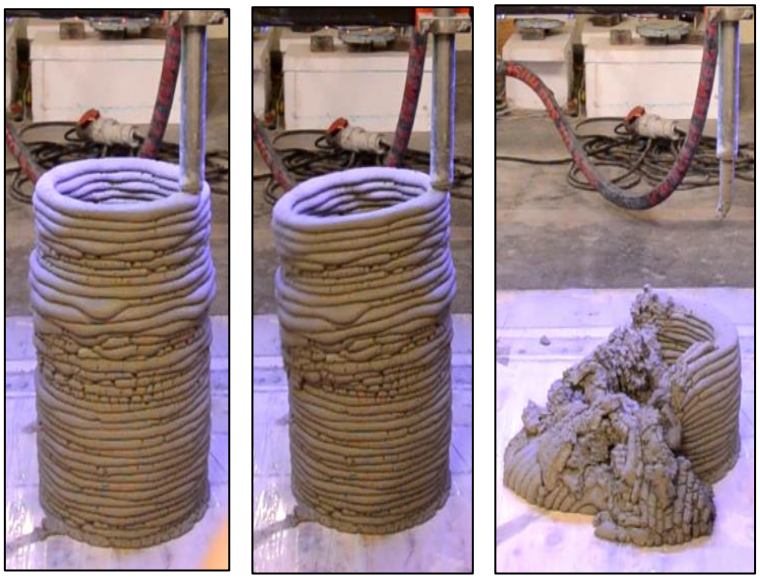

FIGURE 4.17 FA_4 COLUMN FAILURE TRIAL 1

In the first trial, the original mix design used during the characterisation was printed. A high slump of 186.5 mm was measured. False setting was confirmed in a check for rapid stiffness gain on the material left over in the pan as well as the initial extruded concrete. In both samples, the false setting was assumed to be present as the concrete rapidly gained in stiffness. The concrete was supposed to be vibrated throughout the entire print. Bleeding issues inside the hopper forced a reduction in vibration. The vibrator could only be used over short periods and then had to be switched off.

Considering the high measured slump after mixing, the printing process turned out difficult as extrusion problems persisted throughout the print. This can be seen in Figure 4.17 from the inconsistent extrusion of layers. The figure shows the column just before failure, during collapse and after. The extrusion frequency of the hopper had to be increased throughout the print to get a constant extrusion width. A total of 38 layers could be printed before failure. Column failure occurred at the 15th layer. The layers below were of better printing quality and

the layers above of worse quality. Different layer thicknesses were a result of concrete setting and responsive print extrusion speed adjustments to the extrusion issues. The column failure occurred at the thin and badly printed layers. A failure due to instability of the poorly printed layers is assumed to be the reason for collapse. After failure, the concrete from the column was checked for material that had gained stiffness. No obvious sign of concrete that had undergone false setting could be found in the material of the failed column.

For the second trial, the water-cement ratio of the mix was reduced from 0.47 to 0.45. The aim was to solve the bleeding issues and to reduce the slump. A new slump of 182 mm was measured. The vibrator was not used continuously during the print since the mix becomes significantly more flowable when vibrated for longer periods. Only short periods of vibration were used to create a consistent workability inside the hopper.

The overall printing quality was improved with the adjustments. A more consistent layer thickness could be achieved with the reduction in water content. Figure 4.18 shows the failure mechanism for this trial. After printing 36 layers, the column failed at layer 9. A thinner layer can be seen in the failure region. As the width of the printed layer decreases, the stress increases since the load above remains the same. A buckling failure in combination with the poorly printed layers may also be a potential failure mode. A check for false setting after the collapse was again unsuccessful. False setting concrete was deemed to be present if differences in stiffness between the printed material and the material in the hopper could be noted by poking the concrete by hand.

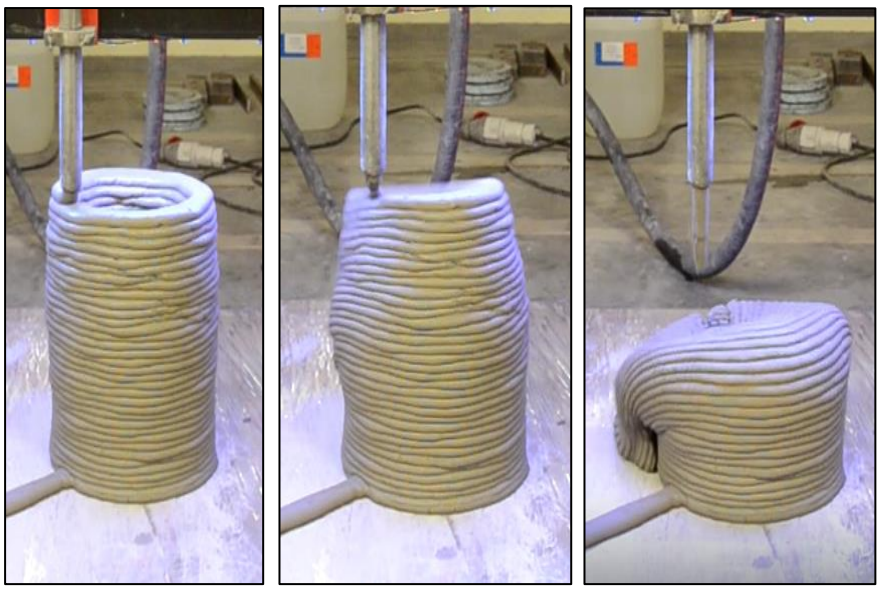

FIGURE 4.18 FA_4 COLUMN FAILURE TRIAL 2

In the third trial, further changes were made for potential buildability improvements. The water-cement ratio was reduced from 0.45 to 0.43. The aim of this was to reduce the slump and to improve the buildability of the mix. A lower slump means that the mix has a lower flowability. The decreased flow capacity means a stiffer mix which in theory should be able to carry more load. A slump of 170 mm was measured. Minimum vibration was used so that

disturbance before pumping was limited. Figure 4.19 shows the failure progression of the FA_4 in the third trial.

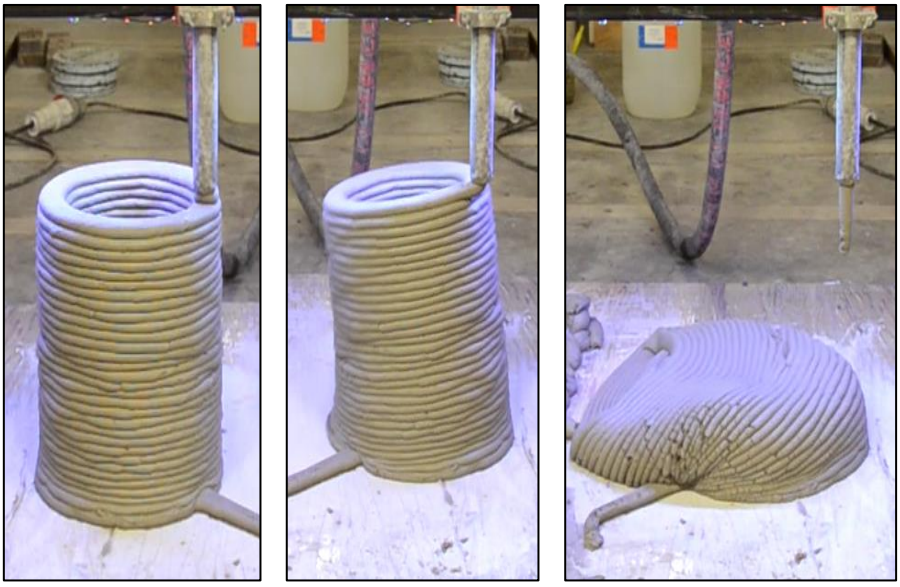

FIGURE 4.19 FA_4 FAILURE MECHANISM TRIAL 3

The reduction of water led to even better printing quality and uniformity in layer thickness and width. From Figure 5.19 it can be noticed that of all trials for the FA_4 mix, the last print produced the most aesthetic column with uniform layer width and thickness. Failure occurred after 33 layers at one of the bottom layers. Figure 4.19 suggests that a material yielding failure took place. Once again, no false setting could be found in the column after failure. The concrete was highly flowable after it collapsed.

To conclude, the reduction in water throughout the trials improved the printing quality significantly. A more uniform column that has a consistent layer thickness was achieved in Trial 3. No buildability improvements were achieved with the adjustments as the total number of printed layers reduced from 38 to 33. Failure in Trial 1 and 2 was caused by poorly extruded layers. The layers below the point of failure seemed to have gained some strength which could indicate false setting. No concrete that showed false setting could be found for all three trials after collapse and therefore no false setting could be confirmed in the column. Only the initial extruded material did false set in each printing trial. This shows that with constant reagetation of the mix inside the hopper, the false setting mechanisms becomes depleted. The vibrator and pump both break the bonds formed while the concrete is inside the hopper. After multiple building and breaking of bonds, the additional calcium sulphate added for false setting becomes depleted. Therefore, only ordinary hydration mechanisms occur in the printed columns.

4.2.1.3 BC_5

The BC_5 mix was printed in 3 trials as shown in Figure 4.20. Adjustments were made to maximise the buildability of the mix. The addition of BCSA caused setting of the concrete within the pipe and therefore the mix had to be handled with caution.

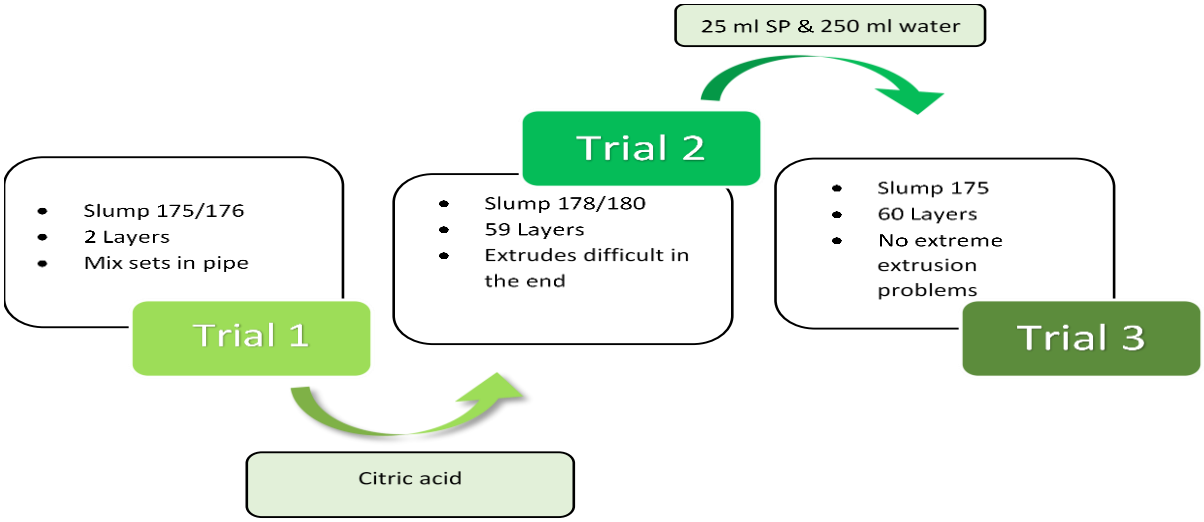

FIGURE 4.20 MIX DESIGN DEVELOPMENT PROCESS BC_5

The original mix design was used for the first trial and had a slump of 175.5 mm. Vibration was once again used to keep consistent workability and improve the concrete pumpability. Only two layers could be printed before no further extrusion was possible. The mix started heating up and set within the pipe. The concrete could not be pumped any further and the print had to be stopped to avoid damage to the pump. This rapid hardening process was a result of the rapid setting BCSA cement in the mix. The added energy by the vibrator and force added by the pump caused immediate setting inside the pipe.

For the second trial, citric acid was added as a retarder. Burris and Kurtis found that the addition of citric acid works well as set retarder for CSA cements. It's addition can have strength enhancing effects at dosages up to 2% of cement mass (Burris & Kurtis, 2018). Literature suggests that 0.35% citric acid with respect to binder content allows for a delay in setting time of about 45 minutes (Rosero, 2020). A linear behaviour between citric acid dosage and start of hydration was found. Therefore 0.1% citric acid was added with reference to binder content. This delays the hydration process of BCSA by about 15 minutes. The concrete was vibrated throughout the entire print and the column failure of the second trial is shown in Figure 4.21.

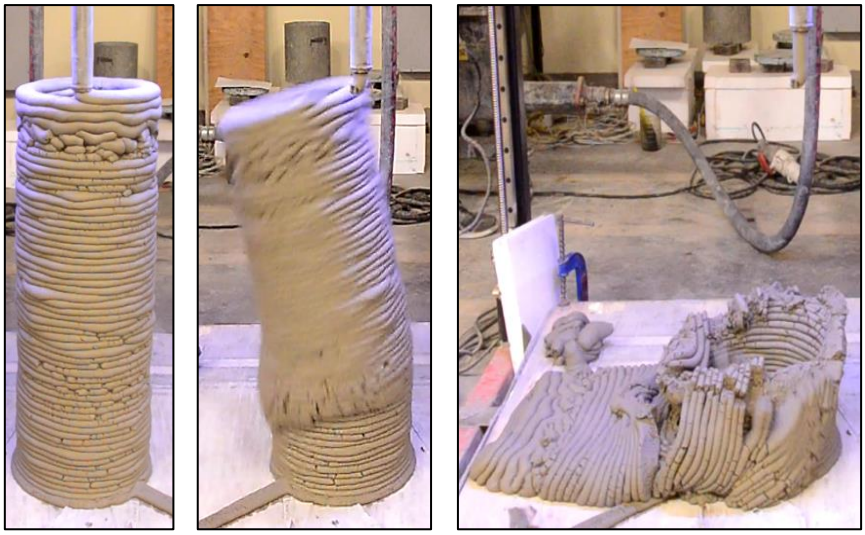

FIGURE 4.21 BC_5 FAILURE MECHANISM TRIAL 2

A total of 59 layers were printed in the second trial. The first 15 layers were easily extrudable and no changes in pumping rate were required. At layer 16, adjustments were required to ensure that the layer width and thickness remained constant. The printing quality issues persisted up until layer 30. No changes were required between layer 30 and layer 51. From the figure, the bad and inconsistently printed layers can be seen in the first image in Figure 4.21. The problem was solved with further pumping rate adjustments, but failure occurred soon after. Failure occurred in and around layer 15. This suggests that the lower layers were able to carry the load and that structuration already took place. The weaker layers then collapsed under the load. It is assumed that more layers could be printed if the layer thickness and printing quality can be kept constant.

For the third trial, the SP dosage and water content were increased slightly. The aim was to create a smoother mix that has improved printability. 25 ml of SP and 250 ml of water were added to the suggested mix design for Trial 2. Citric acid was further used as a retarder for the BCSA hydration. The dosage was not increased since the hydration of BCSA is required to allow for more layers to be printed. Figure 4.22 shows the change in extrusion quality.

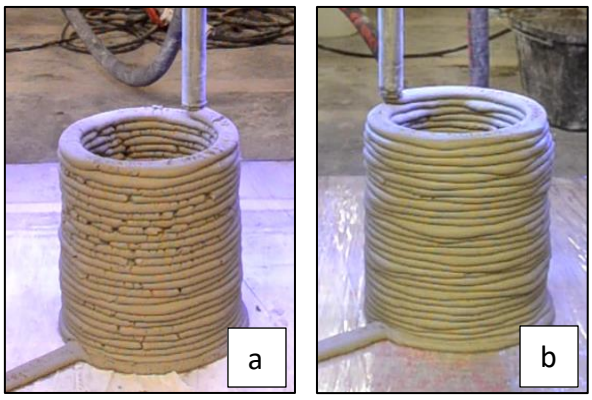

FIGURE 4.22 PRINTING QUALITY IMPROVEMENTS BC_5

As previously discussed, the failure for the Trial 2 column occurred at layer 15. The addition of water and SP was aimed to improve the printing quality of the lower layers. From Figure 4.22, a clear change in printing quality can be seen. In Figure 4.22 a), the layers have gaps and are thinner than in Figure 4.22 b). The column in b) is not as straight as column a) but the extrusion quality is much improved. It can be said that the adjustments worked for the improvement of the bottom layers.

The Trial 3 column failure is shown in Figure 4.23. A total of 60 layers were printed before the column collapsed. With the adjustments made to improve the printability of the mix a smoother and more aesthetic column could be printed. Nonetheless, extrusion rate adjustments were required to keep a consistent layer width. In Figure 4.22 some inconsistent parts are visible in the column but only at about 30 layers onwards. These inconsistencies are a result of pumping rate adjustments. More material is extruded at higher frequency and the extrusion rate must be adjusted so that the layer widths remain the same. Similar to Trial 2, major extrusion issues occurred at the top layers. For Trial 2 the issues started at layer 51 and for Trial 3 at layer 58. This suggests a delay in extrusion issues with the addition of water and SP. The column failure occurred at the base of the printed column. A plastic failure under the above lying layers is the reason for failure. No notable improvements in buildability could be achieved with the adjustments made for Trial 3.

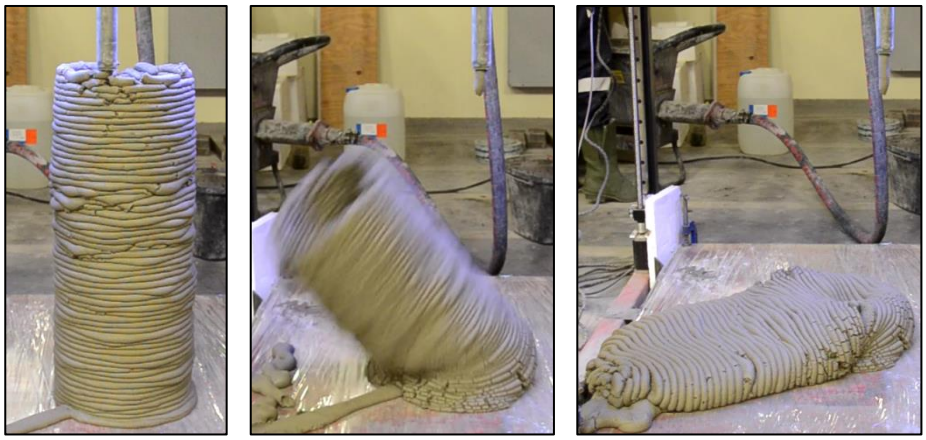

FIGURE 4.23 BC_5 FAILURE MECHANISM FOR TRIAL 3

BCSA cement influences the properties of the concrete significantly. Without any retarder, the energy added by the pump causes the mix to set. The addition of retarder allowed for a longer period of extrusion. Citric acid was only added so that a small delay is caused (Rosero, 2020). A higher dosage can potentially improve the buildability of the BC_5 cement as more layers can be printed without any pumping rate adjustments. The correct balance must be found, because retardation for too long results in loss of structuration which defeats the purpose of the BCSA cement in the mix.

4.2.1.4 FL_0.5

The printing of the FL_0.5 mix was completed in two trials. Figure 4.24 shows the results of each trial as well as the adjustments made between trials.

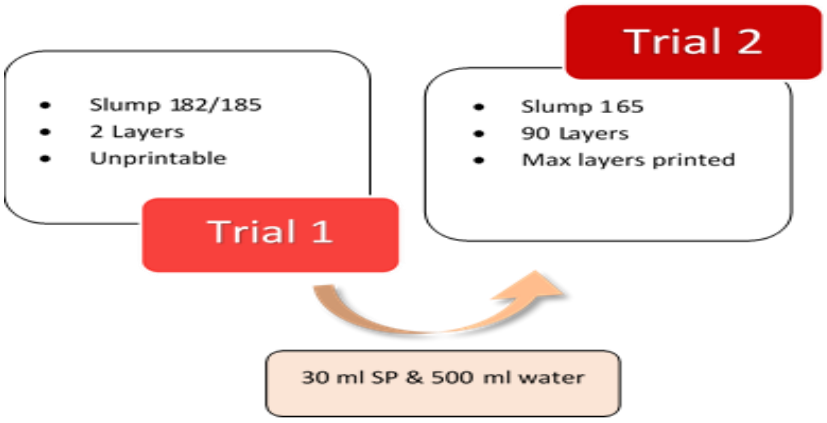

FIGURE 4.24 MIX DESIGN DEVELOPMENT PROCESS FL_0.5

From the UUCT results, the FL_0.5 mix had the best structuration rate. Especially at early ages, the strength development rate is higher than for all other mixtures. The only problem could be the influence of the pump on the flash setting mechanism.

The first trial to print the FL_0.5 mix failed. A few layers could be printed on top of each other, but the cement was far too dry after extrusion. Even though a high slump of 183 mm was measured, the mix remained dry after extrusion. From Figure 4.25 one can see the star-like extruded material. The layers were also not straight on top of each other, and an inconsistent column was printed. Further adjustments to the mix were necessary to make this mix printable.

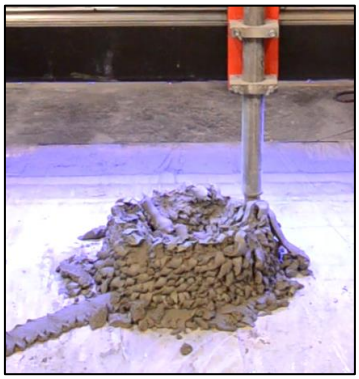

FIGURE 4.25 FL_0.5 TRIAL 1 UNPRINTABLE

Since the mix was far too dry, an additional 500 ml of water was added to the mixture and 30 ml of SP. The aim was to produce a smoother concrete mix even though the slump in the initial trial was already relatively high.

For the second trial, the same mix design was used to produce the FL_0.5 mix. A slump of 160 mm was measured. The additional water and SP were added after the first slump flow test. With the addition of extra water and SP the slump increased to 165 mm. Even though the mix did not become much more flowable in comparison to the first trial, the concrete seemed more workable. Figure 4.26 shows the printing progress for the complete 90-layer column.

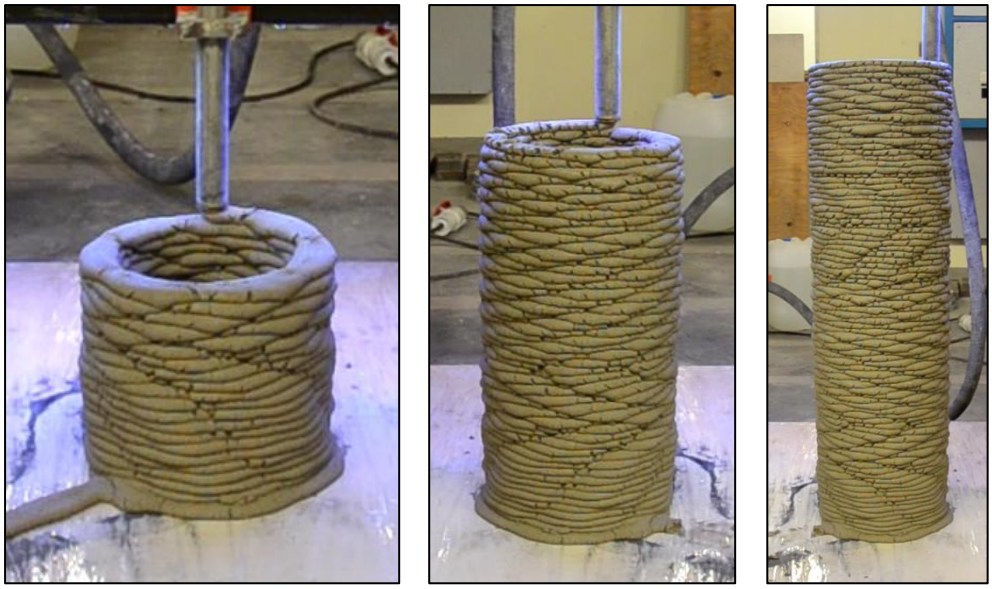

FIGURE 4.26 FL_0.5 COLUMN PRINTING PROCESS

At 90 layers the printing height limit of the 3D printer used has been reached. No failure occurred for this trial and more layers could have potentially been printed. Extrusion speed adjustments for constant layer width were done over the whole printing period. For Trial 2, the FL_0.5 concrete mix was still dry at extrusion in comparison to the other mixes printed. Cracks in the layers of the entire column could be found. These cracks are created when the extrusion rate is slower than the moving rate of the nozzle. The extruded concrete is pulled by the nozzle which creates the crack. Even though these cracks were present the column reached the maximum height of 90 layers. The entire column has a uniform layer thickness with little or no thick/thin sections. The extrusion quality of this mix is not as good as for the BC_5 and FA_4 mixes but has the best buildability. Flash setting could be found in all extruded material. This explains the good buildability as the column gains stiffness more rapid and can withstand higher loads.

A summary of the maximum number of layers that could be printed for each mix is shown in Figure 4.27. All three rapid setting mixes had an improved buildability compared to the REF_3DPC mix. The rapid setting concrete mixtures could all be printed, and the results show the potential such setting mechanisms can have in industry. The presence of mineral additives in REF_3DPC improved the pumpability and extrusion quality of the mixture in comparison to the other mixtures. The adjustments made on BC_5 and FA_4 significantly improved the columns aesthetics. Rapid setting concrete mixtures are more suitable for off-site construction of structural components because elements can be completed in less time. REF_3DPC is designed for on-site printing as its setting behaviour suits large structures better.

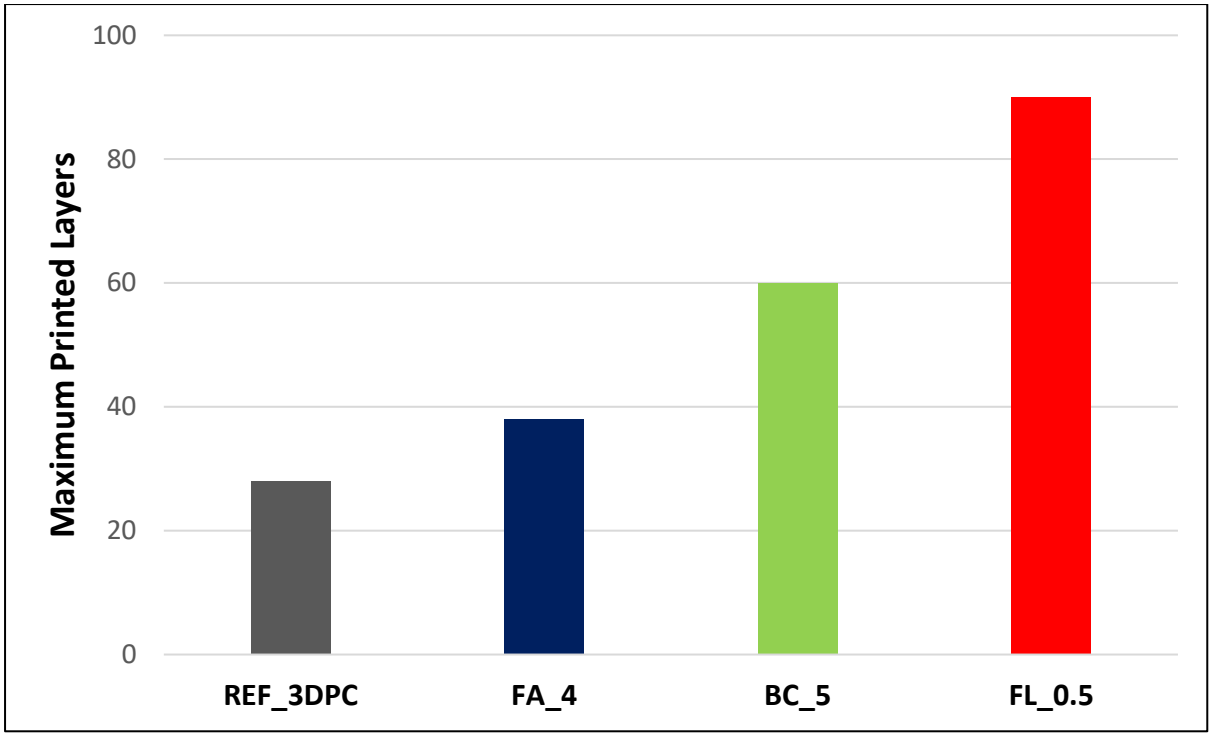

FIGURE 4.27 PRINTING RESULTS SUMMARY

4.2.2 Feasibility of the printed mixes

All rapid setting behaviours had improved buildability characteristics and were induced with the addition of admixtures. The cost of these admixtures influences the production cost of the concrete batch. This section analyses the relationship between increased buildability performance and the cost associated with it.

According to the standard tariffs of Stellenbosch Municipality for 2020-2021, the cost of a kilolitre of water for business, industrial and commercial use is R20.28 (Stellenbosch Municipality, 2020). All other purchase prices in Table 4.6 were obtained from the material suppliers.

TABLE 4.6 MATERIAL COST OBTAINED FROM SUPPLIERS

Material	Price
CEM I 52.5	R 95/50kg
Sand	R 0.13/kg
Water	R 20.28/kL
Superplasticizer Chryso Premia 310	R 60/L
BCSA Cement	R 20/kg
Silica Fumes	R 22.35/kg
Fly Ash	R 2/kg
Calcium sulphate hemihydrate	R 1015.45/kg
Sodium aluminate anhydrous	R 431.02/kg
Citric acid	R 322/kg

From the mix designs used in the buildability study, the production cost per cubic meter of concrete was calculated. In Table 4.7, the quantities of the mix components together with their cost price per cubic metre for the two reference mixes is shown. REF only requires cement, sand, water, and superplasticiser. These are cheap constituents compared to the price of silica fumes for example. As a result, the price of a cubic meter of REF is R1652.61, less than half of R3886.34 for REF_3DPC.

Savings on a project without losing out on quality are preferred by any client. For 3D printed structures, the required quantity of concrete is high since minimal brickwork is used. A reduction in material cost of less than half makes the construction technique more affordable and competitive on the market. The printability characteristics of REF have not been studied in this research but from a financial perspective this mix is recommended instead of REF_3DPC.

TABLE 4.7 COST PER CUBIC METRE FOR REFERENCE MIXES

	REF		REF_3DPC	
	kg/m^3	R/m^3	kg/m^3	R/m^3
CEM I 52.5	670.00	1273.00	579.00	1100.10
Sand	1340.00	175.23	1169.00	152.87
Water	284.75	5.93	261.00	5.43
BCSA Cement		0.00		0.00
SP	3.15	198.45	7.03	442.89
Sodium aluminate anhydrous		0.00		0.00
Calcium sulphate		0.00		0.00
Citric acid		0.00		0.00
Silica Fumes		0.00	83.00	1855.05
Fly ash		0.00	165.00	330.00
SUM	R	1652.61	R	3886.34

The cost of a cubic metre of ordinary concrete, REF, was significantly cheaper than the printable reference mix- REF_3DPC. All rapid setting mixes were based on REF and binder replacements were made to induce a rapid setting behaviour. Table 4.8 provides information on the constituents of each of the three rapid setting mixes together with their associated cost.

From Table 4.8, it becomes clear that the production cost of the FA_4 mix is very expensive, about R23 000 more than for REF_3DPC. The high cost of the calcium sulphate hemihydrate is the reason for the high price. A high unit price in combination with a relatively high

replacement rate results in the significant increase in cost. Both BC_5 and FL_0.5 are cheaper to produce than REF_3DPC but more expensive than REF. The most expensive ingredient of BC_5 is cement. BCSA cement is used to induce the rapid setting behaviour in the cement and costs R669 per cubic metre. This makes Portland cement the most expensive ingredient of the mix which is in contrast to the influence that calcium sulphate hemihydrate has on the cost of FA_4. In FL_0.5, the sodium aluminate added is the most expensive constituent. Its low replacement rate reduces the influence on the overall cost price for production of FL_0.5.

TABLE 4.8 COST PER CUBIC METRE FOR PRINTABLE RAPID SETTING CONCRETE MIXES

	FA_4		BC_5		FL_0.5	
	kg/m^3	R/m^3	kg/m^3	R/m^3	kg/m^3	R/m^3
CEM I 52.5	630.60	1198.14	635.50	1207.45	639.00	1214.10
Sand	1324.26	173.17	1337.90	174.96	1309.95	171.30
Water	295.12	6.14	285.98	5.95	305.04	6.35
BCSA Cement	-	0.00	33.45	669.00	-	0.00
SP	5.57	351.19	5.52	347.69	5.52	347.69
Sodium aluminate anhydrous	-	0.00	-	0.00	3.20	1377.11
Calcium sulphate	25.22	25613.71	-	0.00	-	0.00
Citric acid	-	0.00	0.13	40.25	-	0.00
Silica Fumes	-	0.00	-	0.00	-	0.00
Fly ash	-	0.00	-	0.00	-	0.00
SUM	R	27342.36	R	2445.30	R	3116.55

From the production cost analysis, it suggests that a balance must be found between cost and reward. Reward in this case would come in the form of increased buildability. Figure 4.28 displays the ratio of production cost per cubic metre and the layers printed in the buildability study as well as the maximum number of successively printed layers. A cubic metre of concrete is used as a unit measurement for comparison of the mixes.

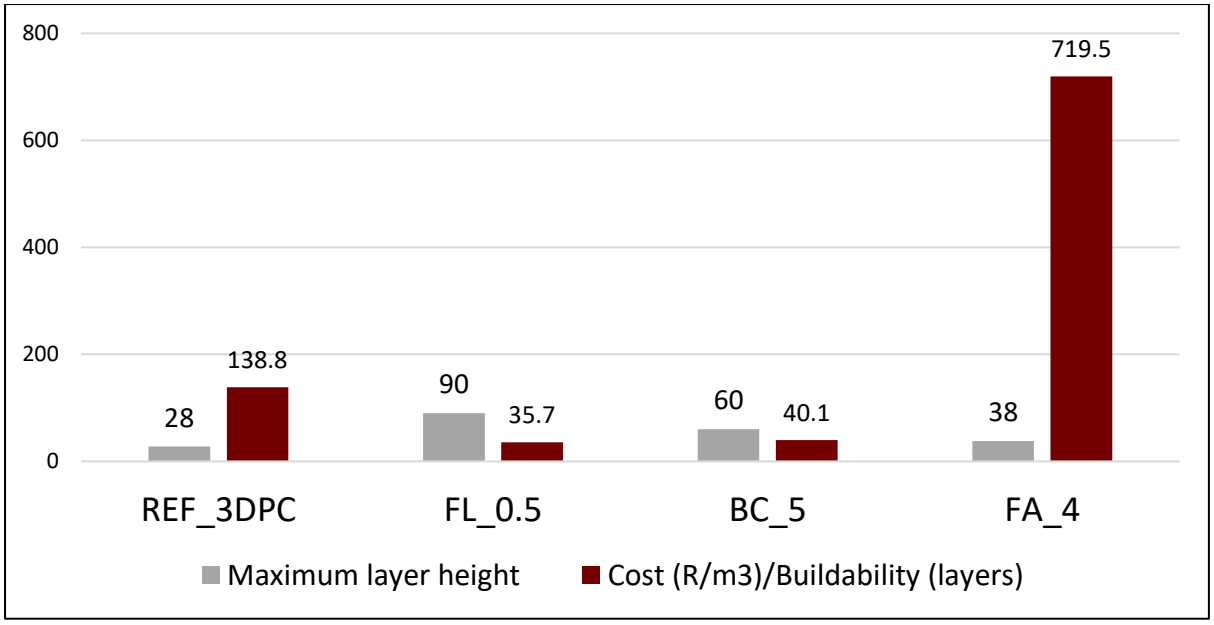

FIGURE 4.28 PERFORMANCE RATIO AND BUILDABILITY RESULTS

To assess the value of using rapid setting cement for 3D concrete printing, the ratio between cost per cubic metre and maximum number of successively printable layers was used, the performance ratio. It allows for conclusions on the usefulness of the induced rapid setting behaviours. The optimum scenario would be a situation where the buildability is improved at minimum cost.

The reference 3D printable mix, REF_3DPC, has a performance ratio of 138.8 (R/m^3)/Layer. Even though the cubic metre price is not much higher than for FL_0.5, the few printed layers before collapse increase the performance ratio. The best performance from a financial point of view for FL_0.5. Its production cost is double than of REF, but more layers could be printed with the concrete. Therefore, the mixture has a lower cost to layer ratio. This means that the addition of sodium aluminate helps to improve the buildability in the most affordable manner. BC_5 has a 12.3% higher performance ratio than FL_0.5. Even though 30 layers less could be printed with the BC_5 mix, the performance ratio is similar. BCSA cement is much cheaper than sodium aluminate or calcium sulphate hemihydrate. A cheaper mix can be produced even though the replacement rate for BC_5 was the highest of all printed mixes, 5% of CEM I 52.5. From Figure 5.28, false setting is not a feasible option in this study. The high material costs have a low reward. Even though ten more layers than for REF_3DPC could be printed, the cost involved to produce a false setting is too high. The cost per printed layer is five times higher than for REF_3DPC.

With the possibility of printing rapid setting ordinary concrete mixes, significant environmental contributions can be made. No formwork is required for the construction process which reduces the amounts of waste produced. Since ordinary concrete mixtures are used for the printing process, the cement quantities used for construction are not significantly influenced. The use of BCSA positively influences the carbon footprint of the construction

industry (Bescher & Kim, 2019), therefore replacing OPC with BCSA has a positive influence on the environment.

In summary, using flash setting and BCSA replacement for buildability improvements is a viable option as the improved buildability performance is worth the extra cost. False setting is not feasible since the cost to increase the buildability by ten layers is too high.

4.2.3 Conclusions

Considering all the results achieved in this study, the aim of this study has been achieved with the FL_0.5 mix. A rapid setting ordinary concrete mix has been developed and the mix has a good buildability. Further adjustments are required to improve aesthetics and an additional increase in water and superplasticiser would possibly solve the problem.

The improved buildability may firstly be a result of the REF mix having a higher static yield stress than the REF_3DPC mix. The higher yield stress allows for more printed layers and therefore a better buildability. Since the REF mix is the basis of all rapid setting mixes, one can expect more printed layers from any of the three selected mixes.

In the UUCT test, the FA_4 and BC_5 mixes showed similar strength gain characteristics. Unfortunately, the UUCT results did not correspond with the buildability results of the FA_4 mix. A maximum of 38 layers was printed. The false setting mechanism is a non-reversable process. After a few cycles of false setting and breaking of the bonds, the calcium sulphate becomes depleted which means that no excess calcium sulphate is available for false setting and the process cannot proceed. Even at minimum vibration and agitation inside the hopper the false setting gets depleted. The concrete is continuously moved during the printing period by the worm inside the hopper which then breaks the bonds that were built up. A continuous pump in a 3D printer may lead to better results since the material does not remain in the hopper for longer periods. The water only gets added close to the pipe which minimises the bond breaking mechanism. False setting concrete is expensive to produce and too high for the buildability improvements gained with it. The use of a continuous mixing system may change the behaviour of the concrete and make it a feasible option.

The BC_5 had twice the buildability rate of the reference mix with 60 successively printed layers before failure. That is a significant improvement and means that one can build twice as high, at a constant rate, with the BC_5 mix compared to the REF_3DPC mix. The rapid setting of the BCSA cement remained an issue. Citric acid worked well as a retarder; the dosage can be adjusted further to improve the buildability of the mix. The additional energy added by the vibrator and pumping worm have an influence on the setting behaviour of the BCSA cement. Nothing exact can be concluded about the extent of the influence, but the rapid build-up of heat in the first trial showed that there is a definite influence on the setting behaviour. A test in a printer with a continuous pump will probably show better results. The contact time of cement and water can be kept constant and most importantly as short as possible. That means, the cement does not remain in the hopper for longer periods and starts to set. BCSA

cement is useful for rapid setting concrete because the additional cost for BCSA is low in comparison to the buildability improvements it brings.

FL_0.5 produced the best buildability results of all tested mixes. The column was printed up to the maximum height of 90 layers. Flash setting was present throughout the print which led to the good buildability of the mix. Slight adjustments to the mix must be done to improve the aesthetics of the printed column. Using flash setting in 3D printing allows structures to be built in less time as more layers can be printed in succession. Depending on the size of the structure the flash setting mechanism can be reduced to avoid cold joints and interlayer bond strength problems. The pumping process does not seem to influence the flash setting mechanism as significantly as for BCSA cement hydration and false setting. The addition of sodium aluminate for flash setting is viable. A doubled production cost of the concrete resulted in a tripled buildability performance. A similar flash setting effect could be achieved with cement that is manufactured specifically for 3D printing with a lower calcium sulphate content.

Summarising, the three rapid setting mechanisms have great potential for 3D printing of concrete. Unfortunately, the batch mixing procedure used for this study significantly influences the setting behaviour of the BCSA containing mixes and especially the false setting concrete. The results obtained show that rapid setting mechanisms improve the buildability of 3DPC. Flash setting produced the best results as its rapid strength gain characteristics were not influenced by the pumping process. From a financial standpoint, the addition of BCSA cement or sodium aluminate influences the buildability of concrete positively. More layers can be printed at a much lower performance ration than for REF_3DPC.

5 Conclusions and recommendations

5.1 Conclusions

The aim of this study was to 3D print rapid setting ordinary concrete mixtures and to characterise the influence of the rapid setting mechanisms on the properties of concrete. A characterisation was used to determine the compressive strength both short-term and long-term, measure the hydration temperature and to obtain the setting times of these rapid setting mechanisms: false setting, flash setting and BCSA replacement. Thereafter, the buildability of each rapid setting concrete mixture was determined, and the economic feasibility of the mixtures was established.

The following conclusion can be drawn on utilising rapid setting in ordinary concrete mixtures:

- False setting was induced by using calcium sulfate hemihydrate which increases the calcium sulfate contents in the mixture. Sodium aluminate addition to ordinary concrete mixtures causes flash setting due to an increased availability of aluminates. The replacement of OPC cement with BCSA cement results in rapid setting of such concrete mixtures.

The following conclusions can be drawn on the fresh and hardened state properties of rapid setting concrete mixtures:

- The compressive strength of concrete was not influenced by false setting and OPC cement replacement with BCSA cement only limits the compressive strength at higher replacement rates. Flash setting has a negative impact on the compressive strength development and the affect increases at higher replacement rates of OPC with sodium aluminate.
- The peak hydration temperature as well as the absolute temperature increase, are higher for false setting mixtures, slight increase in hydration temperature is found for BCSA cement containing mixtures. The initial hydration temperature is increased by flash setting.
- Higher concrete temperature at mixing, accelerates the rate of hydration.
- The setting time of concrete could be reduced in the following order: false setting < BCSA replacement < flash setting. Higher replacement rates of OPC cement with the mineral additives or BCSA cement reduced the setting time even further for each of the three rapid setting behaviours.
- The early age structuration rate was determined with the UUCT test. Peak compressive strength in the first two hours after mixing can be increased as follows: false setting < BCSA replacement < flash setting. Stronger rapid setting due to higher replacement rates increased the compressive strength development of each rapid setting mechanism even further. REF achieves higher compressive strengths in the UUCT test than REF_3DPC.

- A correlation was found between the setting time test results and the UUCT test. Concrete mixes that set faster achieve higher compressive strength in the UUCT test.

The following conclusions can be drawn on the printability and buildability of rapid setting ordinary concrete mixtures:

- All rapid setting ordinary concrete mixtures were printable.
- The buildability could be improved with false setting, BCSA replacement and flash setting.
- False setting increases the buildability by ten layers which is the least of the three rapid setting mechanisms tested. A reduction in the concrete's flowability was an ineffective method to improve the buildability of the FA_4 mixture.
- BCSA replacement increased the buildability significantly and 32 additional layers to REF_3DPC could be printed. Citric acid was successfully used as a retarder for BCSA cement hydration in combination with higher superplasticiser and water contents to improve the buildability of the BC_5 mixture. Improvements in the aesthetics of the printed column were achieved with these changes.
- The flash setting mixture, FL_0.5, had the best buildability characteristics of all tested mixtures. A total of 90 layers were printed which was an increase of 62 layers in comparison to REF_3DPC.

The following conclusions can be drawn on the economic feasibility of 3D printing rapid setting ordinary concrete mixtures:

- 3D printing reduces the amounts of formwork used which has a positive environmental impact. The replacement of OPC with materials such as BCSA cement has a positive impact on the environment by reducing the amounts of OPC cement used in construction.
- Flash setting and BCSA replacement are recommended from an economic point of view as a method to increase buildability of 3D printed concrete. The additional cost of the additives is small compared to the impact they have on the buildability.
- The addition of calcium sulfate hemihydrate is not recommended from an economic point of view. The cost to induce the setting behaviour is seven times mores per layer in comparison to REF_3DPC. In comparison to the small increase in buildability the cost per layer is too high.

From this study it is evident that flash setting improves the buildability of 3DPC the best. The negative of the flash setting mixture is the low compressive strength in comparison to the other mixtures. OPC cement replacement with BCSA cement accelerates the strength gain without compensating on long-term compressive strength. Both, flash setting and BCSA replacement, provided promising results but more research is required to optimise the setting behaviour and to improve the printability characteristics of the mixtures.

5.2 Recommendations for future work

For future studies, the following recommendations can be considered:

- A more detailed study on each of the three rapid setting mechanisms is required:
    - Variation in water-cement ratio will provide insight on the effect water has on the rapid setting concrete's characteristics.
    - The optimal replacement rate for the additives must be determined. This may improve the characteristics of the rapid setting mixtures significantly.
    - Add large aggregate to determine how it influences the rapid setting behaviour of the concrete.
- The rapid setting mixtures can be further tested in a 3D printer with a continuous mixing system:
    - The time between mixing and extrusion is minimised which reduces the chances of material setting in the pipe.
    - Less of the rapidly formed hydration products are reagitated in the hopper which repetitively breaks down the formed bonds.
- Change the mix design of all tested printed mixes to improve the aesthetics of the printed columns.
    - The mix design of all rapid setting concrete mixtures can be adjusted to improve the aesthetics of the printed concrete.
    - The improved extrusion quality may positively influence the mechanical and structural properties of the printed concrete.
- Use the additives causing rapid setting in REF_3DPC:
    - In a well printable mix with good aesthetics, rapid setting is induced to increase the buildability of the mixture.
- 3D printing the REF mix and FA_4 to determine the exact influence on the buildability of concrete:
    - False setting could not specifically be detected in the printed concrete and a comparison of the two mixtures will provide insight if the rapid setting behaviour improves buildability.

6 References

Alonso, M.M., Palacios, M. & Puertas, F. 2013. Compatibility between polycarboxylate-based admixtures and blended-cement pastes. *Cement and Concrete Composites*. 35(1):151–162.

Andersen, M.D., Jakobsen, H.J. & Skibsted, J. 2004. Characterization of white Portland cement hydration and the C-S-H structure in the presence of sodium aluminate by 27Al and 29Si MAS NMR spectroscopy. *Cement and Concrete Research*. 34(5):857–868.

ASTM C136. 2005. Standard test method for sieve analysis of fine and coarse aggregates. Vol 13.

ASTM C403. 2009. Standard test method for time of setting of concrete mixtures by penetration resistance. Vol 14

Bakharev, T., Sanjayan, J.G. & Cheng, Y.B. 1999. Alkali activation of Australian slag cements. *Cement and Concrete Research*. 29(1):113–120.

Beaudoin, J. & Odler, I. 2019. *Hydration, Setting and Hardening of Portland Cement*, in Lea's Cement Chemistry, 5th edition, Butterwirth-Heinemann, pp. 157-250.

Belov, V., Barkaya, T. & Kuliaev, P. 2019. Durability of fine-grained limestone concrete. *E3S Web of Conferences*. 97:1–6.

Bentz, D.P., Ardani, A., Barrett, T., Jones, S.Z., Lootens, D., Peltz, M.A., Sato, T., Stutzman, P.E., et al. 2015. Multi-scale investigation of the performance of limestone in concrete. *Construction and Building Materials*. 75:1–10.

Bentz, D.P., Jones, S.Z., Bentz, I.R. & Peltz, M.A. 2018. Towards the formulation of robust and sustainable cementitious binders for 3-D additive construction by extrusion. *Construction and Building Materials*. 175:215–224.

Bescher, E. & Kim, J. 2019. Belitic Calcium Sulfoaluminate Cement: History, Chemistry, Performance, and Use in the United States. *Conference: 1st International Conference on Innovation in Low Carbon Cement and Concrete Technology*. (July):2–5. [Online], Available: https://www.researchgate.net/publication/334204807_Belitic_Calcium_Sulfoaluminate_Cement_History_Chemistry_Performance_and_Use_in_the_United_States.

Bessinger, J.M.H. 2020. Influence of calcium sulphate to plasticizer/superplasticizer interaction of concrete performance. MEng thesis. Stellenbosch University.

Borštnar, M., Daneu, N. & Dolenec, S. 2020. Phase development and hydration kinetics of belite-calcium sulfoaluminate cements at different curing temperatures. *Ceramics International*. 46(18):29421–29428.

Breilly, D., Fadlallah, S., Froidevaux, V., Colas, A. & Allais, F. 2021. Origin and industrial applications of lignosulfonates with a focus on their use as superplasticizers in concrete. *Construction and Building Materials*. 301:124065.

Bullard, J.W., Jennings, H.M., Livingston, R.A., Nonat, A., Scherer, G.W., Schweitzer, J.S., Scrivener, K.L. & Thomas, J.J. 2011. Mechanisms of cement hydration. *Cement and Concrete Research*. 41(12):1208–1223.

Burgos-montes, O., Palacios, M., Rivilla, P. & Puertas, F. 2012. Compatibility between

superplasticizer admixtures and cements with mineral additions. *Construction and Building Materials*. 31:300–309.

Burris, L.E. & Kurtis, K.E. 2018. Influence of set retarding admixtures on calcium sulfoaluminate cement hydration and property development. *Cement and Concrete Research*. 104(April 2017):105–113.

Butt, H.-J. & Kappl, M. 2018. *Surface and Interfacial Forces*. 2nd ed. John Wiley & Sons.

Canbek, O., Shakouri, S. & Erdoğan, S.T. 2020. Laboratory production of calcium sulfoaluminate cements with high industrial waste content. *Cement and Concrete Composites*. 106(November 2019).

Chen, M., Liu, B., Li, L., Cao, L., Huang, Y., Wang, S., Zhao, P., Lu, L., et al. 2020. Rheological parameters, thixotropy and creep of 3D-printed calcium sulfoaluminate cement composites modified by bentonite. *Composites Part B: Engineering*. 186(May 2019):107821.

Chen, M., Yang, L., Zheng, Y., Huang, Y., Li, L., Zhao, P., Wang, S., Lu, L., et al. 2020. Yield stress and thixotropy control of 3D-printed calcium sulfoaluminate cement composites with metakaolin related to structural build-up. *Construction and Building Materials*. 252:119090.

Chesnut, C.W. 2020. Understanding Workability in Belitic Calcium Sulfoaluminate Concrete Mixtures. Civil Engineering Undergraduate Honors Thesis. University of Arkansas.

Cho, S., Kruger, J., Bester, F., van den Heever, M., van Rooyen, A. & van Zijl, G. 2020. A compendious rheo-mechanical test for printability assessment of 3D printable concrete. *2nd RILEM International Conference on Concrete and Digital Fabrication*.

Chung, C.-W. & Lee, J.-Y. 2011. Premature Stiffening of Cement Paste Caused by Secondary Gypsum and Syngenite Formation (False Set). *Architectural research*. 13(1):25–32.

Danner, T., Justnes, H. & Geiker, M.R. 2015. Effect of Lignosulfonate Plasticizers on the Hydration of C3A Effect of Lignosulfonate Plasticizers on the Hydration of C 3 A. (February 2016).

Danner, T., Justnes, H., Geiker, M. & Andreas, R. 2016. Cement and Concrete Research Early hydration of C 3 A – gypsum pastes with Ca- and Na-lignosulfonate. *Cement and Concrete Research*. 79:333–343.

Diekmann, M.A. 2019. Developing a low embodied carbon-content concrete with conventional concrete properties. [Online], Available: https://scholar.sun.ac.za/handle/10019.1/105732?show=full.

Domone, P. 2003. Fresh concrete, in *Advanced Concrete Technology*. 1st edition. Butterwoth-Heinemann. pp. 3-29.

Domone, P. & Illston, J. 2010. *Construction Materials*. 4th ed. Abingdon: Spon Press.

Donaldson, E. & Alam, W. 2008. *Surface Forces*. Gulf Publishing Company.

Dransfield, J. 2003. Admixtures for concrete, mortar and grout, in *Advanced Concrete Technology*. 1st edition. Butterwoth-Heinemann. Chapter 4.

García-Maté, M., De La Torre, A.G., León-Reina, L., Losilla, E.R., Aranda, M.A.G. & Santacruz, I. 2015. Effect of calcium sulfate source on the hydration of calcium sulfoaluminate eco-

cement. *Cement and Concrete Composites*. 55:53–61.

Gauffinet-Garrault, S. 2012. *The rheology of cement during setting*. Vol. 1. Woodhead Publishing Limited.

Germann Instruments. 2010. ICAR Rheometer. *Product Specifications*. 71–75. [Online], Available: http://www.germann.org/TestSystems/ICAR Rheometer/ICAR Rheometer.pdf.

Han, J., Wang, K., Shi, J. & Wang, Y. 2014. Influence of sodium aluminate on cement hydration and concrete properties. *Construction and Building Materials*. 64:342–349.

Han, Y., Yang, Z., Ding, T. & Xiao, J. 2021. Environmental and economic assessment on 3D printed buildings with recycled concrete. *Journal of Cleaner Production*. 278:123884.

Harrison, T. 2003. Concrete properties :setting and hardening, in *Advanced Concrete Technology: Concrete properties.* 2st edition. Butterwoth-Heinemann. Chapter 4.

Harrison, R.G., Todd, P.W., Rudge, S.R. & Petrides, D.P. 2015. *Bioseparations Science and Engineering*. 2nd ed. Oxford University Press.

Huang, T., Li, B., Yuan, Q., Shi, Z., Xie, Y. & Shi, C. 2019. Rheological behavior of Portland clinker-calcium sulphoaluminate clinker-anhydrite ternary blend. *Cement and Concrete Composites*. 104(March):103403.

Ingaglio, J., Fox, J., Naito, C.J. & Bocchini, P. 2019. Material characteristics of binder jet 3D printed hydrated CSA cement with the addition of fine aggregates. *Construction and Building Materials*. 206:494–503.

Jakuja, M. 2020. THE EFFECT OF RHEOLOGICAL PARAMETERS ON STATIC SEGREGATION OF SELF-COMPACTING CONCRETE MORTAR. Cape Peninsula University of Technology.

Justnes, H. 2010. Acceleration by retardation in hydration process for cement based materials. *Journal of the Chinese Ceramic Society*. 38(9):1618–1622.

Khalil, N., Aouad, G., El Cheikh, K. & Rémond, S. 2017. Use of calcium sulfoaluminate cements for setting control of 3D-printing mortars. *Construction and Building Materials*. 157:382–391.

El Khessaimi, Y., El Hafiane, Y. & Smith, A. 2020. Effect of fineness and citric acid addition on the hydration of ye'elimite. *Construction and Building Materials*. 258:119686.

Krivenko, P., Sanytsky, M. & Kropyvnytska, T. 2018. Alkali-sulfate activated blended portland cements. *Solid State Phenomena*. 276 SSP(L):9–14.

Kruger, P.J. 2019. Rheo-mechanics modelling of 3D concrete printing constructability. Doctoral dissertation. Stellenbosch University.

Kruger, J., Zeranka, S. & van Zijl, G. 2019. 3D concrete printing: A lower bound analytical model for buildability performance quantification. *Automation in Construction*. 106.

De Laubier, R., Wunder, M., Sven, W. & Rothballer, C. 2018. Will 3D Printing Remodel the Construction Industry? *The Boston Consulting Group*. 21.

Lay, J. 2003. The effects of natural aggregates on the properties of concrete, in *Advanced Concrete Technology*. 1st edition. Butterwoth-Heinemann. Chapter .

Le, T.T., Austin, S.A., Lim, S., Buswell, R.A., Law, R., Gibb, A.G.F. & Thorpe, T. 2012. Hardened

properties of high-performance printing concrete. *Cement and Concrete Research*. 42(3):558–566.

Lewis, R., Sear, L., Wainwright, P. & Ryle, R. 2003. Cementitious additions, in *Advanced Concrete Technology*. 1st edition. Butterworth-Heinemann. Chapter 3.

Li, P., Gao, X., Wang, K., Tam, V.W.Y. & Li, W. 2020. Hydration mechanism and early frost resistance of calcium sulfoaluminate cement concrete. *Construction and Building Materials*. 239:117862.

Lin, Y., Yan, J., Wang, Z., Fan, F. & Zou, C. 2019. Effect of silica fumes on fluidity of UHPC: Experiments, influence mechanism and evaluation methods. *Construction and Building Materials*. 210:451–460.

Liu, X., Ma, B., Tan, H., Gu, B., Zhang, T., Chen, P., Li, H. & Mei, J. 2020. Effect of aluminum sulfate on the hydration of Portland cement, tricalcium silicate and tricalcium aluminate. *Construction and Building Materials*. 232:117179.

Maltese, C., Pistolesi, C., Bravo, A., Cella, F., Cerulli, T. & Salvioni, D. 2007. Effects of setting regulators on the efficiency of an inorganic acid based alkali-free accelerator reacting with a Portland cement. *Cement and Concrete Research*. 37(4):528–536.

McCarthy, L.M. 2010. Analysis of alternative water sources for use in the manufacture of concrete. Doctoral dissertation. Queensland University of Technology.

Mewis, J. & Wagner, N.J. 2009. Thixotropy. *Advances in Colloid and Interface Science*. 147–148(C):214–227.

Moelich, G.M., Kruger, J. & Combrinck, R. 2021. Cement and Concrete Research Modelling the interlayer bond strength of 3D printed concrete with surface moisture. *Cement and Concrete Research*. 150(September):106559.

Moir, G. 2003. Cements, in *Advanced Concrete Technology*. 1st edition. Butterworth-Heinemann. Chapter 1.

Muthukrishnan, S., Ramakrishnan, S. & Sanjayan, J. 2021. Technologies for improving buildability in 3D concrete printing. *Cement and Concrete Composites*. 122(June):104144.

Nguyen, H., Kunther, W., Gijbels, K., Samyn, P., Carvelli, V., Illikainen, M. & Kinnunen, P. 2021. On the retardation mechanisms of citric acid in ettringite-based binders. *Cement and Concrete Research*. 140:106315.

Paul, S.C., van Zijl, G.P.A.G. & Gibson, I. 2018. A review of 3D concrete printing systems and materials properties: current status and future research prospects. *Rapid Prototyping Journal*. 24(4):784–798.

Purnomo, J., Sumarni, S. & Saputro, I.N. 2019. Effect of citric acid on setting-time and compressive strength of concrete. *IOP Conference Series: Materials Science and Engineering*. 578(1).

Van Der Putten, J., De Schutter, G. & Van Tittelboom, K. 2019. Surface modification as a technique to improve inter-layer bonding strength in 3D printed cementitious materials. *RILEM Technical Letters*. 4(July):33–38.

Van Der Putten, J., Van Olmen, A., Aerts, M., Ascione, E., Beneens, J., Blaakmeer, J., De

Schutter, G. & Van Tittelboom, K. 2020. 3D Concrete Printing on Site: A Novel Way of Building Houses? *RILEM Bookseries*. 28(July):712–719.

Rassokhin, A.S., Ponomarev, A.N. & Figovsky, O.L. 2018. Silica fumes of different types for high-performance fine-grained concrete. *Magazine of Civil Engineering*. 78(2):151–160.

Rosero, I.A. 2020. Effect of Citric Acid on Slump , Compressive Strength , and Setting Time of Belitic Calcium Sulfoaluminate Concrete. *Graduate Theses and Dissertations. R*etrieved from https://scholarworks.uark.edu/etd/3898

Rößler, C., Möser, B. & Stark, J. 2007. Influence of Superplasticizers on C 3 A Hydration and Ettringite Growth in Cement Paste. *12th International Congress on the Chemistry of Cement.*

Sanjayan, J.G. & Nematollahi, B. 2019. 3D Concrete Printing for Construction Applications. in *3D Concrete Printing Technology*. 1–11.

SANS 3001-AG1:2014. Particle size analysis of aggregates by sieving. South Africa.

Santhanam, M. & Gettu, R. 2009. Early-age properties of concrete. in *ICE Manual of construction materials*. 135–144.

Soriano, E. 2019. The Influence of Citric Acid on Setting Time and Temperature Behavior of Calcium Sulfoaluminate- Belite Cement.

Stellenbosch Municipality. 2020. *Tariffs 2020/2021*.

Suiker, A.S.J., Wolfs, R.J.M., Lucas, S.M. & Salet, T.A.M. 2020. Elastic buckling and plastic collapse during 3D concrete printing. *Cement and Concrete Research*. 135(June):106016.

Taylor, H.F.W. 1997. Cement Chemistry . 2nd edition. Thomas Telford. London.

Wade, S.A., Nixon, J.M., Schindler, A.K., Barnes, R.W. & M.ASCE. 2010. Effect of temperature on the stress-deformation of concrete. *Journal of Materials in Civil Engineering*. 22(3):214–222.

Wang, X., Pang, Y., Lou, H., Deng, Y. & Qiu, X. 2012. Effect of calcium lignosulfonate on the hydration of the tricalcium aluminate-anhydrite system. *Cement and Concrete Research*. 42(11):1549–1554.

Wei, X., Li, Z., Xiao, L. & Thong, W. 2006. Influence of calcium sulfate state and fineness of cement on hydration of Portland cements using electrical measurement. *Journal Wuhan University of Technology, Materials Science Edition*. 21(4):141–145.

Winnefeld, F., Martin, L.H.J., Müller, C.J. & Lothenbach, B. 2017. Using gypsum to control hydration kinetics of CSA cements. *Construction and Building Materials*. 155:154–163.

Wolfs, R.J.M., Bos, F.P. & Salet, T.A.M. 2018. Early age mechanical behaviour of 3D printed concrete: Numerical modelling and experimental testing. *Cement and Concrete Research*. 106(May 2017):103–116.

Zhang, H. 2011a. Concrete. in *Building materials in civil engineering*. 81–149.

Zhang, H. 2011b. Cement. in *Building materials in civil engineering*. 46–80.

Zou, D., Zhang, Z. & Wang, D. 2020. Influence of citric acid and sodium gluconate on hydration of calcium sulfoaluminate cement at various temperatures. *Construction and Building Materials*. 263:120247.

Zunino, F. & Scrivener, K. 2019. The influence of the filler effect on the sulfate requirement of blended cements. *Cement and Concrete Research*. 126(August):105918.

Appendix A: Rheology test results

	t (min)	REF_3DPC Stress (Pa)	t (min)	REF Stress (Pa)
Rthix	0.00	520.19	0.00	1103.44
	0.17	541.16	0.17	1131.14
	0.33	562.14	0.33	1158.84
	0.50	583.11	0.50	1186.54
	0.67	604.08	0.67	1214.24
	0.83	625.05	0.83	1241.94
	1.00	646.02	1.00	
	1.50	708.94	1.50	
	2.00	771.86	2.00	
Athix	4.32	1064.03	0.95	1261.07
	15.00	1528.63	15.00	2150.65
	30.00	2181.28	30.00	3100.27
	45.00	2833.93	45.00	4049.89
trf SM	4.32	min	0.94	min
Rthix	2.09	Pa/s	2.77	Pa/s
Athix	0.73	Pa/s	1.06	Pa/s

Appendix B: Compressive strength test results

	Compressive strength (MPa)				
	1 day	3 day	7day	14 day	28 day
REF	15.87	28.12	36.77	32.72	41.34
REF_3DPC	16.02	18.67	33.93	38.24	46.68
FA_2	15.33	20.45	35.46	32.61	41.78
FA_4	15.62	29.52	39.15	40.71	41.97
BC_5	16.07	29.28	36.08	34.50	41.86
BC_10	16.52	26.21	33.59	35.88	38.36
FL_0.5	12.44	24.25	26.54	29.21	33.19
FL_1	5.05	16.28	19.10	19.98	21.78

Appendix C: UUCT test results

	Maximum Force (N)							
Time (min)	REF	REF_3DPC	FA_2	FA_4	BC_5	BC_10	FL_0.5	FL_1
2	28.09	6.93	22.24	22.50	28.26	23.03	36.56	62.98
4	27.17	4.52	19.29	27.05	27.20	23.69	53.97	71.39
6	27.22	6.98	19.00	25.64	32.27	24.71	45.09	77.09
8	34.19	7.13	23.76	27.33	30.15	27.90	68.73	74.75
10	44.63	5.68	23.49	32.15	30.06	31.34	89.41	88.46
12	47.47	7.58	25.40	27.14	29.53	36.19	96.37	86.27
14	40.31	8.75	20.55	27.37	37.52	36.15	96.09	89.50
16	40.09	9.85	22.61	27.24	38.95	41.71	112.04	92.56
18	35.94	6.62	20.40	24.58	35.04	41.96	109.89	81.55
22	41.41	8.43	24.62	32.75	44.53	47.62	126.11	88.00
24	40.31	10.17	29.59	25.56	38.65	47.72	125.88	101.79
26	44.46	11.84	27.49	35.32	45.70	57.32	134.27	98.81
30	43.03	13.64	30.06	58.07	46.74	62.75	143.91	103.64
60	52.52	17.77	31.93	59.43	74.30	99.60	204.20	139.00
90	69.95	18.74	40.23	104.22	91.08	137.46	231.96	176.84
120	95.46	23.19	62.05	144.33	127.13	170.11	273.06	226.00

Appendix D: Purchase price of materials calculated per kilogram

	R/kg
CEM I 52.5	1.90
Sand	0.13
Water	0.02
BCSA Cement	20.00
SP	63.00
Sodium aluminate anhydrous	431.02
Calcium sulphate	1015.45
Citric acid	322.00
Silica Fumes	22.35
Fly ash	2.00